



Norwegian University
of Life Sciences

Master's Thesis 2019 30 ECTS
Faculty of Science and Technology

Analysis of solar thermal systems for domestic hot water production in a nursing home

Anette Tangård
Environmental Physics and Renewable Energy

PREFACE

This thesis is the finishing piece of my master's degree in Environmental Physics and Renewable Energy at the Norwegian University of Life Sciences (NMBU). It reflects 4.5 months of work, from the preliminary ideas of its content to the completion of this paper. During these months, I have, above all, learned that time is precious. I have also learned to appreciate the value of a second, or more, pair of eyes to evaluate one's work.

From the time I first heard of the project VarmtVann2030, I found the issues interesting and meaningful. This was the main reason for choosing to collaborate with SINTEF Byggforsk, ending in this thesis, "Analysis of solar thermal systems for domestic hot water production in a nursing home". The specifications of the thesis were determined in close cooperation with Åse Lekang Sørensen and Harald Taxt Walnum in SINTEF Byggforsk. I would like to thank these two for excellent guidance and support during this process.

I would also like to thank my supervisor at NMBU, Jorge Mario Marchetti, for valuable feedback when needed. Additionally, I am grateful to Malin Helander in SGP Armatec for her unbound cooperation and Matthias Haase in SINTEF Byggforsk for his introduction into Polysun. To my family and friends, thank you for always being there.

I hope you enjoy your reading.

Anette Tangård

Tønsberg, 13.05.2019

ABSTRACT

The current state of climate change urges the world to consider alternatives concerning the use of energy. In Norway, electricity is a common energy source in buildings, but heating is a purpose which can be conducted using other energy carriers. In 2017, SINTEF Byggforsk and NTNU initiated the project VarmtVann2030 to improve the knowledge about the use of domestic hot water (DHW) in the country. This thesis examines the possibilities of using solar collectors as energy source for the heating of DHW in a nursing home. Some of the results are based on measurements carried out on a nursing home in Drammen, as a part of VarmtVann2030.

The capacity of the sun is 15 000 times larger than the earth's population's total need for energy. Solar collectors transform radiation energy from the sun into heat, which again is transferred to an energy carrier, most often a liquid. A solar thermal facility is usually dimensioned to produce 300-600 kWh/m²_{sc} and cover 40-60 % of the energy needed for DHW during a year. The annual DHW energy demand for the Drammen nursing home is 53.9 MWh. The existing standard on DHW energy use at nursing homes, SN/TS 3031, gives consumption values which are almost twice as large.

Simulations were done using a software called Polysun Designer and calculations were performed in Excel. The focus was on a pressurised system in combination with an electric water heater. A solar thermal system was chosen based on advices from SGP Armatec, a supplier of pressurised installations in Norway. SGP Armatec also offered examples of prices of materials. Considering different sizes of solar collector areas and accumulator tanks, the most profitable solution was found. The most profitable system was the one with the lowest Levelised Cost of Energy (LCOE) out of solar collector areas of 10-100 m² with accumulator tank dimensions of 50 l/m²_{sc}, 62.5 l/m²_{sc} and 75 l/m²_{sc}. The best tilt angle was found doing specified simulations. In addition to the LCOE, the payback period and annual cost were considered. Technical parameters included in the results were the solar fraction, area specific collector field yield and maximum collector temperature.

The most profitable system based on the collected consumption data from the nursing home consisted of a solar collector area of 40 m² with a tilt angle of 50° and an accumulator tank of 2000 l. For this solution, the LCOE was 66.9 øre/kWh, the payback period was 23.2 years and

the annual cost was 17 798 NOK/year. The solar fraction was 38 %, the area specific field yield was 512 kWh/m²_{sc} and the maximum collector temperature was 90 °C.

Alterations in accumulator tank volume and collector area gave various effects in the parameters. A large tank gave the best technical performance because of the increased storage capacity and the lowest economic values occurred for a tank of 1500 l. Regarding construction size, a small system achieved better outcomes than a large one due to its adaptation to the DHW consumption, but the one at 40 m² was most profitable. For the large system (80 m²), the LCOE was 75.7 øre/kWh, the payback period was 27.2 years, the solar fraction was 56 %, the area specific field yield was 388 kWh/m²_{sc} and the maximum collector temperature was 130 °C. For the small system (20 m²), the LCOE was 73.9 øre/kWh, the payback period was 26.3 years, the solar fraction was 22 %, the area specific field yield was 594 kWh/m²_{sc} and the maximum collector temperature was 76 °C. The annual cost was subject to negligible changes for different system sizes.

Sensitivity analyses were done on the most profitable system for both the investment cost and the electricity price, with alterations of ± 30 %. Not surprisingly, all the economic parameters favoured a low investment cost. The minimum values were an LCOE of 46.8 øre/kWh, a payback period of 15.2 years and an annual cost of 15 928 NOK/year. For variations in the electricity price, changes in the LCOE was negligible. The payback period and annual cost was subject to larger effects, their lowest values being 16.9 years and 14 329 NOK/year, respectively.

Additional outcomes of the thesis research gave indications that the DHW consumption should be of a certain magnitude for the use of solar collectors to be adequately profitable. A tripling of the Drammen nursing home DHW demand gave an LCOE of 53.3 øre/kWh. Simulations of a demand based on SN/TS 3031 gave reason to believe that the standard overestimates the best size of solar thermal facilities for nursing homes. SN/TS 3031 resulted in a most profitable system size of 50 m². All the parameters, with an exception of the annual cost and solar fraction, achieved worse results than expected from the standard when implementing the measured DHW consumption on the 50-m² construction. This kind of estimation of the demand can give very different outcomes than predicted.

The results in this thesis show the importance of enhanced research on the use of domestic hot water. Both costs and use of energy can be minimised if the actual consumption of the building in each individual case is examined in advance of the installation of a solar thermal construction. A decrease in the costs of solar thermal facilities and/or an increase in the electricity price would make it a more desirable alternative.

SAMMENDRAG

De pågående klimaendringene stiller krav om omstillinger innen verdens energibruk. I Norge er elektrisitet en vanlig energikilde i bygg, men oppvarming kan utføres ved hjelp av andre energibærere. I 2017 satte SINTEF Byggforsk og NTNU i gang prosjektet VarmtVann2030, som har som mål å øke kunnskapen innen bruk av varmtvann her i landet. Denne masteroppgaven undersøker mulighetene for bruk av solfangere som energikilde til å varme opp varmtvann i et sykehjem. Noen av resultatene er basert på målinger utført ved et sykehjem i Drammen, som en del av VarmtVann2030.

Solens kapasitet er 15 000 ganger større enn hele jordens befolknings energibehov. Solfangere omformer strålingsenergien fra sola til varme, som igjen overføres til en energibærer, som oftest består av en væske. Et solfangeranlegg dimensjoneres normalt for å produsere 300-600 kWh/m²_{sc} og dekke 40-60 % av varmtvannsenergiebehovet i løpet av et år. Den årlige energibruken til varmtvann på sykehjemmet i Drammen er på 53.9 MWh. Den eksisterende standarden for energibruk til varmtvann på sykehjem, SN/TS 3031, gir forbruksverdier som er nesten dobbelt så høye.

Simuleringene ble gjort ved hjelp av en programvare kalt Polysun Designer og utregningene ble utført i Excel. Fokuset var på et trykksatt system i kombinasjon med en elbereder. Valg av solfangersystem ble basert på råd fra SGP Armatec AS, en leverandør av trykksatte installasjoner i Norge. SGP Armatec tilbød også eksempler på materialpriser. En vurdering av ulike størrelser av solfangerarealer og akkumulatortanker ledet til den mest lønnsomme løsningen. Det mest lønnsomme systemet var det med den laveste energikostnaden over levetiden (LCOE) av solfangerarealer på 10-100 m², og akkumulatortankdimensjoner tilsvarende 50 l/m²_{sc}, 62.5 l/m²_{sc} og 75 l/m²_{sc}. Den beste helningsvinkelen ble funnet ved gitte tester. I tillegg til LCOE ble tilbakebetalingstiden og den årlige kostnaden vurdert. Tekniske parametere inkludert i resultatene var solfraksjonen, energiutbytte per solfangerareal og maksimal kollektortemperatur.

Det mest lønnsomme systemet basert på oppsamlede forbruksdata fra sykehjemmet bestod av et solfangerareal på 40 m² med en helningsvinkel på 50° og en akkumulatortank på 2000 l. For denne løsningen ble LCOE 66.9 øre/kWh, tilbakebetalingstiden 23.2 år og den årlige kostnaden

17 798 NOK/år. Solfraksjonen var på 38 %, energiutbyttet per solfangerareal var 512 kWh/m²_{sc} og maksimal kollektortemperatur var 90 °C.

Forandringer i akkumulatortankvolum og solfangerareal gav endringer i de forskjellige parameterne. En stor tank var best ut fra et teknisk ståsted på grunn av den økte lagringskapasiteten og en 1500-l tank gav de laveste økonomiske verdiene. I forbindelse med de ulike systemstørrelsene oppnådde et lite system bedre resultater enn et stort fordi det var bedre tilpasset varmtvannsbehovet, men systemet på 40 m²_{sc} var mest lønnsomt. For det store systemet (80 m²) var LCOE 75.7 øre/kWh, tilbakebetalingstiden 27.2 år, solfraksjonen 56 %, energiutbyttet per solfangerareal 388 kWh/m²_{sc} og maksimal kollektortemperatur 130 °C. For det lille systemet (20 m²) var LCOE 73.9 øre/kWh, tilbakebetalingstiden 26.3 år, solfraksjonen 22 %, energiutbyttet per solfangerareal 594 kWh/m²_{sc} og maksimal kollektortemperatur 76 °C. Den årlige kostnaden endret seg svært lite for ulike systemstørrelser.

Sensitivitetsanalyser på det mest lønnsomme systemet ble utført for både investeringskostnaden og elektrisitetsprisen, med endringer tilsvarende ± 30 %. Som forventet gav en lav investeringskostnad i de beste økonomiske resultatene. Minimumsverdiene var en LCOE på 46.8 øre/kWh, en tilbakebetalingstid på 15.2 år og en årlig kostnad på 15 928 NOK/år. LCOE endret seg svært lite for variasjoner i elektrisitetsprisen. Tilbakebetalingstiden og den årlige kostnaden var utsatt for større endringer, med de laveste verdiene på henholdsvis 16.9 år og 14 329 NOK/år.

Andre resultater i denne oppgaven gav indikasjoner på at varmtvannsforbruket burde være av en viss størrelse for at bruken av solfangere skal bli lønnsom nok. En tredobling av varmtvannsbehovet på sykehjemmet i Drammen ga en LCOE på 53.3 øre/kWh. Simuleringer av varmtvannsbehovet basert på SN/TS 3031 gav grunn til å tro at standarden overestimerer den beste størrelsen på solfangeranlegg for sykehjem. SN/TS 3031 resulterte i at 50 m² var den mest lønnsomme systemstørrelsen. Alle parameterne, med unntak av den årlige kostnaden og solfraksjonen, oppnådde verre resultater enn forventet fra standarden når det målte varmtvannsforbruket ble simulert i anlegget på 50 m². Slike estimeringer av behovet kan gi helt andre utfall enn forutsett.

Resultatene i denne masteroppgaven får frem viktigheten av økt forskning på bruken av varmtvann. Både kostnader og energibruk kan minimeres dersom det faktiske

varmtvannsforbruket i en bygning i hvert tilfelle blir vurdert på forhånd av installasjon av et solfangeranlegg. Lavere investeringskostnader og/eller økte elektrisitetspriser vil føre til at solfangere blir et mer attraktivt alternativ.

TABLE OF CONTENTS

Preface	i
Abstract.....	iii
Sammendrag.....	vii
List of figures	xv
List of tables.....	xix
Abbreviations	xxi
1 Introduction	1
2 Theory	5
2.1 Physics	5
2.1.1 The sun as a resource.....	5
2.1.2 Solar radiation.....	7
2.1.3 Thermal conduction.....	8
2.1.4 Thermal convection.....	9
2.1.5 Fluid dynamics.....	10
2.2 Hot water distribution systems.....	11
2.2.1 Storage heaters	11
2.2.2 Mixing valve	13
2.2.3 Circulation system.....	13
2.3 Solar collectors.....	13
2.3.1 Types	13
2.3.1.1 Flat plate collector.....	14
2.3.1.2 Evacuated tube collector	15
2.3.2 Positioning	16
2.3.3 Efficiency.....	17
2.4 Solar thermal system	21
2.4.1 Dimensioning.....	24
2.5 Costs	26

2.5.1	Investment costs	26
2.5.2	Operating and maintenance cost	28
2.5.3	Electricity cost.....	28
2.6	DHW consumption.....	29
2.6.1	The nursing home.....	29
2.6.2	SN/TS 3031.....	30
3	Methods	33
3.1	Analysis of the nursing home data	33
3.1.1	Conversion of the electrical energy into volume flow	33
3.2	The simulation program – Polysun Designer.....	36
3.2.1	Features.....	36
3.2.2	Settings in Polysun	37
3.3	Chosen DHW system	38
3.4	Assumptions and limitations.....	40
3.5	Estimation of the investment cost	41
3.6	Finding the best tilt angle	43
3.7	Finding the most profitable solution	44
3.8	Parameters to be represented	46
3.8.1	Economic	46
3.8.1.1	Payback period.....	46
3.8.1.2	Annual cost.....	47
3.8.2	Technical.....	47
3.9	Simulations	48
3.9.1	Nursing home consumption	48
3.9.2	Larger DHW consumption	48
3.9.3	Consumption based on SN/TS 3031	48
4	Results	51
4.1	Results based on the nursing home consumption	51

4.1.1	Finding the best configuration	51
4.1.2	The most profitable solution	53
4.1.3	Larger and smaller accumulator tank	58
4.1.4	Large system	61
4.1.5	Small system	63
4.1.6	Comparison between system sizes	65
4.1.7	Sensitivity analyses	69
4.1.7.1	Investment cost	69
4.1.7.2	Electricity price	70
4.2	Larger consumption	72
4.3	Results based on normed inputs from SN/TS 3031	75
4.3.1	Finding the best configuration	75
4.3.2	The most profitable solution	77
5	Discussion	83
5.1	Assumptions	83
5.1.1	Maximum solar collector area and accumulator tank volume	83
5.1.2	Irradiation and shading	83
5.2	Weather data and DHW consumption	84
5.3	System choices	85
5.3.1	Pipes	85
5.3.2	Solar collector	85
5.3.3	Accumulator tank	85
5.3.4	Solar liquid	86
5.3.5	Temperatures	86
5.3.6	Heat and pressure losses	86
5.3.7	Water heater and pumps	87
5.4	Methods limitations	88
5.4.1	Result parameters	88

5.4.2	Software.....	89
5.4.3	Dimensioning.....	89
5.4.4	Construction lifetime.....	89
5.5	Choice of costs.....	90
5.5.1	Installation cost.....	90
5.5.2	Accumulator tank cost.....	90
5.5.3	Investment cost.....	90
5.5.4	Electricity price.....	92
5.6	Results discussion.....	93
5.6.1	SN/TS 3031.....	93
5.6.2	LCOE.....	93
5.6.3	Payback period.....	95
5.6.4	Annual cost.....	96
5.6.5	Area specific collector field yield.....	96
5.6.6	Solar fraction.....	97
5.6.7	Maximum collector temperature.....	98
5.6.8	Temperature out of the accumulator tank.....	98
5.6.9	Usefulness.....	99
6	Conclusion.....	101
6.1	Further research.....	103
7	References.....	105
	Appendix A: Components in Polysun.....	
	Appendix B: Controllers in Polysun.....	
	Appendix C: Specifications of solar collector and accumulator tank.....	

LIST OF FIGURES

FIGURE 1: The global horizontal solar irradiance of a typical meteorological year (TMY) in Drammen	6
FIGURE 2: Daily average clear-sky horizontal solar irradiance in March, June, September and December in Drammen.....	6
FIGURE 3: A hot water circulation system, as illustrated in Polysun.....	11
FIGURE 4: Illustrations of series and parallel connection of water heaters	12
FIGURE 5: An illustration of a structure of a flat plate solar collector	14
FIGURE 6: One type of an evacuated tube solar collector	15
FIGURE 7: Monthly solar irradiation estimates onto a collector with various tilt angles in Drammen (59.7°N).....	16
FIGURE 8: Accumulated irradiation over the year onto collectors with various tilt angles in Drammen	17
FIGURE 9: Heat transfer processes in a solar thermal collector	18
FIGURE 10: Typical flat plate collector efficiencies against a range of temperature differences, from 0 °C to 100 °C, at various irradiances.....	21
FIGURE 11: Solar collector system for hot water preparation as illustrated in Polysun.....	22
FIGURE 12: Development of the percentage of the installation costs in relation to the investment cost.....	28
FIGURE 13: The yearly energy consumption for DHW at the Drammen nursing home, given in Wh/m ²	29
FIGURE 14: Average 24 hours DHW energy consumption profile for the nursing home in Drammen based on the collected data	30
FIGURE 15: 24 hours DHW energy consumption profile for nursing homes based on the standard SN/TS 3031.....	31
FIGURE 16: Average 24 hours DHW energy consumption profile for the nursing home in Drammen and based on SN/TS 3031	31
FIGURE 17: The yearly variation of energy consumption for DHW at the Drammen nursing home and based on values from SN/TS 3031.....	32
FIGURE 18: Cold water profile over a year, made in Polysun	35
FIGURE 19: Illustration of the isothermal layers in the tanks in Polysun.....	36
FIGURE 20: The chosen system diagram as it is shown in Polysun	39
FIGURE 21: The accumulator tank price as a function of tank volume	41

FIGURE 22: The accumulator tank price as a function of solar collector area.....	42
FIGURE 23: The change in the total investment cost with increasing collector area up to 100 m ²	42
FIGURE 24: The development of the investment cost per collector area with increasing area from 10 m ² to 100 m ²	43
FIGURE 25: The collector field yield relating to gross area for collector areas of 40 m ² and 80 m ² at different tilt angles, based on the Drammen nursing home consumption	51
FIGURE 26: The LCOE at different solar collector areas from 10 m ² to 100 m ² based on the Drammen nursing home consumption.....	53
FIGURE 27: The solar fraction for each month of the year.	55
FIGURE 28: The heat energy delivered to the system, divided into the two energy sources – the solar thermal system and the electric heating element.....	55
FIGURE 29: The collector field yield together with the hot water demand in week 1 of 2019	56
FIGURE 30: The collector field yield together with the water temperature out of the accumulator tank (pipe 1) in week 1 of 2019.....	56
FIGURE 31: The collector field yield together with the hot water demand in week 26 of 2018	57
FIGURE 32: The collector field yield together with the water temperature out of the accumulator tank (pipe 1) in week 26 of 2018.....	57
FIGURE 33: The energy flow diagram of the most profitable system	58
FIGURE 34: The LCOE at accumulator tank volumes of 1000 l, 1500 l, 2000 l, 2500 l and 3000 l	58
FIGURE 35: The payback period at accumulator tank volumes of 1000 l, 1500 l, 2000 l, 2500 l and 3000 l.....	59
FIGURE 36: The annual cost at accumulator tank volumes of 1000 l, 1500 l, 2000 l, 2500 l and 3000 l.....	59
FIGURE 37: The solar fraction at accumulator tank volumes of 1000 l, 1500 l, 2000 l, 2500 l and 3000 l.....	60
FIGURE 38: The collector field yield relating to gross area at accumulator tank volumes of 1000 l, 1500 l, 2000 l, 2500 l and 3000 l.....	60
FIGURE 39: The maximum collector temperature at accumulator tank volumes of 1000 l, 1500 l, 2000 l, 2500 l and 3000 l	61

FIGURE 40: The LCOE for a system of 80 m ² with tank volumes of 4000 l (50 l/m ² _{sc}), 5000 l (62.5 l/m ² _{sc}) and 6000 l (75 l/m ² _{sc})	62
FIGURE 41: The LCOE for a system of 20 m ² with tank volumes of 1000 l (50 l/m ² _{sc}), 1250 l (62.5 l/m ² _{sc}) and 1500 l (75 l/m ² _{sc})	64
FIGURE 42: The LCOE for system sizes of 20 m ² , 40 m ² and 80 m ²	66
FIGURE 43: The payback period for system sizes of 20 m ² , 40 m ² and 80 m ²	66
FIGURE 44: The annual cost for system sizes of 20 m ² , 40 m ² and 80 m ²	67
FIGURE 45: The solar fraction for system sizes of 20 m ² , 40 m ² and 80 m ²	67
FIGURE 46: The collector field yield relating to gross area for system sizes of 20 m ² , 40 m ² and 80 m ²	68
FIGURE 47: The maximum collector temperature for system sizes of 20 m ² , 40 m ² and 80 m ²	68
FIGURE 48: The LCOE with changes in the investment cost of ± 30 %	69
FIGURE 49: The payback period with changes in the investment cost of ± 30 %	69
FIGURE 50: The annual cost with changes in the investment cost of ± 30 %.....	70
FIGURE 51: The LCOE with changes in the electricity price of ± 30 %	70
FIGURE 52: The payback period with changes in the electricity price of ± 30 %	71
FIGURE 53: The annual cost with changes in the electricity price of ± 30 %.....	71
FIGURE 54: The LCOE for increasing DHW consumption equivalent to the double and triple of the nursing home demand.....	72
FIGURE 55: The payback period for increasing DHW consumption equivalent to the double and triple of the nursing home demand	72
FIGURE 56: The annual cost for increasing DHW consumption equivalent to the double and triple of the nursing home demand	73
FIGURE 57: The solar fraction for increasing DHW consumption equivalent to the double and triple of the nursing home demand.....	73
FIGURE 58: The collector field yield relating to gross area for increasing DHW consumption equivalent to the double and triple of the nursing home demand	74
FIGURE 59: The maximum collector area for increasing DHW consumption equivalent to the double and triple of the nursing home demand	74
FIGURE 60: The collector field yield relating to gross area for collector areas of 40 m ² and 80 m ² at different tilt angles, based on SN/TS 3031	75
FIGURE 61: The LCOE at different solar collector areas from 10 m ² to 100 m ² based on SN/TS 3031	77

FIGURE 62: The LCOE of a construction with 50 m ² solar collector area for two different consumption profiles	78
FIGURE 63: The payback period of a construction with 50 m ² solar collector area for two different consumption profiles	78
FIGURE 64: The annual cost of a construction with 50 m ² solar collector area for two different consumption profiles.	79
FIGURE 65: The solar fraction of a construction with 50 m ² solar collector area for two different consumption profiles	79
FIGURE 66: The collector field yield relating to gross area of a construction with 50 m ² solar collector area for two different consumption profiles	80
FIGURE 67: The maximum collector temperature of a construction with 50 m ² solar collector area for two different consumption profiles.....	80
FIGURE 68: The LCOE as a function of two different pump control mode.	88
FIGURE 69: Historical electricity prices for industry consumers	92

APPENDIX FIGURE 1: Screenshot of the settings for the cold-water inlet of the chosen system in Polysun.

APPENDIX FIGURE 2: Screenshot of the settings for the pipes of the chosen system in Polysun.

APPENDIX FIGURE 3: Screenshot of the settings for the heat exchanger of the chosen system in Polysun.

APPENDIX FIGURE 4: Screenshot of the settings for the pumps of the chosen system in Polysun.

APPENDIX FIGURE 5: Screenshot of the settings for the solar collector of the chosen system in Polysun.

APPENDIX FIGURE 6: Screenshot of the settings for the tap of the chosen system in Polysun.

APPENDIX FIGURE 7: Screenshot of the settings for the pump controllers of the chosen system in Polysun.

APPENDIX FIGURE 8: Screenshot of the settings for the heating element controller of the chosen system in Polysun.

APPENDIX FIGURE 9: Screenshot of the settings for the mixing valve controller of the chosen system in Polysun.

LIST OF TABLES

TABLE 1: Unit costs of different components included in a solar thermal construction, based on SGP Armatec’s products.....	27
TABLE 2: The annual hot water demand set in Polysun for the two different consumption profiles	37
TABLE 3: The different temperatures set in the system to avoid Legionella formation	38
TABLE 4: A summary of the numerical values relating to the components in the solar thermal system	40
TABLE 5: A summary of the chosen economic factors for calculation of the different parameters	47
TABLE 6: Collector field yield relating to gross area for a variation of collector areas and tilt angles, based on the Drammen nursing home consumption.....	52
TABLE 7: The LCOE, payback period and annual cost for the most profitable system	54
TABLE 8: The solar fraction, collector field yield relating to gross area and maximum collector temperature over a year for the most profitable system	54
TABLE 9: The LCOE, payback period and annual cost for the large system.....	63
TABLE 10: The solar fraction, collector field yield relating to gross area and maximum collector temperature over a year for the large system.....	63
TABLE 11: The LCOE, payback period and annual cost for the small system	65
TABLE 12: The solar fraction, collector field yield relating to gross area and maximum collector temperature over a year for the small system.....	65
TABLE 13: Collector field yield relating to gross area for a variation of collector numbers and tilt angles, based on SN/TS 3031	76

APPENDIX TABLE 1: Specifications of the solar collector used in the chosen system.

APPENDIX TABLE 2: Specifications of the accumulator tank used in the chosen system.

ABBREVIATIONS

AM	Air mass
AR5	Fifth Assessment Report
DHW	Domestic hot water
IPCC	The Intergovernmental Panel on Climate Change
KPN	Knowledge-Building Project for Industry
LCOE	Levelised Cost of Energy
NOK	Norwegian kroner
NSF	The Norwegian Solar Energy Society
NTNU	Norwegian University of Science and Technology
NVE	The Norwegian Water Resources and Energy Directorate
PU	Polyurethane
PVGIS	Photovoltaic Geographical Information System
sc (index)	Solar collector
SN/TS 3031	SN/TS 3031:2016
TMY	Typical meteorological year

1 INTRODUCTION

Our climate is changing. The latest assessment report (AR5) from the Intergovernmental Panel on Climate Change (IPCC) states that it is clear that human activity impacts the climate and that continued “business as usual” will cause long-lasting changes in the environmental system (IPCC, 2014). In an attempt to mitigate this impact, one of the aims of the Paris Agreement, which entered into force in November 2016, is to limit the global temperature increase to 1.5 °C above pre-industrial levels (United Nations Framework Convention on Climate Change, n.d.). Based on this agreement, Norway has legislated several goals concerning greenhouse gas emissions within the country, including a 40 % decrease in 2030 and a 80-95 % decrease in 2050, both compared to values from 1990 (Klima- og miljødepartementet, 2017).

There exist several areas with potential for improvements in our society, regarding minimisation of environmental impact. One of them is the energy use in buildings. Several specifications are found in “Regulations on technical requirements for building works”, including points on energy efficiency and proscriptions against the use of fossil fuels (Kommunal- og moderniseringsdepartementet, 2017). In Norway, electricity is the energy source which is most commonly used in buildings, according to Enova’s statistics from 2017 (Enova, 2019). According to The Norwegian Water Resources and Energy Directorate (NVE), 54 % of the power consumption in buildings was directly connected to the heating of space and water in 2016 (Spilde et al., 2018). Heat is a form of energy which can be produced by other means than electricity. This thesis will concentrate on such an alternative energy carrier.

Solar collectors are examples of devices which transform the irradiation from the sun into thermal energy. In addition to space heating, this energy can warm domestic hot water (DHW). The energy demand for DHW is much less dependent on the outside temperature than space heating, and remains approximately constant throughout the year (Andresen, 2008). For this reason, the extensive solar irradiation in summer can be taken better advantage of. DHW heating has a share of around 15-20 % of the total energy consumption in Norwegian residential buildings (SINTEF Byggforsk, 2011). The energy efficiency of buildings will probably increase in the future. In consequence, the heating of DHW will require a larger part of the building’s total energy use.

In 2017, SINTEF Byggforsk and NTNU initiated the project “Energy for domestic hot water in the Norwegian low emission society”, in short “VarmtVann2030” (SINTEF Byggforsk, n.d.). This is a Knowledge-Building Project for Industry (KPN) in cooperation with building owners and suppliers. Among the reasons for creating this project was the low level of knowledge about the actual demand of energy for DHW in Norway. Further research on this topic could help form a basis for future development. The gathering of information about energy use is in progress and one of the next steps will be to explore possibilities regarding effective and environmentally friendly solutions. This thesis is a part of the project VarmtVann2030 in collaboration with SINTEF Byggforsk. The focus will be on the use of solar collectors in nursing homes.

By the end of 2016, the global capacity of solar thermal collectors in operation was 457 GW_{th}, 71 % of which installed in China, according to the report *Solar Heat Worldwide* (Weiss & Spörk-Dür, 2018). Estimations for new installations in 2016 gives 38.3 MW_{th} as the equivalent value for Norway. The annual energy yield worldwide from water-based solar collectors in 2016 was 375 TWh, giving CO₂ savings of 130 million tons. Heating of DHW make up the largest part of applications, with a share of 94 % of the energy production worldwide in 2016 (Weiss & Spörk-Dür, 2018).

Several studies on the use of solar collectors to heat DHW has been done in Norway. Among these are reports written by SINTEF which analyse the principles (Andresen, 2008; SINTEF Byggforsk, 2011) and costs (Skeie et al., 2016) of introducing a solar thermal construction to a building. In 2015, the Norwegian Solar Energy Society (NSF) and Asplan Viak informed of the status quo of the use of solar collectors in the country (Norsk Solenergiforening & Asplan Viak, 2015). Statsbygg sponsored a project which, among others, consisted of implementing a solar collector installation on a student residence building in Evenstad (Selvig et al., 2017). Different implementations which have been examined in other papers include industrial halls (Fidorów-Kaprawyl & Dudkiewicz, 2017), districts (Fredly, 2014), office buildings (Keul, 2010), sheltered housing (Larsen et al., 2011), educational facilities (Moratal & Bermejol, 2013) and single-family buildings (Starakiewicz, 2018). The extensive research show that the use of solar collectors as energy source is an area of interest and a realistic, provident choice.

Research on an existing solar thermal facility at a hotel in Trondheim, by Aashammer (2016), gave indications of the actual functioning of the system. There appeared to be a deviation

between projected and measured values on the share of contribution from the solar collector installation of larger than 50 %. Aashammer means that a reason for this could be errors in the projecting phase of the solar collector construction based on assumptions from the supplier. SINTEF has written a report on experiences of house owners which has implemented solar collectors at their residence (Hauge et al., 2014). The report argued, among others, that improved competence among professionals in the area is necessary. Hence, continued measures are needed to assure the best possible performance of solar heat installations.

An estimated energy yield potential, given that all of Norway's residents have a correctly dimensioned solar collector construction delivering heat to their DHW, is around 5 TWh yearly (SINTEF Byggforsk, 2011). This amount of energy could replace almost 10 Alta hydro power plants. The focus in this thesis will be on the possibility of using solar collectors as energy source for the heating of DHW in nursing homes.

Measurements on DHW energy use has been collected by SINTEF Byggforsk over one year from a nursing home in Drammen. These values will act as a basis to dimension solar thermal constructions, using a software called Polysun Designer (Vela Solaris, 2019). Only pressurised systems with a liquid water solution energy carrier, and in combination with an electric water heater, will be assessed. The configuration which ends up with the lowest Levelised Cost of Energy (LCOE) is considered to be the best one. This thesis examines the most profitable solar collector facility for measured and standard based DHW consumptions in nursing homes, and changes in various economic and technical parameters with specified alterations.

The issues which will be explored are:

- What is the most profitable system configuration based on the measured Drammen nursing home DHW consumption?
- What characteristics do the most profitable solution have?
- What changes are noticeable when the accumulator tank size and solar collector area is altered?
- How dependent are the economic parameters on alterations in the investment cost and electricity price?
- What changes are noticeable on the most profitable system for the Drammen nursing home when the DHW consumption is increased?

- What is the most profitable system configuration based on the standard (SN/TS 3031) for nursing homes?
- What would be the outcomes if the most profitable solution based on SN/TS 3031 was implemented for the Drammen nursing home DHW consumption?

Chapter 2 will explain the relevant background theory. This includes both physics and information about solar thermal systems and DHW consumption. Chapter 3 describes the analysis done, the methods used and the assumptions taken in the research. Chapter 4 represents the results and objective observations of these. Chapter 5 comprises a discussion of the assumptions and the results in a broader perspective. Chapter 6 will conclude on the most important aspects and outcomes in the thesis.

2 THEORY

The following chapter will cover the physics relevant to solar collectors. Further, principles of solar collectors and its system are explained, in addition to a representation of the related costs. A description of hot water distribution systems is also included. Lastly, the energy measurements for DHW at the Drammen nursing home and the standard SN/TS 3031 are depicted.

2.1 PHYSICS

2.1.1 THE SUN AS A RESOURCE

One of our natural energy sources is the sun. The radiation energy from this massive star is in fact the origin of life on earth (Engvold, 2018). The capacity of the sun is 15 000 times larger than the earth's population's total need for energy (Norsk solenergiforening et al., 2017). This illustrates the huge potential of the sun as an energy source.

According to NVE (2018), Norway receives between 700 kWh/m² and 1000 kWh/m² from the sun on a horizontal surface each year. At higher latitudes, the intensity is lower because the same amount of radiation energy is spread over a larger area (Norges vassdrags- og energidirektorat, 2018). NSF et al. (2017) state that the southeastern part of the country has the highest potential concerning solar radiation intensity. Naturally, the elevation of the surroundings and the weather conditions play an additional part on a local perspective. The solar irradiance is also dependent on the time of the year and day (Norsk solenergiforening et al., 2017). Figures 1 and 2 show the yearly and daily variation, respectively, in Drammen. The visualisations are derived from Photovoltaic Geographical Information System (PVGIS), which is a web application developed at the European Commission Joint Research Centre (European Commission, 2017). A typical meteorological year (TMY) is a selection of hourly meteorological data for a given location, based on a time frame of normally 10 years or more (European Commission, 2019). Each month is represented by data from the most "typical" year for that month, e.g. January might be from 2010 while July is from 2008 etc.

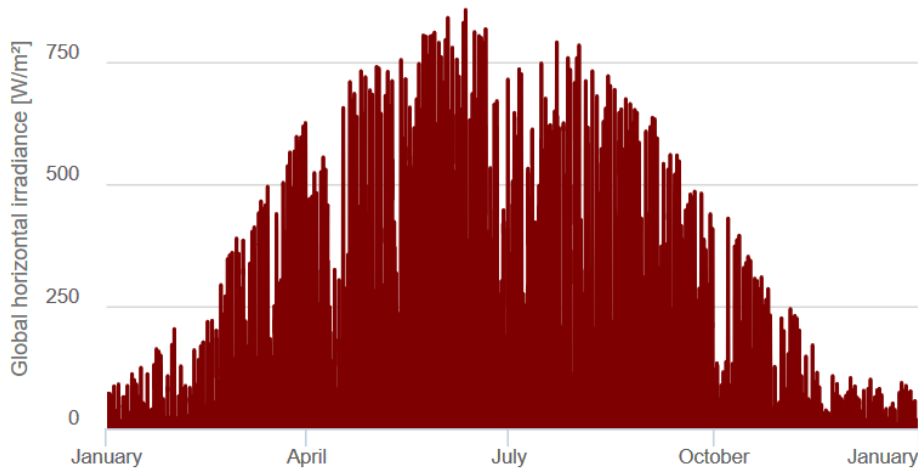


FIGURE 1: The global horizontal solar irradiance of a typical meteorological year (TMY) in Drammen, based on the years 2006-2017. Source: PVGIS

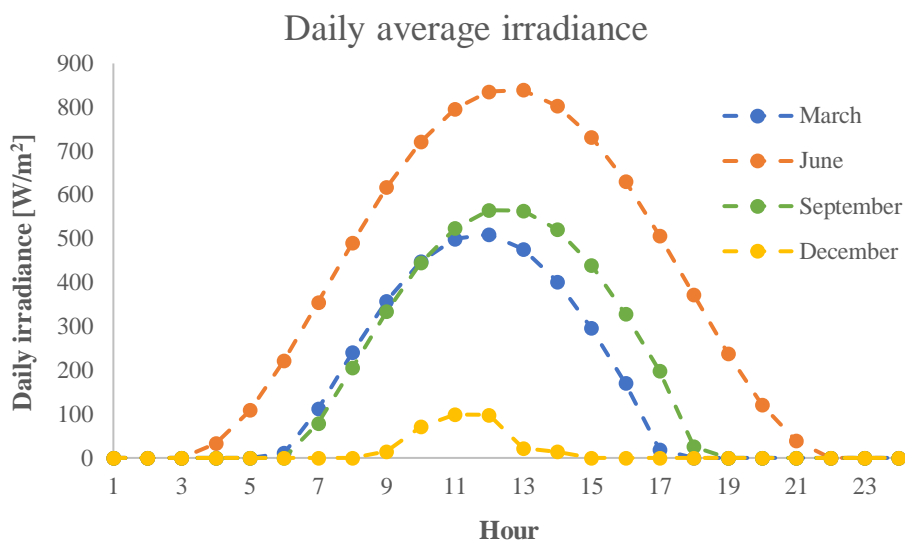


FIGURE 2: Daily average clear-sky horizontal solar irradiance in March, June, September and December in Drammen. Database: PVGIS-SARAH.

It is clear from Figure 1 that summer is the season when the irradiance from the sun is strongest, with a peak in June. Figure 2 shows that the maximum radiation intensity occur in the middle of the day and that it is non-existent at night. There are large differences between the months, both in irradiance peak value and day length. Collectively, weather variations form a complex pattern which might make it difficult to rely on solar radiation as a sole source of energy.

2.1.2 SOLAR RADIATION

All objects having a temperature above absolute zero emit radiant energy and interact with other objects (Young & Freedman, 2012). Emission describes radiation outwards while absorption, reflection and transmission are processes referring to the reception of such energy. The interactions happening on a specific surface depend on properties of both the object and the radiation (Twidell & Weir, 2006). Total absorptance depends on the different wavelengths of the incident radiation and it is the absorbed energy which is considered useful when discussing solar collectors.

Solar radiation is a form of electromagnetic energy including infrared, visible and ultraviolet light (Twidell & Weir, 2006). Spending time outside on a sunny day, it is inevitable to feel the sun's capability of energy transfer. It is the infrared portion of the radiation we feel as heat (Hanania et al., 2019). Heat transfer by radiation is a product of interaction between photons in the radiation and the molecules making up the absorbing body. The molecules move faster, which in consequence lead to an increase in the internal temperature (Hanania et al., 2017). This energy transfer will continue until the contributing components reach the same temperature. The radiation is still present, but the exchange has ceased.

The sun is often considered to be a blackbody, which means that it absorbs all wavelengths contained in the radiation which hits it and reflects or transmits nothing. Similarly, it emits radiant energy comprising a specter of wavelengths dependent on its temperature. This spectrum is given by Planck's law and the peak frequency can be derived from Wien's Displacement Law. The emissivity, e , of a blackbody is equal to 1. (Twidell & Weir, 2006)

To get a notion of the value of the solar flux, Stefan-Boltzmann law, given below, can be used.

$$P = Ae\sigma T^4 \quad (1),$$

where P is the radiated power [W], A is the surface area [m^2], e is the emissivity [-], $\sigma = 5.67 \cdot 10^{-8} \text{ W/m}^2\text{K}^4$ is the Stefan-Boltzmann constant and T is the temperature [K]. All the values refer to the radiating object. (Twidell & Weir, 2006)

It is obvious from equation (1) that the radiation power is highly dependent the sun's temperature. Taking into consideration the weakening of the radiation from the sun because of spreading and the distance from earth, the yearly average solar radiation intensity on our planet is 1367 W/m^2 (Amin et al., 2018). The amount of radiation which actually reaches the surface of the earth depends on cloud cover, particles in the atmosphere and the angle of incidence. For standardisation purposes, the unit air-mass is defined. At air-mass zero (AM0) the power density is 1367 W/m^2 , referring to the solar radiation outside the atmosphere. At AM1.5 it is 1000 W/m^2 and this value is typically used as a standard when testing solar technology because it is considered as "normal" air mass. As a result of radiative interactions in the atmosphere and on the earth's surface, there will always be diffuse radiation, in addition to direct (Twidell & Weir, 2006). Diffuse radiation can for instance be reflection from clouds or windows.

Equation (1) explains the emitted radiation by a body, but it does not show the interaction between two radiating surfaces. Considering two bodies – 1 and 2 – emitting radiation equally in all directions and having no absorbing body between them. The net radiative heat flow, Q_{rad} , from 1 to 2 is then given by:

$$Q_{rad} = \sigma(T_1^4 - T_2^4)A_1F'_{12} \quad (2),$$

where σ is the Stefan-Boltzmann constant, T_1 and T_2 are the temperatures (in Kelvin) of bodies 1 and 2 respectively, A_1 is the surface area of 1 and F'_{12} is the exchange factor. The exchange factor depends on the proportion of the emitted radiation from 1 which reaches 2, dependent on the geometry of the bodies involved, the area ratio and the emittance of the surfaces. (Twidell & Weir, 2006)

2.1.3 THERMAL CONDUCTION

Thermal conduction is an essential process in solar collectors, explaining the energy transfer to the energy carrier. Unlike radiation energy, conduction can only happen between materials which are in contact. Similar to radiation energy, the warmer object causes vibrations of the atoms in the colder object. The vibrations spread throughout the medium between atoms and free electrons and cause a gradual temperature rise. Different materials have different conduction abilities, denoted thermal conductivity. Metals are for example good conductors because of their large number of free electrons. (Cooper, n.d.)

The equation explaining heat conduction can be given in the form:

$$Q_{cond} = -kA \frac{\Delta T_{cond}}{\Delta x} \quad (3),$$

where Q_{cond} is the heat transfer rate, k is the thermal conductivity, A is the contact area, ΔT_{cond} is the temperature difference and Δx is the distance. All the values refer to the connection between the surfaces. The minus sign is added to emphasise that the energy flows to the coldest place. (Twidell & Weir, 2006)

From equation (3) it can be derived that the energy travels faster with increased conductivity, surface area and temperature difference. Likewise, it slows down with growing distance between the points of different temperatures.

2.1.4 THERMAL CONVECTION

The last mechanism of heat transfer is convection. This type of energy exchange only happens to or from a fluid in motion. There are two kinds of convection, natural and forced. When a fluid is heated, it expands and hence becomes less dense, which in turn makes it rise. This is natural convection and it is the driving force behind wind on the earth's surface. Forced convection is a result of influence from an external impact, for instance an air fan or a water pump. The initial heating process, before the fluid moves, happens by conduction from a hot surface. (Twidell & Weir, 2006)

The complexity of the convection process requires simplifications for calculation purposes. Equation (4) is based on the assumption that the fluid is not moving in the boundary layer. The boundary layer is the area closest to the heating surface. Hence, an expression for convective heat transfer, Q_{conv} , can take the following form:

$$Q_{conv} = Ah_v \Delta T_{conv} \quad (4),$$

where A is the cross-sectional area of the boundary layer, h_v is the convective heat transfer coefficient and ΔT_{conv} is the temperature difference across the boundary layer. h_v is dependent on the surface shape and fluid flow, in addition to the thermal conductivity of the fluid. (Twidell & Weir, 2006)

2.1.5 FLUID DYNAMICS

A fluid in motion is called a flow. This thesis will concentrate on liquid flowing in tubes, and for that reason specific theory regarding other types of flow is excluded. A pipe flow is physically limited on all sides and is driven by either pressure or gravity. For simplicity, liquids are usually considered incompressible even though this is not entirely true. (Jones, 2017)

For simplification, a flow is often considered as steady, which means that its properties do not change with respect to time. Additionally, a flow can be either laminar or turbulent. A laminar flow is smooth, but not necessarily linear, while a turbulent flow moves anywhere with no apparent pattern. (Jones, 2017)

The value commonly used to determine whether a flow is laminar or turbulent is Reynolds number, Re :

$$Re = \frac{\rho v l}{\mu} \quad (5),$$

where ρ is the density, v is the flow velocity, l is the characteristic length of the container and μ is the dynamic viscosity (Engineering ToolBox, 2003c). The characteristic length is equal to the diameter if the container is a circular tube or duct (Engineering ToolBox, 2003b). The velocity relates to the cross section area of the fluid container (Engineering ToolBox, 2008b). With increasing Re , the flow grows in turbulence.

A flow consists of potential, kinetic and pressure energy. Losses are unavoidable and in the case of fluids in motion the majority is due to friction. Considering flow in a tube, these losses can be expressed by the D'Arcy-Weisbach equation:

$$\Delta p_{loss} = \lambda \frac{l}{d_h} \frac{\rho v^2}{2} \quad (6),$$

where λ is the friction coefficient, l is the length of the pipe, d_h is the hydraulic diameter, ρ is the fluid density and v is the flow velocity. Equation (6) is valid for a fully-developed, steady and incompressible flow (Engineering ToolBox, 2003a). The friction coefficient depends on

the degree of turbulence of the flow and the roughness of the tube surface, and can be found by solving the Colebrook equation (Engineering ToolBox, 2008a).

2.2 HOT WATER DISTRIBUTION SYSTEMS

A hot water distribution system consists of one or multiple water heaters, a piping system, valves and the tap (Zijdemans, 2014). Figure 3 displays a possible structure. There are different types of water heaters, mainly divided into flow heaters and storage heaters. In flow heaters, the water is heated at the tap, while storage heaters accumulate hot water in a tank. In this thesis, the focus will be on storage heaters since they provide inertia in the system.

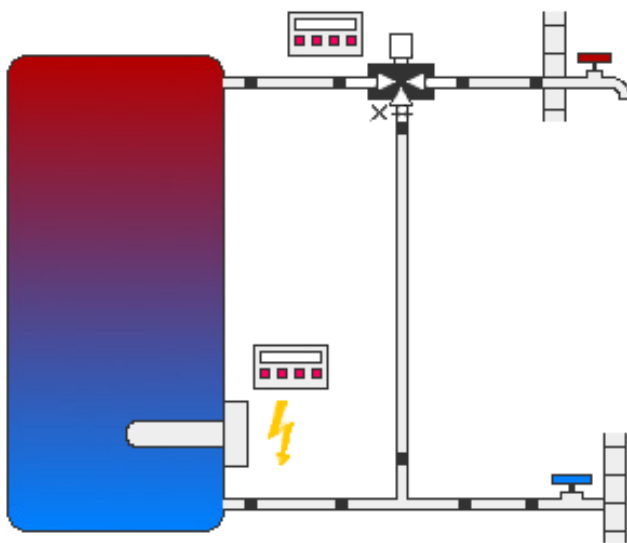


FIGURE 3: A hot water circulation system, as illustrated in Polysun. This comprises a direct storage heater. Used with kind permission from Vela Solaris.

2.2.1 STORAGE HEATERS

Storage heaters can be separated into direct and indirect types. Direct heating happens by means of an electric heating element which is placed inside the tank in contact with the water. Due to low installation and electricity costs, this is the most common type of storage heaters in Norway. In standard direct storage heaters, the heating element is normally located in the bottom of the tank to heat its entire contents, as in figure 3. Fast heaters also exist, in which the top tank water is heated first to ensure that the water in the tap becomes hot as quickly as possible. (Zijdemans, 2014)

An indirect storage heater usually contains a spiral pipe (coil) or an external heat exchanger. The coil is placed inside the tank and holds a medium of higher temperature than the accumulated water, thereby heating it up. Coil heaters are mostly used in large facilities and may be part of combination systems. The external heat exchanger is commonly of the plate type. A circulation pump carries the cold water from the bottom of the tank, through the heat exchanger and delivers the heated water to the top. Indirect and direct storage heaters can be combined, for instance by achieving a certain temperature indirectly and using an electric heating element for reheating. There are several energy sources which can provide heat energy to such a system, e.g. heat pumps, bio energy or solar collectors. (Zijdemans, 2014)

For larger buildings it might be necessary to connect multiple water tanks (Zijdemans, 2014). In principle, there are two ways of doing this: series and parallel. In a series connection (to the left in figure 4), the water flows through each tank in turn and this solution works well with an external heat exchanger. This is also a suitable method to attain good temperature stratification. Water density changes with temperature and this makes the hotter part lighter (Norsk solenergiforening et al., 2017). As a consequence, the warm water will lie as a layer on top of the colder in a tank. Thermal stratification is the division of these layers. When the tanks are connected in parallel (to the right in figure 4), the water is divided equally into each tank (Zijdemans, 2014). In direct storage heaters, a parallel connection might be beneficial because all the heating elements will kick in at the same time, resulting in a shorter heating time and even use.

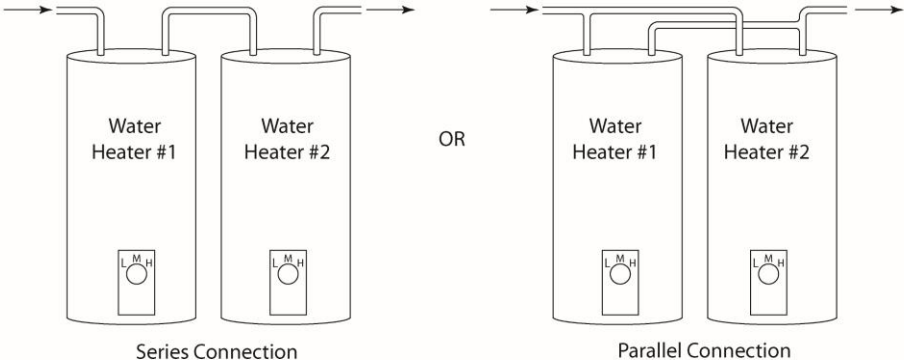


FIGURE 4: Illustrations of series and parallel connection of water heaters (Fuchs, 2013).

2.2.2 MIXING VALVE

The temperature in an electrically heated water tank is often set to be higher than the desired tap temperature. The reason for this is to achieve a large energy capacity in the tank. Between the tank and the tap, the hot water is mixed with cold water by means of a mixing valve, illustrated in figure 3. The mixing valve can function both thermally and mechanically. The thermally based types continually adjust the mix ratio to get a given temperature. In the mechanical mixing valves, the ratio between hot and cold water is constant. (Zijdemans, 2014)

2.2.3 CIRCULATION SYSTEM

After periods of no use, there might take some time before the hot water reaches the tap because the water lying in the pipes has been cooled. This leads to excessive use of water. To avoid such water waste and waiting time, a circulation system may be applied. A circulation system consists of pipes which lead the heated water in a circuit between the tap and the mixing valve. This prevents the water from being still over a longer period. The system is dimensioned in order to always circulate a given amount of water, and there exist several variants. Heat losses increase with higher water temperatures, such as in a circulation system. The size of these losses is dependent on the length of the pipes, which is usually largest from the water heater to the tap. This results in more heat losses with circulation than without. An alternative to a circulation system is to install heat tracers alongside the pipes, underneath the insulation layer. (Larsen, 2014)

2.3 SOLAR COLLECTORS

A solar collector transforms radiation energy from the sun into heat, which again is transferred to a carrier, usually a liquid. The most important component in a collector is the absorber, as it is the part which does the work of energy transfer. The absorber should have good absorption characteristics and is therefore often coloured black. A selective coating further increases the absorber performance by decreasing the emittance of infrared radiation. This coating usually have an absorbance of around 98 %. (SINTEF Byggforsk, 2011)

2.3.1 TYPES

Among liquid based solar collectors there are two types which are most widely used: flat plate and evacuated tube.

2.3.1.1 FLAT PLATE COLLECTOR

By the end of 2016, 83 % of the total capacity of solar collectors in Europa was of the type flat plate (Weiss & Spörk-Dür, 2018). Flat plate collectors also form the majority in Norway (Norsk solenergiforening et al., 2017). The basic design consists of a plane absorber, channels or tubes for the heat carrier, glazing and insulation, illustrated in figure 5 (Alternative Energy Tutorials, 2019b). The glazing is added to increase the temperature in the collector (SINTEF Byggforsk, 2011). It is made of a transparent material (e.g. glass or plastic) and keeps the heat inside by admitting shortwave radiation but hindering the longwave radiation from escaping, like a greenhouse. Insulation in the bottom and on the sides decreases the heat loss even more, especially the conduction losses (Norsk solenergiforening et al., 2017). The absorber plate is usually framed in aluminium.

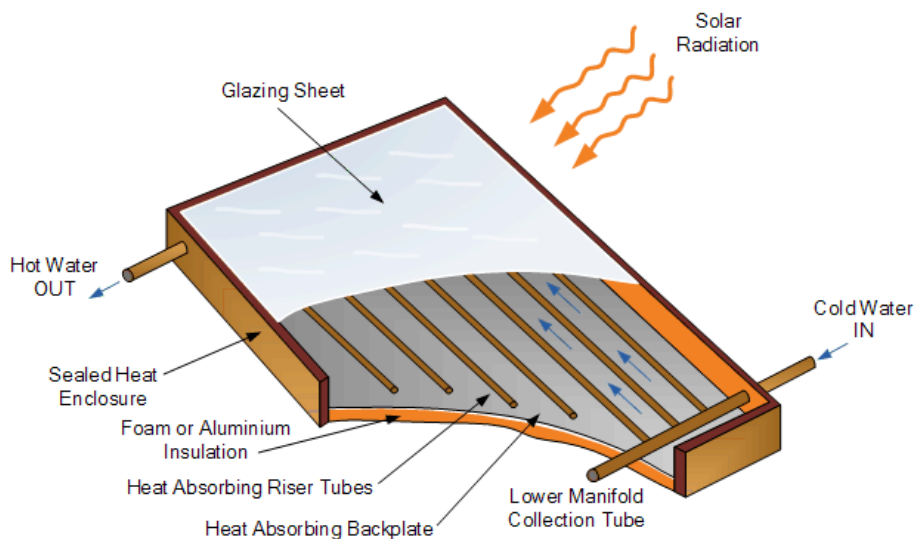


FIGURE 5: An illustration of a structure of a flat plate solar collector. The glazing, pipes, absorber and insulation is shown. The cold water enters at the bottom and the flow divides between the pipes. On its way to the top it is heated and the flows meet again before leaving the collector with a warmer temperature. The figure is used with kind permission from Alternative Energy Tutorials (2019b).

The absorber can be made of aluminium, copper or plastic (polymer). The choice of material depends on the type of system. Solar collectors with metal absorbers deliver higher temperatures and has a higher efficiency compared to those with polymer absorbers. The heat medium is often contained in tubes which are welded on the backside of the absorber. (Norsk solenergiforening et al., 2017)

2.3.1.2 EVACUATED TUBE COLLECTOR

In China, 92 % of the solar thermal capacity was provided by evacuated tube solar collectors by the end of 2016. The equivalent number in Europe was 14 % (Weiss & Spörk-Dür, 2018). Evacuated tube collectors consist of two-layered glass cylinders with vacuum in between (Alternative Energy Tutorials, 2019a). The vacuum works as an insulator against convection and radiation losses to the surroundings. The absorber, an aluminium or copper sheet, is placed inside the inner tube and connected to a metal pipe containing the liquid, as can be seen in figure 6.

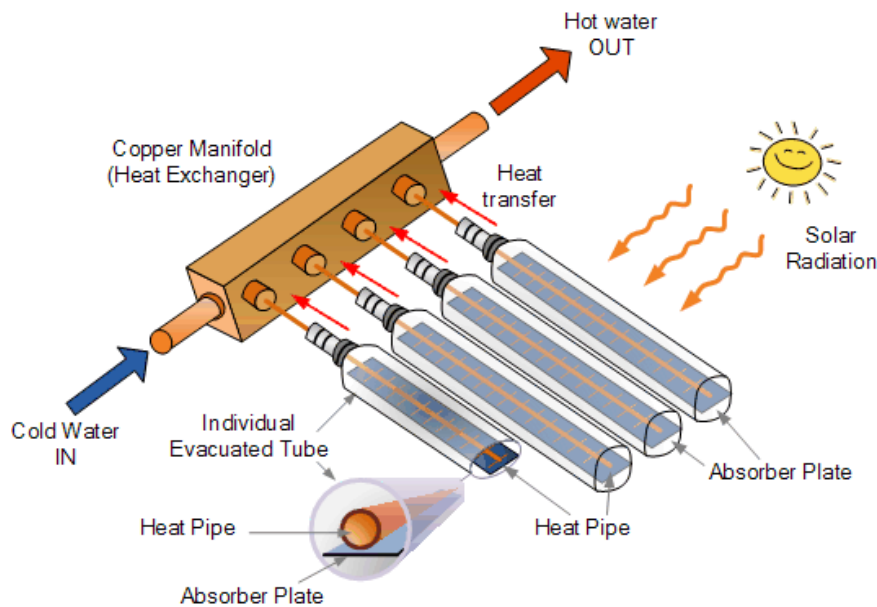


FIGURE 6: One type of an evacuated tube solar collector, consisting of four tubes with absorber plates and heat pipes. On the top there is a heat exchanger in which the solar liquid flows. The figure is used with kind permission from Alternative Energy Tutorials (2019a).

There are some different possibilities regarding the construction and functioning of evacuated tube collectors (Alternative Energy Tutorials, 2019a). For instance, the heat carrier can flow directly through the tube in a U-bend (direct flow) or it can receive energy by the use of a heat exchanger (heat pipe). The degree of flexibility and efficiency are among the properties which vary with choice of configuration.

Several individual tubes are connected via a manifold to form the collector. Because of the cylindrical shape, evacuated tube collectors have the benefit of always receiving sunlight perpendicularly independent of its position on the sky. Large irradiation angles, leading to a high degree of reflection, is a common problem with flat plate solar collectors. The benefit of

the round shape together with excellent insulation characteristics, results in the production of high temperatures and a good overall efficiency. However, due to the vacuum insulation, evacuated tube collectors are prone to overheating. (Alternative Energy Tutorials, 2019a)

2.3.2 POSITIONING

In addition to the location of the solar collector, orientation and tilt angle are also important aspects. How to position a collector is dependent on the specific need (Norsk solenergiforening et al., 2017). An orientation towards south is optimal to take the most advantage of insolation, but deviations of less than 45° does not affect the energy yield considerably (SINTEF Byggforsk, 2011). Having a relatively low sun in Norway, the tilt angle should be quite steep. An inclination of 10° below the latitude of the location is a general rule for estimation purposes. NSF (2017) propose a collector slope of around 45° for a solar collector which will be used for heating DHW exclusively. Figure 7 shows the effect of tilt angle on solar irradiation over the year, based on data from Meteonorm via Polysun.

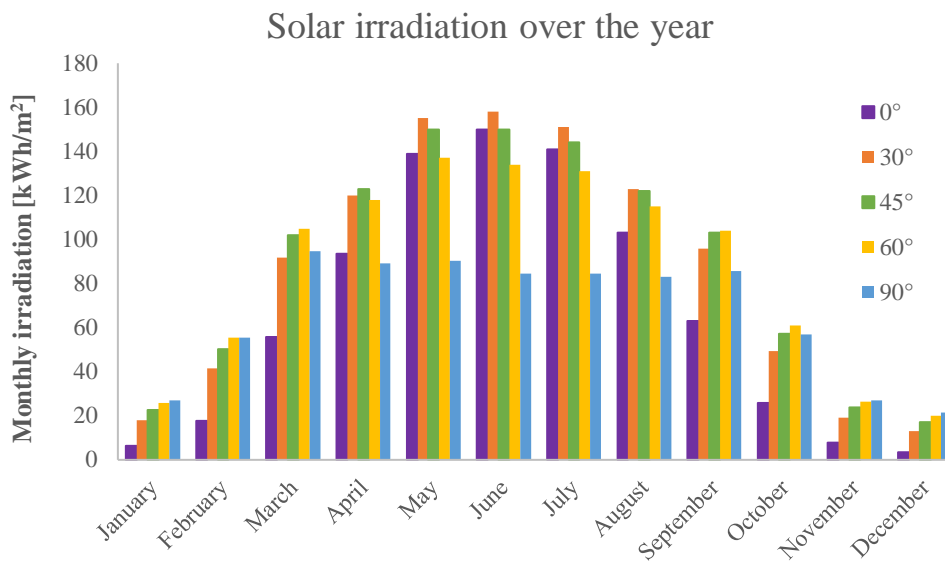


FIGURE 7: Monthly solar irradiation estimates onto a collector with various tilt angles in Drammen (59.7°N). The graphs are based on data from Meteonorm.

In summer, a 30° inclination receives most radiation, while during autumn, winter and spring, a larger angle can seem to be best in this regard. It is clear that the height of the sun affects the optimal tilt angle of a collector. For this reason, it is beneficial to define the use as detailed as possible before installing a solar thermal construction. To get a notion of what the best choice of collector slope would be throughout the year, the monthly values are added and shown in

figure 8. An inclination of 45° receive most irradiation on a yearly basis, which corresponds well with both the general rule and NSF’s suggestion.

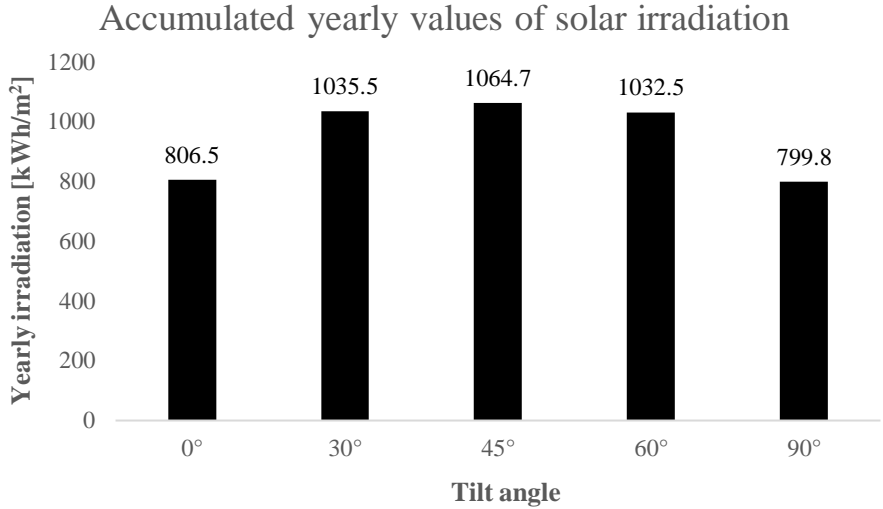


FIGURE 8: Accumulated irradiation over the year onto collectors with various tilt angles in Drammen. The graphs are based on data from Meteonorm.

2.3.3 EFFICIENCY

The efficiency of a solar collector describes how well it is able to utilise the energy it receives from the sun. There are several means of heat losses in a collector, dependent both on material properties and external conditions. The main parts of these losses are due to radiation and convection. Figure 9 shows the processes happening in a flat plate solar collector. For simplification, only flat plate collectors will be considered in this chapter. (Quaschnig, 2004)

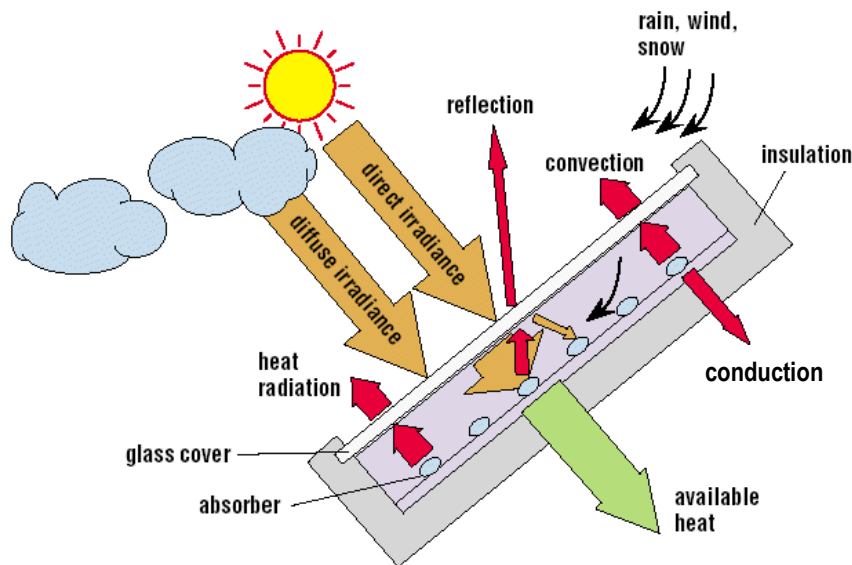


FIGURE 9: Heat transfer processes in a solar thermal collector. The irradiance from the sun is both transmitted and reflected when striking the glazing. Inside the frame it reflects some of the outgoing infrared radiation from the absorber while another part is let out. Additionally, there are both radiation and conduction losses from the absorber. The heat remaining after the losses is denounced as available heat, represented by the green arrow. The figure is used with kind permission from Volker Quaschnig (2004).

Solar radiation hits the collector in both direct and diffuse form. Reaching the glazing, the majority of the radiation is transmitted, but some of it is also reflected. The amount which is reflected vary with the angle of incidence of the sun, as illustrated in figure 7. The characteristics of the absorber defines how much heat it is able to receive and keep, a selective coating acquiring the highest amounts. The reflective properties of the glazing has a positive effect as well, trapping the emitted heat radiation from the absorber inside the collector. However, a part of the emittance also manages to leave through the cover. (Quaschnig, 2004)

The difficulty of completely air sealing the collector makes it exposed to convection losses. These losses will be highly dependent on the prevailing weather conditions. Strong winds will for instance maximise the losses because the heated air masses will continually be removed. (Quaschnig, 2004)

In a flat plate solar collector, the radiant power captivated by the absorber, P_{abs} , is given by

$$P_{abs} = \tau_{cov} \alpha_p A_p E \quad (7),$$

where τ_{cov} is the transmittance of the glazing (cover), α_p is the absorptance of the absorber (plate), A_p is the area of the absorber and E is the irradiance at the absorber. τ , α and A are usually specified for a given collector while E can be measured. (Twidell & Weir, 2006)

To account for the heat losses, a simplified expression is used. All the three forms of heat transfer – conduction, convection and radiation – are dependent on the temperature difference between the two bodies participating in the process, as can be seen in equations (2), (3) and (4). Each of these transfer forms have a thermal resistance related to it:

$$R_{cond} = \frac{\Delta x}{k_p A_p} \quad (8),$$

R_{cond} is the conductive resistance where Δx is the distance between the absorber and the surroundings of different temperature, k_p is the thermal conductivity of the absorber plate and A_p is the absorber area. (Twidell & Weir, 2006)

$$R_{conv} = \frac{1}{h_v A} \quad (9),$$

R_{conv} is the convective resistance where h_v is the convective heat transfer coefficient and A is the cross-sectional area of the boundary layer. (Twidell & Weir, 2006)

$$R_{rad} \approx \frac{1}{4\sigma A_p F'_{pa} T_{av}^3} \quad (10),$$

R_{rad} is an estimation of the thermal resistance for radiation when $(T_p - T_a) \ll T_p, T_a$, which is often the case. T_p and T_a is the temperature of the absorber and the surroundings (ambient) respectively. σ is the Stefan-Boltzmann constant, A_p is the surface area of the absorber, F'_{pa} is the exchange factor and $T_{av} = (T_p + T_a)/2$ is the mean temperature. The temperatures are given in Kelvin. (Twidell & Weir, 2006)

The heat loss part of the energy balance equation combines these resistances into one equivalent thermal resistance R_L . The resulting formula for the captured radiant power, P_{cap} , is

$$P_{cap} = \tau_{cov}\alpha_p A_p E - \frac{T_p - T_a}{R_L} = \eta_{cap} A_p E \quad (11),$$

where T_p and T_a is the temperature of the absorber and the surroundings respectively. η_{cap} is the capture efficiency divided into optical losses and heat transfer losses. (Twidell & Weir, 2006)

It can be derived from equation (11) that the losses due to heat transfer grow in size with increasing temperature difference until η_{cap} reaches zero and no heat is captured in the absorber. The temperature in this situation is called the equilibrium, or stagnation, temperature.

So far, only the energy captured by the absorber has been considered. Another factor must be added to illustrate the amount which is delivered to the heat carrier. The useful power, P_u , in the liquid is given by

$$P_u = \dot{m}c(T_2 - T_1) = \eta_{tran} P_{cap} \quad (12),$$

where \dot{m} is the mass flow, c is the specific heat capacity and T_1 and T_2 is the temperature of the inlet and outlet, respectively. η_{tran} is the efficiency of the heat transfer between the absorber and the heat carrier. (Twidell & Weir, 2006)

Multiplying η_{cap} and η_{tran} from equations (11) and (12) gives the total efficiency of the collector:

$$\eta_c = \eta_{cap}\eta_{tran} = \frac{P_u}{A_p E} \quad (13).$$

In a well-designed solar collector, the transfer efficiency is almost independent of the operating conditions, typically $\eta_{tran} = 0.85$. R_L would vary linearly with temperature if not for the radiative thermal resistance, which decreases rapidly with increasing T_p . (Twidell & Weir, 2006)

Volker Quaschnig gives a graphic description of how the efficiency varies with the difference between T_p and T_a , displayed in figure 10. These curves are estimations based on measurements with distinct irradiances. The optical losses are governed by τ_{cov} and α_p and are constant for a given collector. There will always be an amount of thermal loss, its magnitude depending on the E and the temperature difference. With an increase in irradiance, the thermal losses shrink, which can also be seen from equation (11). The dependence of $T_p - T_a$ is also noticeable in equation (11) as in the figure below.

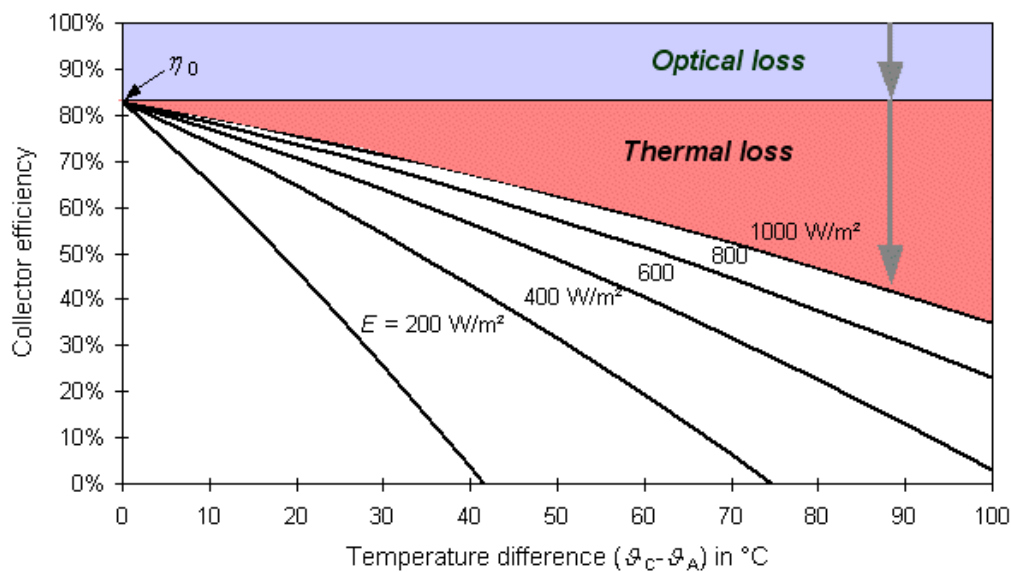


FIGURE 10: Typical flat plate collector efficiencies against a range of temperature differences, from 0 °C to 100 °C, at various irradiances. The constant optical loss is illustrated on the top, while the thermal loss is dependent on the irradiance and temperature difference. The curve gets steeper with decreasing radiation intensity. The figure is used with kind permission from Volker Quaschnig (2004).

There are several means of improving the efficiency of a solar collector. To minimise optical losses, it is important to have a glazing with high transmittance and an absorber with selective properties. The glazing will also decrease the convective losses. Additionally, proper insulation weakens conductive losses. Finally, a low inlet temperature of the liquid to the collector will increase its conductive heat transfer abilities. (SINTEF Byggforsk, 2011)

2.4 SOLAR THERMAL SYSTEM

There are two main types of system: pressurised and non-pressurised (drain-back). In a pressurised system, the heat medium is situated in the collector all year round. For this reason, antifreeze – normally ethylene glycol or propylene glycol – is needed for the fluid to stay in the

liquid form in sub-zero climates. Drain-back systems, on the contrary, use pure water because the medium is drained as soon as the temperature is outside predefined limits. (Norsk solenergiforening et al., 2017) This thesis will focus on pressurised systems with a liquid water solution energy carrier.

The two main components of a solar collector system is the solar collector and heat storage. To connect and control these parts are pipes, heat exchanger(s), pumps, valves and a management system. Figure 11 illustrates this. After circulating the solar collector, the heat carrier flows in the pipes through a heat storage where the liquid transfers the energy obtained, e.g. via a heat exchanger, to the water inside. The heat storage is usually an insulated container which is called an accumulator tank. From the accumulator tank, the heated water supply energy to the hot water distribution system when needed. An additional energy source is included to give peak load on days when the solar heating construction does not manage to cover the need by itself. (Norsk solenergiforening et al., 2017)

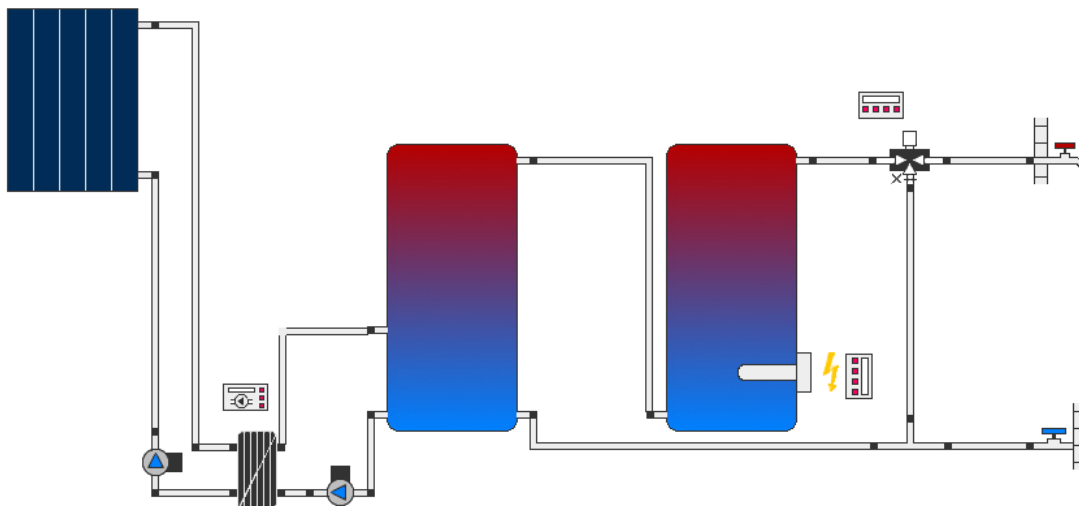


FIGURE 11: Solar collector system for hot water preparation as illustrated in Polysun. The system consists of a collector and an accumulator tank with pipes connecting them. In addition, a water heater with an electric heating source is connected to the accumulator tank in series. Two pumps, a mixing valve and controllers are also shown. The figure is used with kind permission from Vela Solaris.

The accumulator tank provides inertia in the heating system. It stores the energy for the time of need and its capacity depends on insulation, size, temperatures and the actual use. Thermal stratification is an important concept in the storage tank and this mechanism is utilised in a solar collector system. For the stratification to be as good as possible, a minimised amount of circulation is wanted. This is dependent on the height of the tank and the velocity of the inlet

and outlet water. The solar collector is usually connected to the bottom part of the tank due to the fact that it is most efficient at lower temperatures. (Norsk solenergiforening et al., 2017)

Water expands when it freezes and might for that reason cause damage to the pipes in a collector. There are several properties which are changed by adding antifreeze to the solar liquid. With increasing concentration of antifreeze, the heat capacity weakens and the viscosity gets larger. Additionally, the boiling point increases while the freezing point decreases. At a propylene glycol percentage of at least 33 %, the liquid freezes in a grainy gelatinous form which is not harmful to equipment. (Vela Solaris, 2018)

Since the heat carrier in a pressurised system contains antifreeze, this liquid is not used directly as tap water (SINTEF Byggforsk, 2011). The system is classified as indirect, which means that the solar fluid is kept in a closed circuit. A heat exchanger is needed. There exist different types of heat exchangers in a solar thermal system, some more common than others. Two widely used solutions are internal coil and external plate heat exchanger (Vela Solaris, 2018). The internal coil heat exchanger is a spiral pipe, situated in the cold-water part inside of the tank. The solar liquid flows in the coil and transfers its heat through the conducting material of the pipe. Convection forces contribute to spread the heat throughout the tank. In an external plate heat exchanger, the two liquids are thermally connected by flowing in opposite directions, only separated by thin plates. By this method, up to 99 % of the heat of one liquid can be transferred to the other. After being heated, the water is usually brought to the tank by means of a pump. An external heat exchanger normally has a greater heat transfer efficiency than an internal coil (Vela Solaris, 2018). On the other hand, such a configuration demands an extra circulation pump and has a higher cost. For this reason, external heat exchangers are mostly used in large systems.

In a system with roof mounted solar collectors, the accumulator tank is usually placed inside the building at a lower level. For the system to work efficiently, pumps are integrated in the circuit (SINTEF Byggforsk, 2011). The pumps circulate the water between the solar collector and the storage tank, governed by temperature sensors in each place. When the liquid in the solar collector has a higher temperature than the tank water by a specified amount of degrees, the pumps are activated. This temperature difference is typically 5-8 °C (Andresen, 2008). A non-return valve ensures that the flow is not reversed at night, avoiding heat losses (SINTEF Byggforsk, 2011). Expanders are fitted to account for volume variations with temperature. An

automatic management system may be necessary to control and monitor the process to ensure the highest possible energy yield. To make sure that the heating works as anticipated, the management system should also offer a logging function.

There are several possibilities in types of energy sources which can be combined with solar collectors. This thesis will focus on electricity as the secondary source, which is also the simplest solution. In larger systems, the accumulator tank provides the storage. The inlet water for the solar collector is usually taken from the bottom of the tank, where it is coldest. The heated outlet water is delivered above this, but still at a relatively low level. Since the system is indirect, the heat carrier is contained in closed pipes. The accumulator tank is connected to a water heater with an electrical source to ensure the correct temperature. The water can either be heated to the wanted temperature entirely by the solar collectors or electricity can provide the last temperature increase. (Norsk solenergiforening et al., 2017)

2.4.1 DIMENSIONING

In Norway, a well dimensioned solar thermal construction should deliver 300-600 kWh/m²_{sc} during a year (SINTEF Byggforsk, 2011). The dimension and specifications of the system depend on the energy use and available area. Overdimensioning can lead to a large accumulation of heat in the collectors, causing high temperatures and risk of boiling in a pressurised system. Optimally, the system should not produce more heat than the building consumption and the storage capacity at low loads allow (Norsk solenergiforening et al., 2017). Extensive heat production in combination with minimum heat need is most likely to happen during the summer. For this reason, information about the demand in these periods is the most important basis of dimension calculation. According to NSF (2017), constructions aimed for the heating of only DHW will normally be dimensioned to cover around 40-60 % of the annual DHW energy demand. This demand is dependent on both the amount and temperature level of the water needed and the consumption profile.

It can be difficult to find the proper size of a heat storage, avoiding both reduced efficiency and over use of the secondary heating source. According to SINTEF Byggforsk, a short time storage for residences should be able to cover two to three days' heat need during the summer season. A general rule is to have an accumulator tank volume of 50-75 litres for each square meter of solar collectors. (SINTEF Byggforsk, 2011)

There are different aspects to consider in relation to tank size and choice of temperature. A large tank has great capacity, but there is a need for more energy to heat its contents to a certain temperature level. Similarly, higher temperatures hold more energy, but the losses become larger. Considering heat losses, it is beneficial with a large tank compared to several small ones because of the decreased ratio between surface and volume. To minimise these losses, a layer of insulation at 15-30 cm with a conductivity of 0.04 W/mK is normally added. (Vela Solaris, 2018)

The solar collectors are most efficient when the water in the collector is not much hotter than the surroundings, as can be observed in figure 10. The Norwegian Institute of Public Health recommends a minimum temperature of 70 °C in the tank and at least 60 °C in the tap to prevent Legionnaires' disease (Folkehelseinstituttet, 2018), which counteracts a good performance of the solar heating system. For this reason, the solar collectors often deliver heat to give a temperature below the demanded. The needed temperature increase is provided by the auxiliary energy source.

The flow rate of the pumps is dependent on the preferred temperature increase through the collector (Vela Solaris, 2018). A low flow rate (10-20 l/m²_{sc}/h) allows a larger increase than a high flow rate (30-40 l/m²_{sc}/h), because the solar liquid is present in the collector for a longer period. Change in pipe dimensions affect both flow rate and losses. Pipes with large diameter cause more heat loss, but less pressure loss, compared to smaller ones. The pipe material also impacts the flow, copper and steel being widely used. Most important in relation to heat losses is insulation. Some centimetres of insulation material allow for an acceptable decrease in these losses. The European standard EN 12976 recommend at least 20-30 mm insulation (Andresen, 2008).

When placing the installation on a roof, there are several limitations to have in mind. The available area and roof slope govern the structure and size of the construction. Individual collectors might cause shading which affects the choice of distance between the units and their inclination. Other obstructions, like buildings or trees, can also cast shadows and prevent irradiation from reaching the collectors and should be avoided. The solar collectors are able to produce heat despite the appearance of frequent clouds, but the output will be reduced by about the same amount as the shade cover. (Norsk solenergiforening et al., 2017)

In addition to shading considerations, there are some other aspects to have in mind. The installation should be planned in such a way that the pipes are as short as possible. Space for thermostats and grounding cables should also be included. In the events of snow, the tilt angle of the solar collectors should be steep enough for it to slide off, there should be enough area on the roof to room the fallen snow and measures should be done to avoid the snow from doing any harm on possible pedestrians on the ground. Evacuated tube collectors are especially prone to keeping snow upon them because of their good insulation. The roof must be able to resist the load exposed on it, including the construction and any additional load which may arise. Equally, the floor where the storage tank is placed should resist its weight. Lastly, it is important to ensure adequate access to the solar collectors for maintenance and other. (SINTEF Byggforsk, 2011)

2.5 COSTS

There are a number of factors which affect the costs of a solar thermal construction, e.g. the type of collector, the size and structure of the facility and integration with existing systems (Enova, 2016). In addition to the construction itself, these costs include installation and consultation from roofers, electricians and plumbers (SINTEF Byggforsk, 2011).

For this thesis the residual charges are disregarded. The focus will be on investment, operating and maintenance and electricity costs. Cleaning and management costs are assumed to be included in the operating and maintenance costs.

2.5.1 INVESTMENT COSTS

Information on material prices for solar collector facilities was given by one of the largest suppliers of pressurised solar heating systems in Norway, SGP Armatec AS. SGP Armatec shared the prices for the products they offer, including solar collectors with accessories, different solar stations and accumulator tanks of various volumes. These are listed in table 1.

TABLE 1: Unit costs of different components included in a solar thermal construction, based on SGP Armatec’s products. Included in the equipment/accessories post are collector pipes, vents, hoses, roof stands and connections. The solar station consists of a heat exchanger, pumps and an automatic control system.

	Unit prices [NOK]
Flat plate solar collector (2.5 m²)	6 500
Equipment/accessories (per collector)	2 539
Solar liquid (per collector)	314
Solar station:	
Mini (< 20 m ² _{sc})	29 000
Midi (< 50 m ² _{sc})	36 600
Maxi (< 100 m ² _{sc})	44 000
Mega (< 200 m ² _{sc})	116 500
Accumulator tank:	
500 l	22 300
1000 l	28 500
2000 l	36 800
3000 l	42 700
4000 l	59 900
5000 l	84 000
Expansion tank (200 l)	6 500
DHW coil	21 000

The installation costs will be based on its percentage of the total investment cost. Results in an NVE report show that the installation costs represent around 12 % and 8 % for constructions of 12 m² and 300 m², respectively (Sidelnikova et al., 2015). In figure 12, the trend line of the installation costs percentage for different facility sizes is displayed, based on these two values.

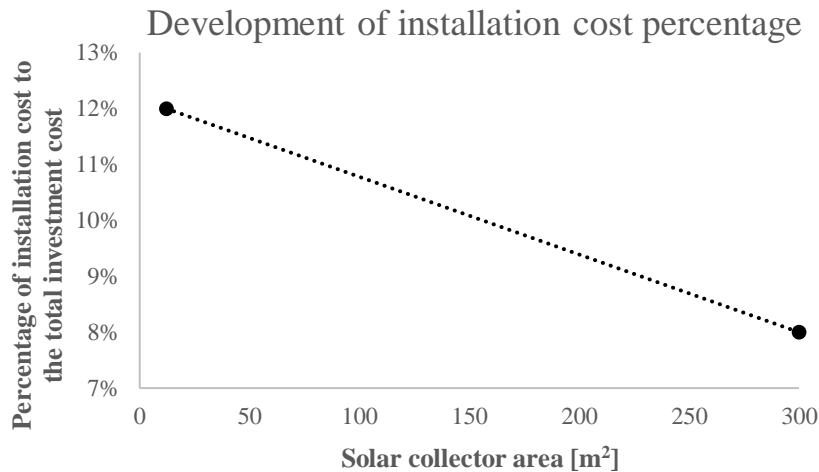


FIGURE 12: Development of the percentage of the installation costs in relation to the investment cost. The line is based on a percentage of 12 % for 12 m² solar collector area and 8 % for an area of 300 m².

At the time of writing, Enova offers financial support of 201 NOK/m² installed solar collector area (Enova, n.d.). The funding has a limit of 1 million NOK and up to 45 % of the investment cost. For future reference of the investment cost, the Enova subsidies are included in the calculation.

2.5.2 OPERATING AND MAINTENANCE COST

The cost for operation and maintenance of a solar thermal construction is estimated to be 1 % of the investment cost each year (Sidelnikova et al., 2015).

2.5.3 ELECTRICITY COST

The power price is estimated by using a forward spot price for the year 2022 of 30.8 øre/kWh, based on Nasdaq OMX (Tekniske Nyheter DA, 2019). Additionally, the electricity price consists of a mark of 1.0 øre/kWh, a consumption tax of 15.8 øre/kWh (Skatteetaten, 2019) and an electricity certificate mark of 2.6 øre/kWh (Tekniske Nyheter DA, 2019). This gives a price of 50.2 øre/kWh, without grid rent. The grid rent is set to 20.7 øre/kWh, based on a weighted average for health and social services from 2017 (Statistisk sentralbyrå, 2018). In total, the electricity price which will be used is 70.9 øre/kWh. These prices are without value added tax.

2.6 DHW CONSUMPTION

2.6.1 THE NURSING HOME

The nursing home is located in the city of Drammen on the southeastern coast of Norway. It has a heated area of 3327 m² and 52 residents. Today, the tap water is heated by electrical means, consisting of three power sources of 25 kW each. The three hot water tanks have a volume of 550 litres each and are connected in parallel. As a part of the project VarmtVann2030, SINTEF Byggforsk has received values for the hourly energy use of the electric heating elements over a year, from January 11th, 2018 at midnight to January 10th, 2019 at 11 p.m.

The annual energy demand for the heating of DHW at the nursing home is 53.9 MWh. Figure 13 shows how this consumption varies throughout the year. The demand span from almost zero to around 11 Wh/m² per hour.

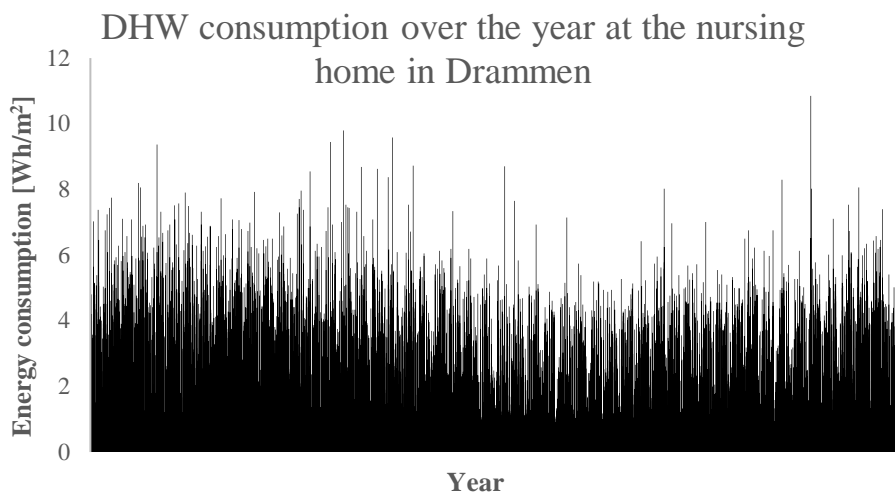


FIGURE 13: The yearly energy consumption for DHW at the Drammen nursing home, given in Wh/m². The data source is the hourly collection done by SINTEF Byggforsk.

An average 24 hours consumption profile is displayed in figure 14, estimated from the entire year's measurements. A protruding morning peak can be observed from 07:00 to 08:00. During the day, a minimum occurs from 14:00 to 15:00, while there are several lower peaks around midday and towards the evening.

Average 24h consumption profile for the nursing home

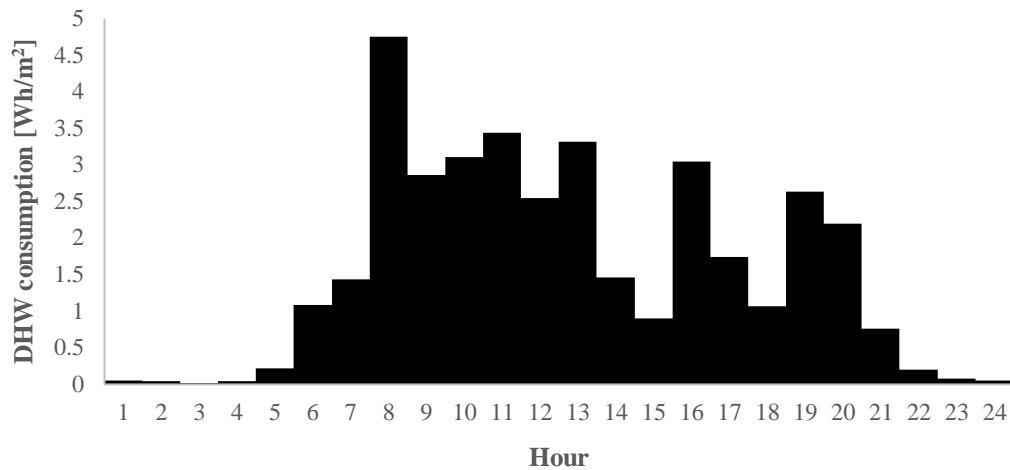


FIGURE 14: Average 24 hours DHW energy consumption profile for the nursing home in Drammen based on the collected data. The consumption at 03:00 is not zero, but it is too small to be visible in this graph.

2.6.2 SN/TS 3031

The standard SN/TS 3031:2016 (SN/TS 3031) is a tool to estimate energy requirements and energy supply in buildings (Standard Norge, 2017). Normed input values for 24 hours are available for, among others, hot water consumption at nursing homes (Standard Norge, 2016). The normed inputs are given in Wh/m^2 . In this standard, the DHW energy use for nursing homes is identical to the one for hotels. The inputs are based on a standard reference year, consisting of hourly meteorological data (NS 3031:2014). Figure 15 illustrates the profile for nursing homes for one day and night. This is compared to the average profile for the Drammen nursing home in figure 16.

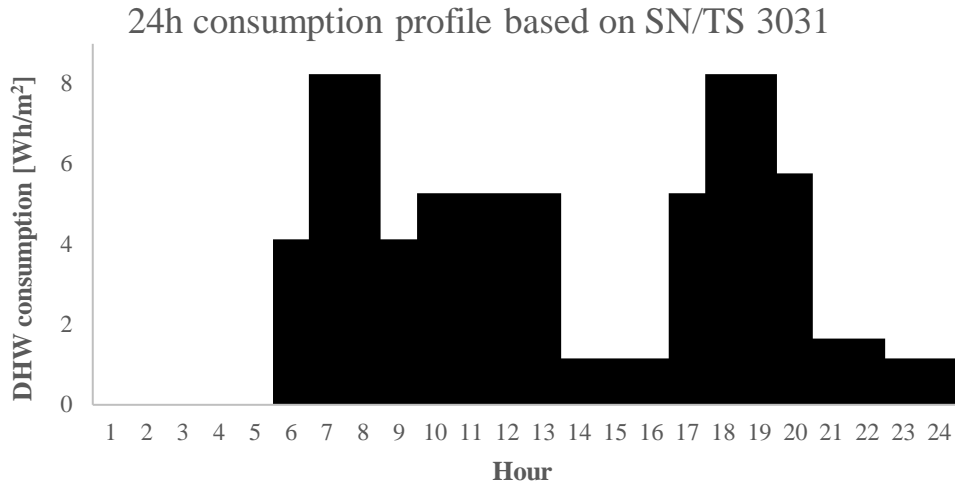


FIGURE 15: 24 hours DHW energy consumption profile for nursing homes based on the standard SN/TS 3031.

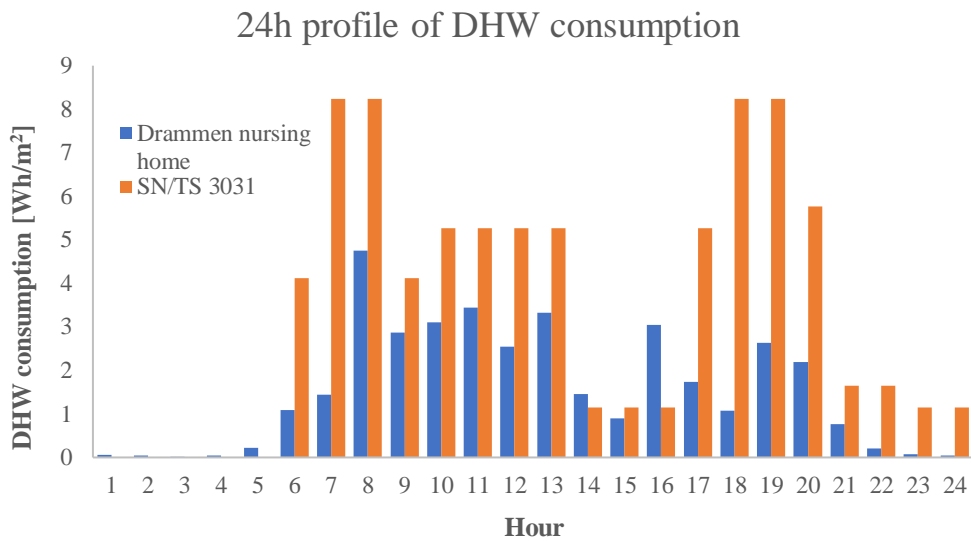


FIGURE 16: Average 24 hours DHW energy consumption profile for the nursing home in Drammen and based on SN/TS 3031. The consumption at the Drammen nursing home is not zero in the night, but it is too small to be visible in this graph.

It is clear that the standard assumes a higher DHW consumption than what is measured in Drammen. Additionally, SN/TS 3031 prolongs the day, most noticeable in the late evening. Most of the time, the standard assumes the highest consumption. However, there is an obvious exception at 16:00 where the collection-based energy demand is more than twice as large as the one based on SN/TS 3031. In summary, there are evident differences between the two profiles.

For a nursing home of the same size as the one in Drammen, the annual DHW energy demand would be around 100 MWh, based on SN/TS 3031. This is nearly twice as high as the measured energy demand.

In the standard, all days are assumed to have the same profile. The consequence of this is that there are no seasonal variations. A comparison between the monthly differences of the collected consumption data at the nursing home in Drammen and the standard is displayed in figure 17. The graph is based on months with an equal length of 365/12 days to achieve a correct ratio. In addition to being constant over the year, the input values from SN/TS 3031 also gives a higher overall consumption than the data from the nursing home. A noticeable consumption decrease in summer for the measured data can also be observed in the figure.

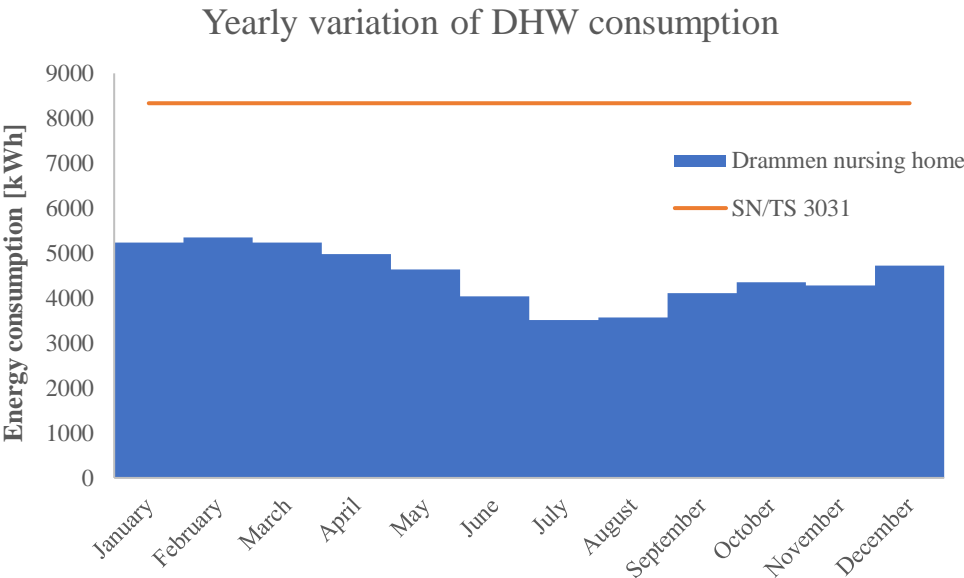


FIGURE 17: The yearly variation of energy consumption for DHW at the Drammen nursing home and based on values from SN/TS 3031. The energy use is accumulated over each month. To ensure the correct ratio, the months are assumed to be equally long, consisting of 365/12 days.

3 METHODS

In this chapter, the methods used in the thesis are presented. It includes a description of the necessary analysis of the collected nursing home data and use of the simulation program. Further, the solar thermal system which will be tested is introduced. Assumptions, estimations and procedures for the simulations and calculations completes this chapter. All the calculations and diagram making were done in Excel.

3.1 ANALYSIS OF THE NURSING HOME DATA

Before starting the simulations, an analysis of the collected data from the nursing home was done. The measurements consisted of the electrical energy used to heat the water at the nursing home. These values were available on an hourly basis for a whole year, from January 11th 2018 at midnight to January 10th 2019 at 11 p.m.

A review of the data set showed some faults in the measurement process. Some of the energy values was zero, even though the heating elements had been active all the time. It was assumed that whenever a zero occurred, the following non-zero number was an accumulated value of the energy not measured in the previous hours. To correct this, the accumulated number was divided equally on the relevant amount of fields. E.g. if three zeros were followed by a positive value, this number was divided by four. Apart from this, the data collection had apparently gone well.

3.1.1 CONVERSION OF THE ELECTRICAL ENERGY INTO VOLUME FLOW

The input in the consumption profiles in Polysun needed to be in litres, while the measured data was in kWh. Additionally, the profile in Polysnu was defined in the tap, which meant that the heat losses from the tanks to the tap needed to be subtracted from the collected data.

For this reason, a conversion was done. The data was sorted from January 1st to December 31st, making sure that the values appeared in the correct order. This was necessary because the values from January 1st including January 10th was from 2019, while the rest belonged to 2018.

The conversion was based on the following equation:

$$E_{el} = Vc\Delta T\rho + E_{loss} \quad (14),$$

where E_{el} is the electrical energy use, V is the volume which is heated, c is the specific heat capacity, ΔT is the temperature difference between the cold inlet water and the warm output water, ρ is the density and E_{loss} refer to the heat transferred to the surroundings. The final result was multiplied by 1000 to achieve an answer in litres.

The heat losses in the DHW system were set to be 0.75 kW, based on measurements done previously in the project (SINTEF Byggforsk, 2019). These were subtracted from the complete set of numbers to get the amount of energy contained in the water at the tap. Another problem arised after the removal of the losses, namely negative numbers of electrical energy use. In this scenario, an opposite direction of energy flow does not make sense, and the negative numbers was changed to zero. These zero values now represented the occasions when the losses were larger than the energy received from the electric heating source. These negative values may have arised because the heat losses in reality were less than 0.75 kW on some occasions. Another reason could be that there was a mismatch between the time of the energy yield and the loss. In any case, the effects of these simplifications are negligible.

After the losses were considered, a unit conversion had to be made. To ensure a correct value, the electrical energy was calculated from being given in kWh to kJ.

The temperature difference, ΔT , which was required for the heating of the water is defined in equation (15).

$$\Delta T = T_{tap} - T_{in} = 65 \text{ }^\circ\text{C} - T_{cold\ water\ profile} \quad (15),$$

where T_{tap} is the demanded temperature in the tap, set to 65 °C, and T_{in} is the cold inlet temperature, given by the profile in figure 18. ΔT vary on a monthly basis, reaching its peak in March.

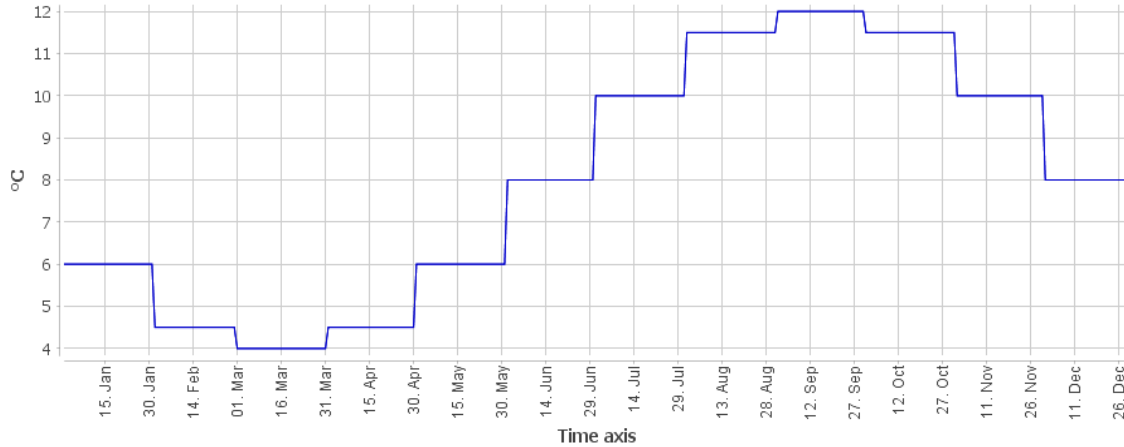


FIGURE 18: Cold water profile over a year, made in Polysun. The mean temperature was set to 8 °C with a range of 4 °C. The values are constant per month with the warmest water in September, due to inertia in the ground temperature. Source: Polysun.

Both the density and the heat capacity of water changes with temperature. Since the volume flow demand is defined in the tap at 65 °C, the table value of the density at this temperature was chosen: 980.55 kg/m³ (Engineering ToolBox, 2003d). The specific heat capacity was found by means of equation (16).

$$c = \frac{\Delta h_f}{\Delta T} = \frac{(272.03 - 20.98) \text{ kJ/kg}}{(65 - 5) \text{ K}} = 4.18 \text{ kJ/kgK} \quad (16),$$

where Δh_f is the change in enthalpy of saturated liquid water caused by a temperature increase of ΔT . The values are found in table B.1.1 in *Fundamentals of Thermodynamics* (Borgnakke & Sonntag, 2013).

The same procedure was applied to convert the normed inputs from SN/TS 3031 from energy (Wh/m²) to volume (l/h). The values were also multiplied by the area of the nursing home.

Polysun calculates values of energy use for DHW from the given volumes using its own conversion method. For this reason, the energy values given in the results may not correspond to the numbers given in the theory chapter.

3.2 THE SIMULATION PROGRAM – POLYSUN DESIGNER

The simulations for this thesis was done in a software called Polysun Designer by Vela Solaris. For this purpose, a student licence with a validity of six months was purchased. Polysun makes it possible to choose among a large number of ready-made templates or create a system from scratch. After simulating a chosen system, a great selection of evaluations are available, including various time steps and component details. (Vela Solaris, 2019)

3.2.1 FEATURES

The catalogs in Polysun comprise standardised versions of all the parts of a solar collector system, in addition to specific products from different manufacturers. These versions exist in a range of sizes and qualities. In the simulations done for this thesis only standardised versions have been used to ensure a high degree of generalisation.

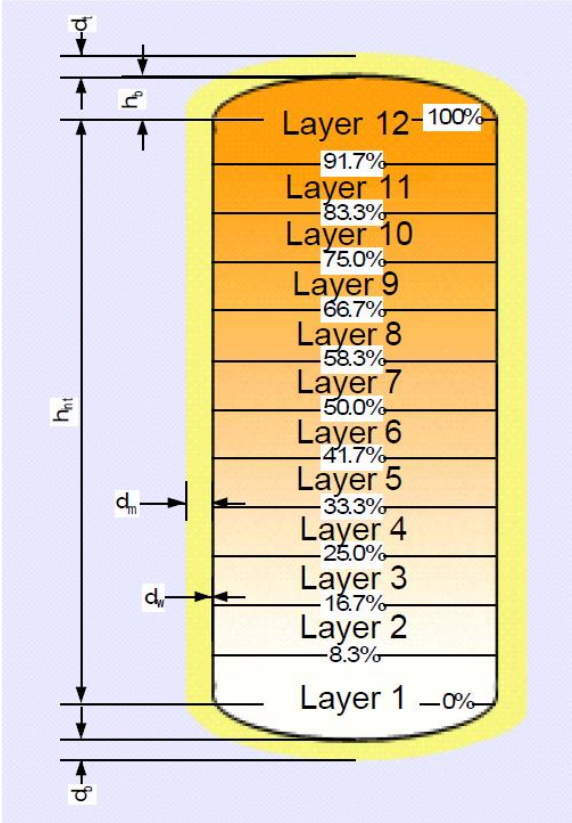


FIGURE 19: Illustration of the isothermal layers in the tanks in Polysun. Pipes and heating elements are positioned by means of percentage values, while temperature sensors are placed in layers. The lines and arrows refer to different heights and thicknesses. The figure is used with kind permission from Vela Solaris (2018).

The interior of the tanks in Polysun is subdivided into twelve isothermal layers, illustrated in figure 19. Due to density differences, the warmest water is on the top and the coldest is in the bottom. The layers are not subject to convective mixing. Components relating to the tank is positioned by means of percentage or layer and correspond to the positions in figure 19. There are ten pieces available for the connection of pipes and such.

3.2.2 SETTINGS IN POLYSUN

The position of the nursing home was chosen as the location in Polysun to ensure the best possible correlation between the weather conditions and the energy required to heat water. The exact location was found using a map, daylight saving time was applied and the site was described as ‘clear’. The elevation was chosen to be 98 m, with reference from a topographical map of Norway (Kartverket, n.d.). Standard outdoor temperature was set to 7 °C, based on the mean temperature in Oslo (Time and Date AS, 2019).

Several options were available for uploading weather data. The option called *Webservice* was chosen, comprising the newest information collected from Meteonorm’s web pages (Vela Solaris, 2018). The Meteonorm services use both ground-based weather stations and satellites to gather the relevant data (Meteotest, n.d.). No specific horizon for shading was defined, to keep the position as generalised as possible.

In order to be able to use the measured energy data as an input in Polysun, a new consumption profile had to be imported into the program. After finishing the conversion process, the resulting volume values was copied into an Excel template with the hours referred in seconds. This new file was selected as a consumption profile for the simulations of a solar collector construction in Polysun. The annual demand was set according to table 2, based on the collected data from the nursing home and the normed standard inputs. Applying SN/TS 3031, the consumption is about twice as large as with the measured data.

TABLE 2: The annual hot water demand set in Polysun for the two different consumption profiles.

	Annual demand
Drammen nursing home	729 m ³
SN/TS 3031	1465 m ³

To avoid the formation of Legionella, measures was done to keep the temperature at around 70 °C in the tank and 65 °C in the tap. The solution for this was to change some of the inputs in the auxiliary heating controller, the tap and the mixing valve controller. Table 3 lists the relevant temperature settings. The temperature shift in the mixing valve is set to account for heat losses in the pipes connecting it to the tap.

TABLE 3: The different temperatures set in the system to avoid Legionella formation. The cut-in/off tank temperature controls when the heating element is switched on/off. The “tap temperature” refers to the temperature in the tap on the row above.

	Temperature [°C]
Auxiliary heating controller:	
Cut-in tank temperature	67.5
Cut-off tank temperature	72.5
Tap	65
Mixing valve controller	Tap temperature + 5

The heat medium in the solar loop was chosen to be a solution of 40 % propylene glycol in water. This mixture is used by SGP Armatec. The solar liquid, TYFOCOR L, has a freezing point at -21.5 °C at a concentration of 40 % (TYFOROP Chemie GmbH, 2015). The corresponding boiling temperature is 146 °C.

To ensure security of supply of hot water, all controllers in the system is set to be available at all times. Polysun has a function which gives a warning if the energy demand is not met.

3.3 CHOSEN DHW SYSTEM

In order to achieve a certain degree of usefulness of the results, advices on system structure was inquired from SGP Armatec (2019). It was suggested to use flat plate solar collectors instead of the evacuated tube type, because of the costs. For the energy transfer between the solar liquid and the water, an external heat exchanger was recommended in favour of a spiral in the tank. This choice was contemplated by a spiral having a much smaller heat transfer area and the possibility of dimensioning the heat exchanger for a specific use. Additionally, they suggested to dimension the system based on the hot water demand during the warm season. This corresponds well with advices given by NSF.

Bearing these advices in mind, a ready-made template was chosen from the collection in Polysun. This template consists of a solar collector field, a heat exchanger, two pumps, one

accumulator tank (I), one electrically heated water tank (II), a mixing valve, inlet of cold water and the tap. Connecting these components are a number of pipes and controllers for the pumps, the auxiliary heating element and the mixing valve. Figure 20 shows the system design.

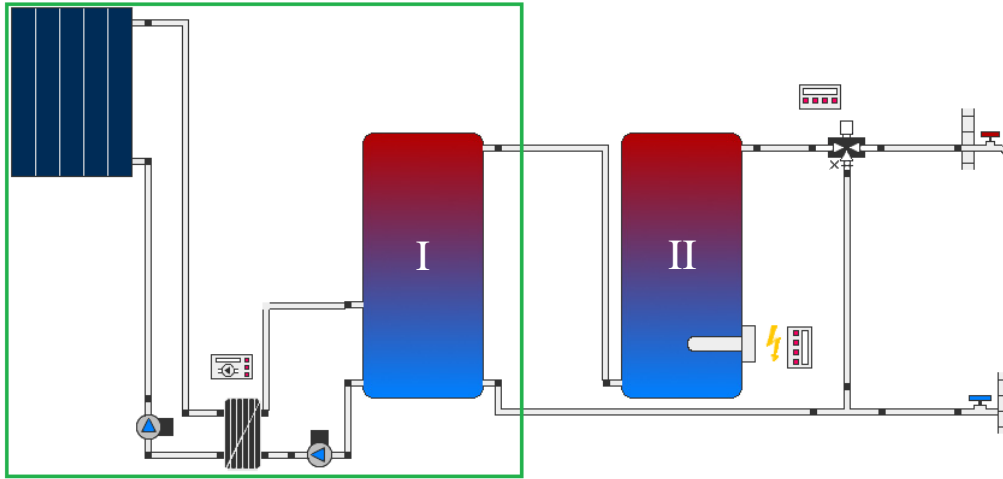


FIGURE 20: The chosen system diagram as it is shown in Polysun. The green square frames the solar thermal part of the system. The part which is not framed represents a system which is needed for the hot water distribution, independently of the solar thermal system. The figure is used with kind permission from Vela Solaris.

The focus in this thesis is not on the pipes and, for this reason, permanent values for their characteristics was set. The pipes are made of copper with an external diameter of 22 cm and a thickness of 1 cm. The insulation is made of 100 mm thick loose glass fibres and mineral wool to minimise heat losses. All the 13 pipes in the system was given a length of 1 m each, regardless of their position. They have a linear form factor of 1, assuming they are all straight (Vela Solaris, 2018). In addition, the friction factor is set to zero which means that all pressure losses are neglected.

Tank II in figure 20 represents an electrically heated water tank which is needed for the hot water distribution, independently of the solar thermal system. The volume of this tank was set to 1000 l and the heating element was given a power of 30 kW. The heating element was positioned at 10 % (layer 2) in the tank and the temperature sensors was placed in layer 3, corresponding to figure 19.

The two pumps are electrically powered with a flow rate setting of 27.5 l/h per m² solar collector area. This flow rate lies in the middle of the minimum and maximum value (15-40 l/h per m² solar collectors) for the pumps used in the largest solar stations supplied by SGP Armatec (SGP

Armatec AS, n.d.-b). When the temperature difference between the output of the solar collectors and the bottom layer in the accumulator tank exceeds 6 °C, the solar loop pump is switched on. It is switched off again when the temperature difference is 2 °C. The choice of heat exchanger was an external flat plate type with a transfer capacity of 10 000 W/K, defined in Polysun.

Remaining are the two variables for the simulations, namely the number of solar collectors and the accumulator tank volume. In all the simulations, flat plate collectors of “good quality” with an individual area of 2 m² oriented towards the south will be tested. They will all be assembled on one array. These collectors have similar characteristics to De Dietrich CH250, which was recommended by SGP Armatec (De Dietrich, 2017). Although the tanks will differ in volume, they will all be set to be 2 m high and made of 3 mm thick stainless steel. The insulation will consist of a 150 mm layer of rigid PU foam, based on the recommendations from Vela Solaris (2018).

Table 4 summarises the numerical values relating to the components.

TABLE 4: A summary of the numerical values relating to the components in the solar thermal system.

Pipes:	
External diameter	22 cm
Thickness	1 cm
Insulation	100 mm loose glass fibres
Total length	13 m
Water heater volume	1000 l
Heating element power	30 kW
Pump flow rate	27.5 l/h per solar collector area
Solar loop temperatures:	
On	6 °C
Off	2 °C
Heat exchanger transfer capacity	10 000 W/K
Solar collector area	2 m ²
Accumulator tank:	
Height	2 m
Thickness	3 mm
Insulation	150 mm rigid PU foam

3.4 ASSUMPTIONS AND LIMITATIONS

- There are no specified space limitations.
- The roof is assumed to be flat.
- A collector area of 100 m² will be an upper limit to confine the research extent.

- There will be no distinction between kWh_{th} and kWh_{el}.

3.5 ESTIMATION OF THE INVESTMENT COST

The accumulator tank prices attained from SGP Armatec are only for the volumes they offer, displayed in figure 21. A helping line is added to see the development.

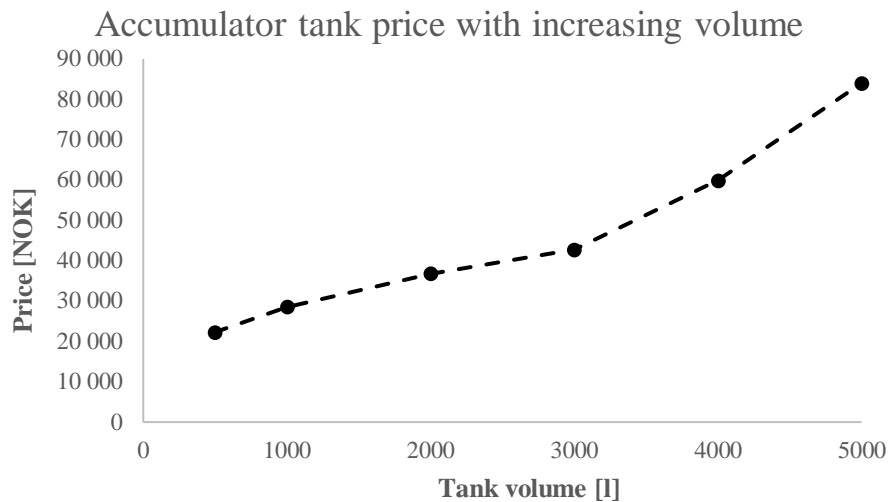


FIGURE 21: The accumulator tank price as a function of tank volume, based on the values in table 1.

To observe the possible development in tank prices with solar collector area, trend lines were estimated for three different dimensioning principles, as figure 22 shows. The accumulator tank dimensions of 50 l/m²_{sc}, 62.5 l/m²_{sc} and 75 l/m²_{sc} is based on the general rule of 50-75 l/m²_{sc} storage capacity (SINTEF Byggforsk, 2011). An exponential trend was found to be a suitable fit.

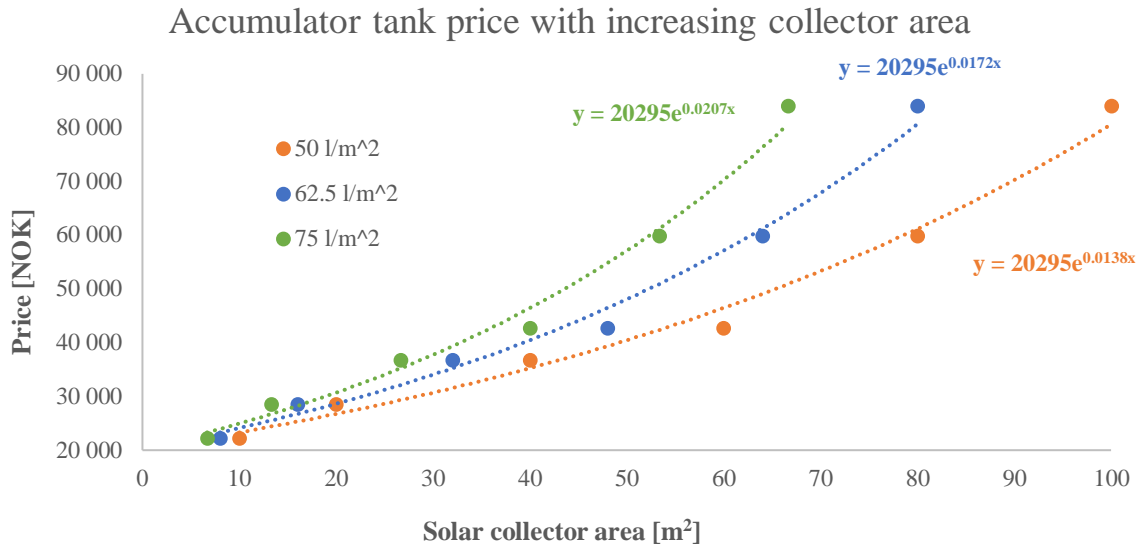


FIGURE 22: The accumulator tank price as a function of solar collector area. The tank is dimensioned by means of 50 l/m²_{sc}, 62.5 l/m²_{sc} and 75 l/m²_{sc}. The graph also includes trend lines of exponential form and their formulas.

This principle was used to calculate the total investment cost, including the material costs, the installation cost and the financial support from Enova. Graphs showing the development of the investment cost with increasing collector area is displayed in figure 23. The formulas of the trend lines in figure 22 were used to extrapolate the accumulator tank prices for a construction of up to 100 m².

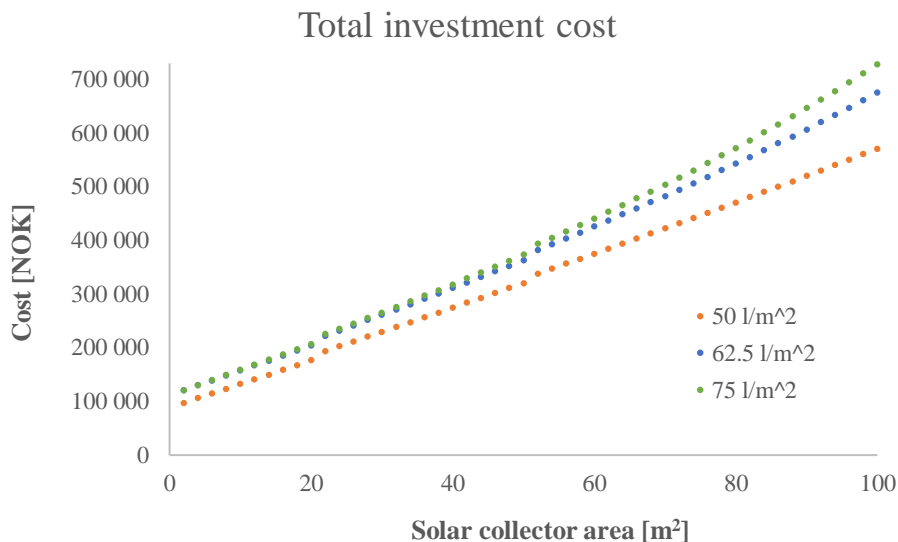


FIGURE 23: The change in the total investment cost with increasing collector area up to 100 m², based on data from table 1 and the trend lines of figures 12 and 22. The tank is dimensioned by means of 50 l/m²_{sc}, 62.5 l/m²_{sc} and 75 l/m²_{sc}.

Figure 24 shows the investment cost per solar collector area as a function of this area. The tank dimensioning 75 l/m^2_{sc} is used as an example; the other dimension principles gave a similar result. It is clear that the investment cost per area decreases rapidly up to a solar collector system size of around 16 m^2 . For larger areas, the reduction is much less, and the minimum is reached at 80 m^2 .

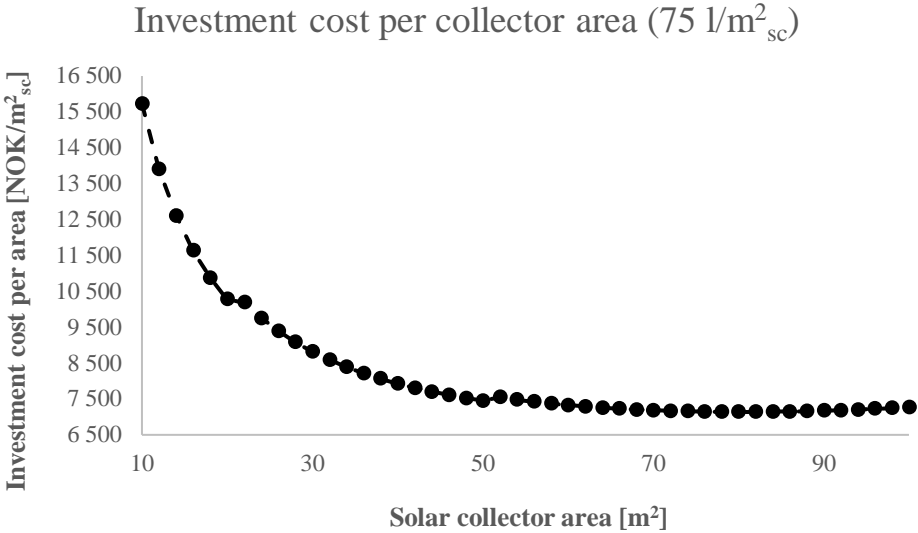


FIGURE 24: The development of the investment cost per collector area with increasing area from 10 m^2 to 100 m^2 , based on data from table 1 and the trend lines of figures 12 and 22. The tank is dimensioned by means of 75 l/m^2_{sc} .

3.6 FINDING THE BEST TILT ANGLE

Figure 8 showed that a solar collector with a slope of 45° received most irradiation over the year at the position of the nursing home, compared to 0° , 15° , 30° , 60° and 90° . However, the energy yield from the solar collectors also depends on the actual consumption and the total collector area.

To find the best tilt angle, a function in Polysun called *Log and parametrize* was used. The parametrize feature enables the user to simulate a range of chosen inputs and receive preferred outputs in the form of an Excel sheet. Two rounds of parametrization were done, enumerated below. In the simulations, the tank volume was set to $10\,000 \text{ l}$ to avoid possible limitations in storage capacity.

1. Estimating the best tilt angle between 0° and 90° for two different solar collector areas, based on the given DHW consumption.

Inputs:

'Tilt angle' from 0° to 90° , in steps of 10° .

'Number of collectors' at 20 and 40.

Output: 'Collector field yield relating to gross area'.

The reason for the choice of two collector areas was to get a notion of the change with different construction sizes. These simulations gave maximum two preferred tilt angles, one for each facility size.

2. Analysing a selection of tilt angles based on the results from round 1 for a range of solar collector areas, to observe the trend.

Inputs:

'Number of collectors' from 5 to 50 in steps of five.

A range of 'tilt angles' in steps of 5° . This range included the preferred collector slope(s) from round 1 in addition to one value below and one above.

Output: 'Collector field yield relating to gross area'.

The reason for choosing the extra tilt angles was to achieve a broader perspective and hopefully exclude any coincidences.

The outcomes of these tests were taken into account when choosing which tilt angle to use in the final simulations.

3.7 FINDING THE MOST PROFITABLE SOLUTION

The criterion for the most profitable combination of the solar thermal system was the lowest Levelised Cost of Energy (LCOE). This value express the cost of each produced unit of energy

over a time period equal to the lifetime of the facility (Sidelnikova et al., 2015). The LCOE may be compared to the electricity price to determine a construction's profitability.

The present value is found by using the standard NS 3454:2013. It is the value of a future cost related to a base year, depending on a given discharge rate. Equation (17) gives the means of calculation.

$$PV_T = \sum_{t=0}^T \frac{C_t}{(1+d)^t} \quad (17),$$

where T is the analysis period, PV_T is the present value of the costs over the analysis period, t is a given year, C_t is the cost in year t and d is the discharge rate (given in decimals). C_t includes investment, operating, maintenance and electricity costs.

NVE assumes a solar thermal construction lifetime of 25 years and a discount rate of 6 % (revised) in their cost analyses (Isachsen, 2017; Sidelnikova et al., 2015). These values will be used in the calculations of the economic parameters.

The LCOE is estimated as shown in equation (18) and is given in NOK/kWh (Sidelnikova et al., 2015):

$$LCOE = \frac{PV_{T, costs}}{PV_{T, produced energy}} \quad (18),$$

where PV_T is the present value as given in equation (17). In this case the electricity costs represent the costs of operating the pumps.

In Polysun, the 'electricity consumption of pumps' will be the parameter used to find the electricity costs for the LCOE. The 'solar thermal energy to the system' represents the produced energy.

To achieve the correct result, the LCOE was calculated for a range of solar collector areas from 10 m² to 100 m². This approach was done for tank volumes of 50 l/m²_{sc}, 62.5 l/m²_{sc} and 75 l/m²_{sc}, given by the general rule. For each collector area, the best tilt angle was selected, based on the parametrizations.

In addition to the above-mentioned economic considerations, for the system to be well-functioning it is crucial that the solar collector liquid does not start to boil. The most obvious disadvantage of boiling is the waste of energy. Another issue is that the glycol might get lumpy and cause damage to the components (SGP Armatec AS, 2019; Stickney, 2017). Boiling in the collectors is usually prevented by avoiding an overdimensioned solar collector area. The maximum collector temperature will be limited to 140 °C, based on the characteristics of TYFOCOR L and a pressure of 4 bar in the solar collector (TYFOROP Chemie GmbH, 2015).

The combination resulting in the lowest LCOE will be chosen as the best solution, given that the maximum collector temperature is below the limit. To ensure this, a final simulation of the chosen combination is done, checking this temperature.

3.8 PARAMETERS TO BE REPRESENTED

3.8.1 ECONOMIC

Besides the LCOE, the payback period and the annual cost will be analysed in the simulations.

3.8.1.1 *PAYBACK PERIOD*

The payback period is the amount of time it takes before the savings in electricity costs equals the costs put into the project. For a construction to be profitable this period must be shorter than its lifetime. It is defined as in equation (19) (G. & Donev, 2017).

$$\text{Payback period} = \frac{\text{Investment costs}}{\text{Annual savings}} = \frac{C_i}{\text{Cost of avoided yearly electricity use} - C_{om}} \quad (19),$$

where C_i and C_{om} is the investment, and operation and maintenance costs respectively.

In Polysun, the *costs of avoided electricity use* were found by first adding ‘total energy consumption’, ‘heat loss to indoor room’ and ‘heat loss to surroundings’. Then the ‘total electricity consumption’ was subtracted from this sum.

3.8.1.2 ANNUAL COST

The annual cost is found by using the standard NS 3454:2013. It is defined as the annuity of the present value over the analysis period. To calculate the annual cost, a parameter called the annuity factor, a , must be decided, calculated as in equation (20).

$$a = \frac{d}{1 - (1 + d)^{-T}} \quad (20),$$

where d is the discharge rate (given in decimals) and T is the analysis period.

The annual cost, AC , is estimated according to equation (21).

$$AC = PV_T \cdot a \quad (21),$$

where PV_T is the present value of the costs over the analysis period given in equation (17) and a is the annuity factor given in equation (20). In this case the electricity costs represent the use of both the heating element and the pump operation.

Table 5 lists the chosen factors for calculation of the economic parameters in this thesis.

TABLE 5: A summary of the chosen economic factors for calculation of the different parameters.

Analysis period (construction lifetime)	25 years
Discharge rate	6 %
Electricity price	70.9 øre/kWh

3.8.2 TECHNICAL

In addition to the maximum collector temperature, two other technical factors will be represented in the results. These are the solar fraction and the field yield per collector area. The (net) solar fraction is given by equation (22) (Vela Solaris, 2018).

$$SF_n = \frac{\text{Solar energy to the system}}{\text{Solar energy to the system} + \text{Auxilliary energy to the system}} \quad (22),$$

The solar fraction is the share of solar contribution of the total energy quantity delivered to the system, as can be derived from equation (22). The field yield per collector area describes the efficiency of the solar thermal facility and is defined by equation (23).

$$\text{Area specific field yield} = \frac{\text{Solar collector field yield}}{\text{Solar collector area}} \quad (23),$$

3.9 SIMULATIONS

3.9.1 NURSING HOME CONSUMPTION

The most profitable system based on the collected DHW energy consumption at the Drammen nursing home was determined. The procedure started with an examination of the best tilt angle for a range of construction sizes. When this was concluded, the LCOE was calculated to find the minimum. A number of figures illustrating some characteristics of the system were also included.

Additionally, larger and smaller accumulator tanks were compared to the most profitable one to observe possible effects on the parameters. Further, two simulations tested a larger system (twice the collector area) and a smaller system (half the collector area). The most profitable accumulator tank size was determined for the larger and smaller system. Finally, these systems sizes were compared to the most profitable one.

Sensitivity analyses with alterations of $\pm 30\%$ on the investment costs and the electricity price were performed on the most profitable system to observe possible changes.

3.9.2 LARGER DHW CONSUMPTION

Tests with larger DHW consumptions on the most profitable system were done, to get a notion of the development of the various parameters. The DHW volume flow of the nursing home was doubled, tripled etc. until the energy demand could no longer be met.

3.9.3 CONSUMPTION BASED ON SN/TS 3031

In addition to simulations with the measured DHW demand, the standard SN/TS 3031 was tested. Using the same methods as with the nursing home data, the goal was to find the system with the lowest LCOE for the standard based demand. The collected DHW consumption was put into the resulting system to observe how the parameters would be affected. This gave useful

information on how well SN/TS 3031 would work as a base for dimensioning of a solar thermal construction in cases where no real consumption information is available.

4 RESULTS

This chapter includes the results of the simulations described in the methods chapter. The outcomes are divided into three different DHW demand bases: the Drammen nursing home, double/triple consumption and the standard, SN/TS 3031.

4.1 RESULTS BASED ON THE NURSING HOME CONSUMPTION

4.1.1 FINDING THE BEST CONFIGURATION

Figure 25 graphically represents the area specific collector field yield for various tilt angles, resulting from round 1 of the parametrization. For a collector area of 40 m², the maximum value occurs at a 50° angle, while the maximum value for an area of 80 m² is 60°.

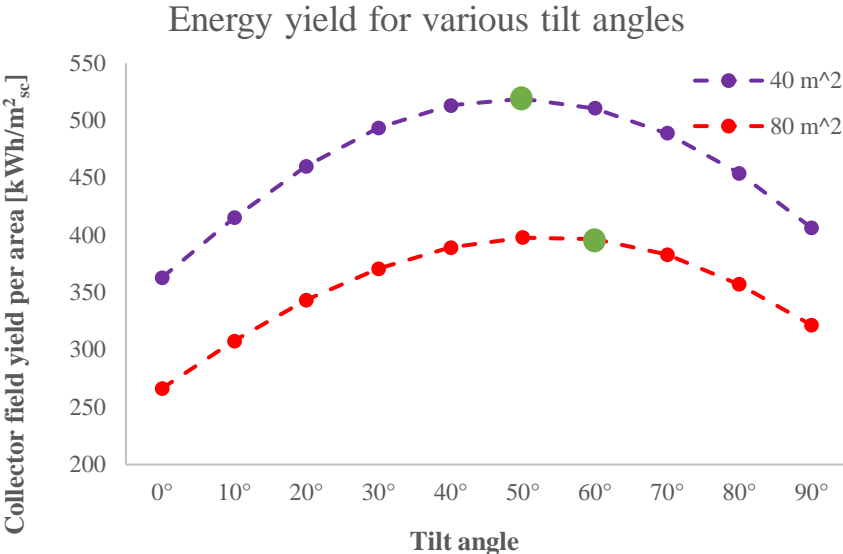


FIGURE 25: The collector field yield relating to gross area for collector areas of 40 m² and 80 m² at different tilt angles, based on the Drammen nursing home consumption. The maximums occur at 50° and 60° respectively and are marked with green dots.

In round 2 of the parametrization, the collector field yield per area was examined at tilt angles 45°, 50°, 55°, 60° and 65°. Comparing the energy yield at the five different tilt angles gave an overview of the best solutions in the range of collector areas. Table 6 gives a representation of the results.

TABLE 6: Collector field yield relating to gross area for a variation of collector areas and tilt angles, based on the Drammen nursing home consumption. For an area of 10-20 m² 45° have the highest value, for 30-70 m² the maximum is at 50° and for 80-100 m² 55° is preferred. 60 ° and 65° is not the best tilt angle for any of the collector areas in the range. The relevant values are marked in green.

Collector area [m ²]	Collector field yield per area [kWh/m ² _{sc}]				
	45°	50°	55°	60°	65°
10	654.97	653.51	647.86	638.00	624.13
20	608.17	607.87	603.43	595.09	582.79
30	560.65	561.19	557.96	550.75	539.99
40	517.92	518.97	516.52	510.71	501.55
50	481.06	482.55	480.84	475.86	467.89
60	449.93	451.88	450.78	446.22	438.87
70	421.57	424.05	424.01	420.49	413.81
80	394.64	397.82	398.64	396.58	391.49
90	370.08	373.79	374.95	373.69	369.79
100	347.28	351.35	353.19	352.78	349.89

In table 6, all the results for 10-100 m² collector areas are reproduced. The tilt angle being the best regarding energy yield varies with collector area, explained more detailed in the table text.

The graphs in figure 26 show the LCOE for different solar collector areas, calculated using equation (18). The minimum is 66.9 øre/kWh and occurs at a solar collector area of 40 m² with an accumulator tank volume of 2000 l.

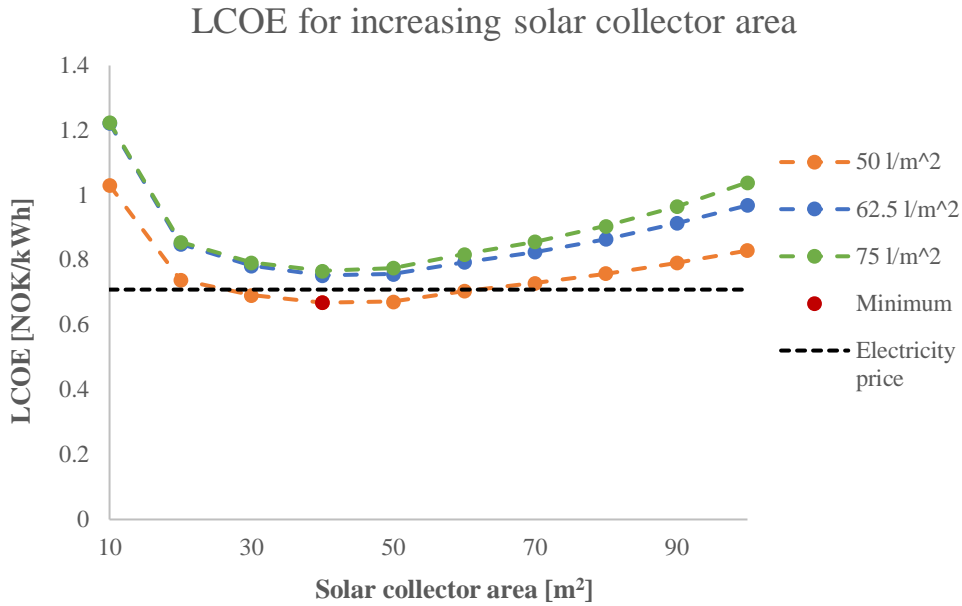


FIGURE 26: The LCOE at different solar collector areas from 10 m² to 100 m² based on the Drammen nursing home consumption. The minimum point occurring at 40 m² with a tank of 2000 l is marked with a red dot. The electricity price is also included.

The maximum collector temperature for the most profitable system was 90 °C, which is below the limit value for boiling.

4.1.2 THE MOST PROFITABLE SOLUTION

Based on these simulations, the following parameters ended up in the best combination:

- Solar collector area – 40 m²
- Accumulator tank volume – 2000 l
- Tilt angle – 50°

Table 7 comprises the economic parameters together with the values which are part of the calculations. The LCOE, payback period and annual cost are based on equations (18), (19) and (21) respectively. The LCOE is smaller than the electricity price and the payback period is shorter than the lifetime. Both of these coherences pledge that the system is profitable.

TABLE 7: The LCOE, payback period and annual cost for the most profitable system. The economic factors needed for the calculations are also included.

Most profitable system - economic	
Discharge rate	6 %
Construction lifetime	25 years
Electricity price	70.9 øre/kWh
Investment cost	273 660 NOK
Operating and maintenance costs	2737 NOK/year
Pump electricity cost	19 NOK/year
Total energy demand	56 289 kWh/year
Produced solar energy	20 491 kWh/year
Electricity use	35 798 kWh/year
LCOE	66.9 øre/kWh
Payback period	23.2 years
Annual cost	17 798 NOK/year

Table 8 comprises the technical parameters. All the numbers refer to a time frame of one year. The solar fraction is calculated using equation (22) and is just below the recommended range. The area specific field yield is calculated using equation (23) and is within the suggested interval.

TABLE 8: The solar fraction, collector field yield relating to gross area and maximum collector temperature over a year for the most profitable system.

Most profitable system - technical	
Solar fraction	37.6 %
Collector field yield per area	512 kWh/m ² _{sc}
Maximum collector temperature	89.9 °C

Figure 27 shows the monthly values of the solar fraction over one year.

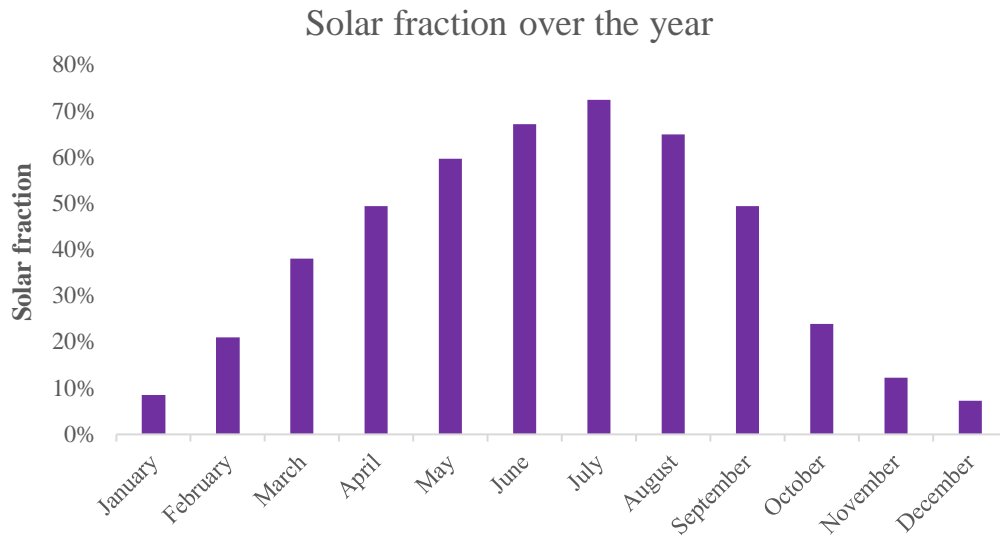


FIGURE 27: The solar fraction for each month of the year.

In figure 28, the division of energy contribution between the solar collectors and the heating element is represented.

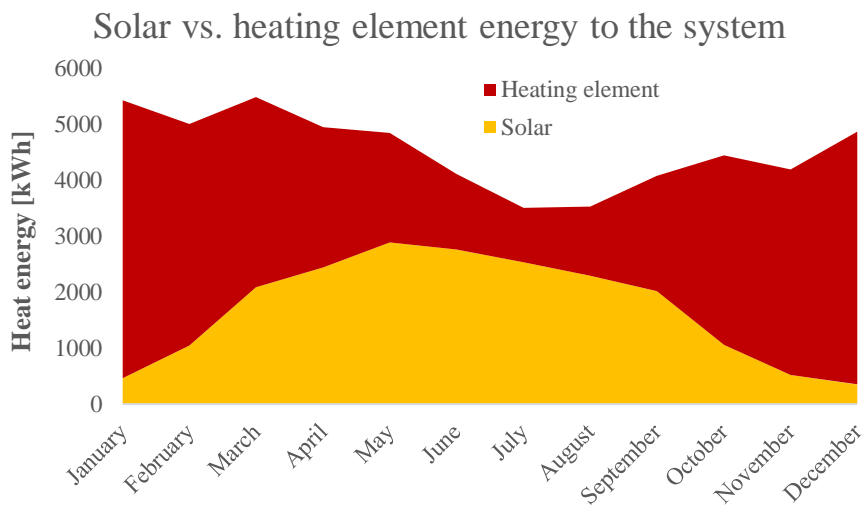


FIGURE 28: The heat energy delivered to the system, divided into the two energy sources – the solar thermal system and the electric heating element. The combined areas show the total amount.

Figures 29, 30, 31 and 32 show the collector field yield, DHW demand and water temperature from the accumulator tank in week 1 (January) of 2019 and week 26 (June/July) of 2018. The two weeks differ in all parameters. In January, the consumption peak is at around 24 kW (figure 29), while it is around 19 kW in June/July (figure 31). The demand does not vary much from

day to day in week 1, in contrast to the solar energy contribution. In week 26, the field yield is more stable and cover the majority of the energy for the DHW consumption. In January, the temperatures from the accumulator tank range from 4 °C to 18 °C (figure 30). In June/July, the corresponding temperatures are higher and has a larger span, with a minimum value of 33 °C and a maximum value of 82 °C (figure 32).

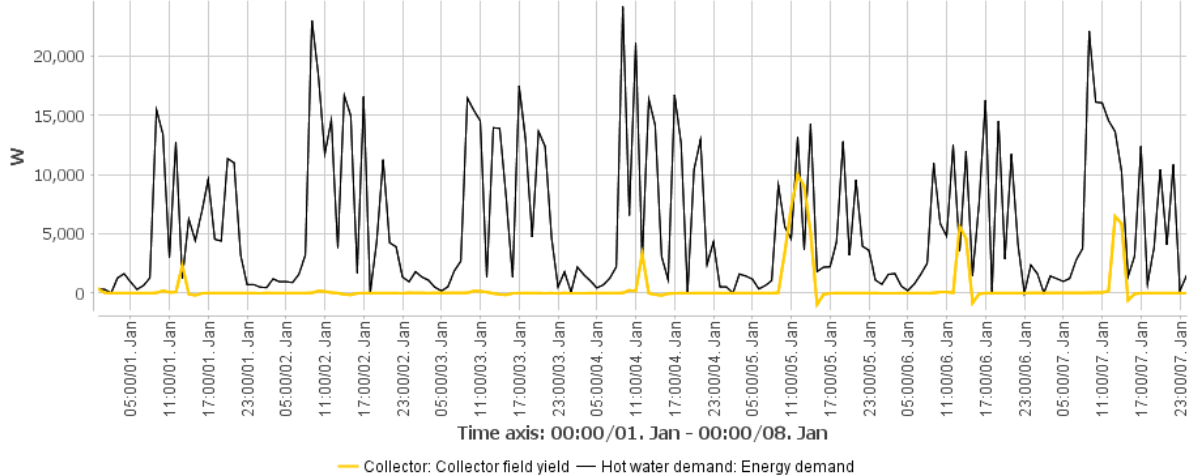


FIGURE 29: The collector field yield together with the hot water demand in week 1 of 2019. Source: Polysun.

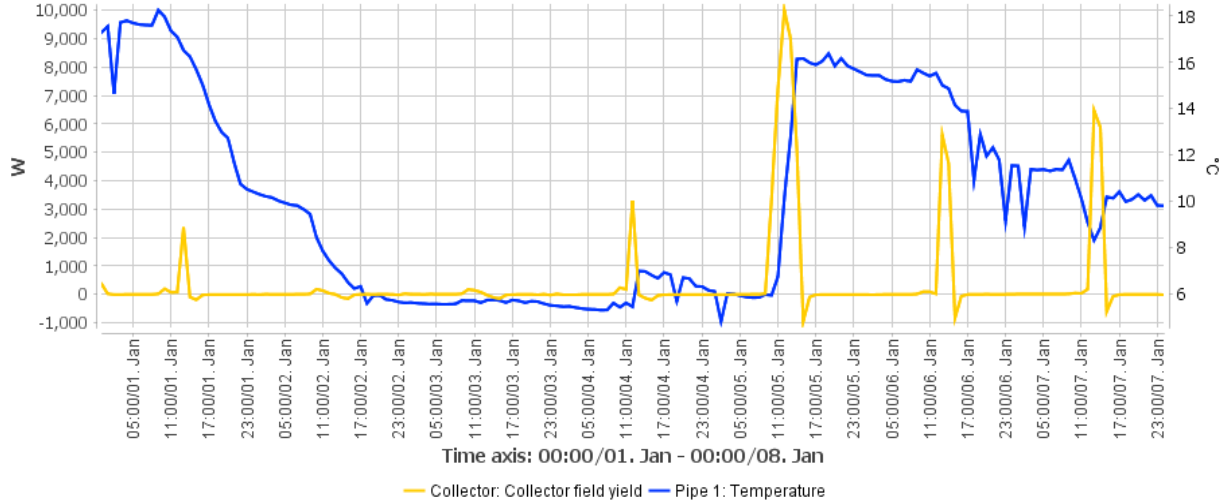


FIGURE 30: The collector field yield together with the water temperature out of the accumulator tank (pipe 1) in week 1 of 2019. Source: Polysun.

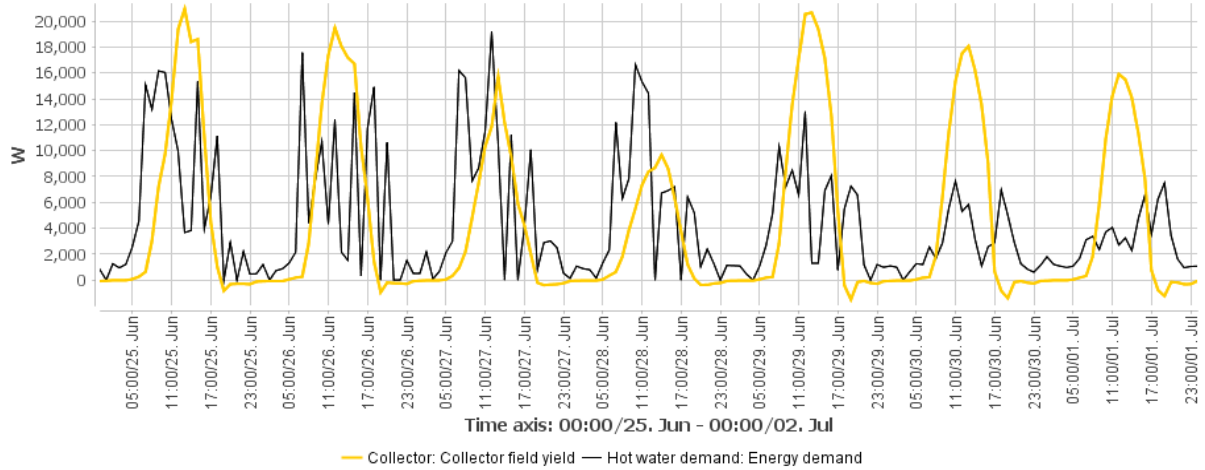


FIGURE 31: The collector field yield together with the hot water demand in week 26 of 2018. Source: Polysun.

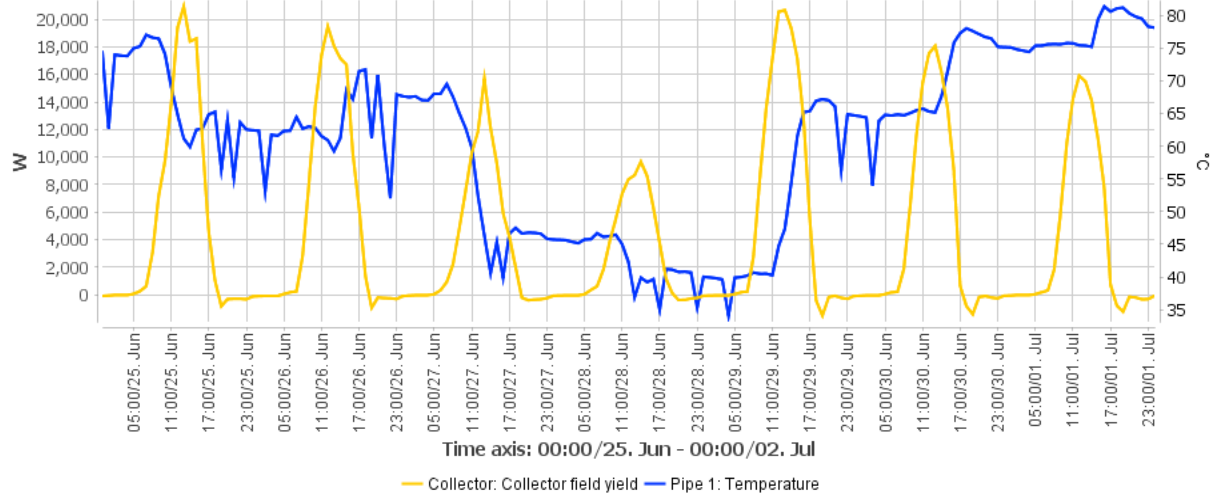


FIGURE 32: The collector field yield together with the water temperature out of the accumulator tank (pipe 1) in week 26 of 2018. Source: Polysun.

The energy flow diagram of the most profitable system is displayed in figure 33. The solar factor of almost 40 % can be observed.

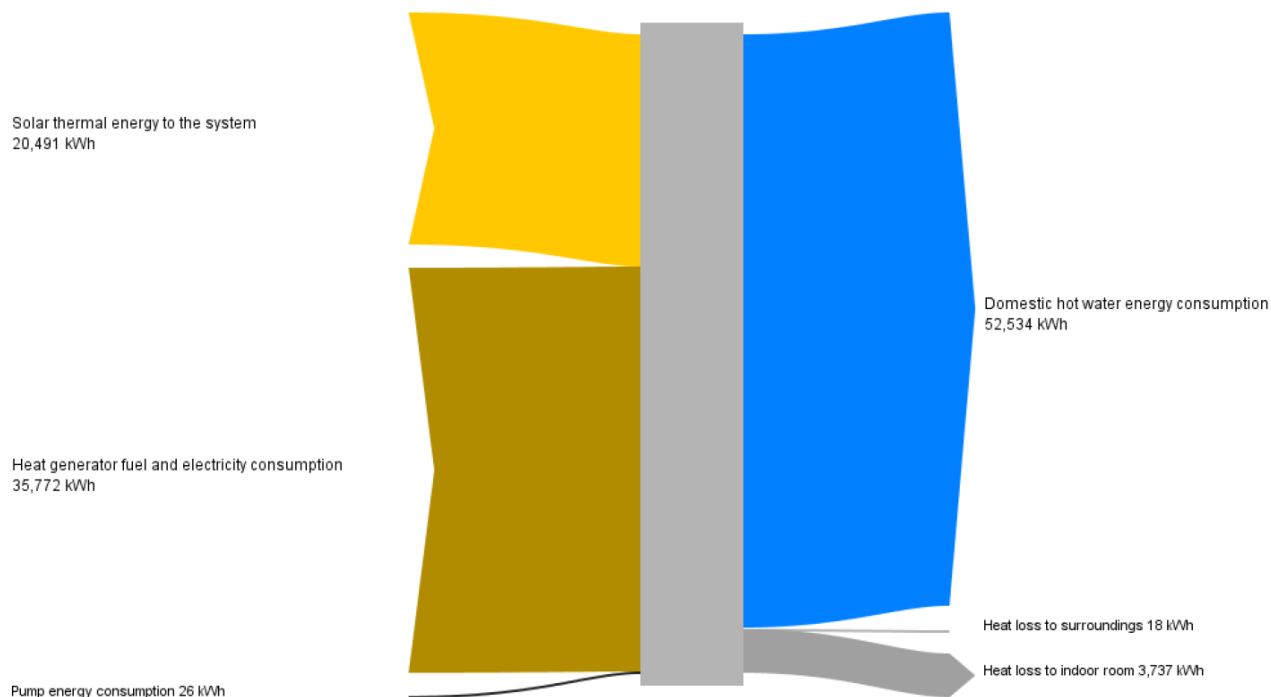


FIGURE 33: The energy flow diagram of the most profitable system. The electricity consumption is divided into the part used by the heating element and the fraction which goes to the pump. Heat loss is separated between (outdoor) surroundings and indoor room.

4.1.3 LARGER AND SMALLER ACCUMULATOR TANK

The changes in the economic parameters when the accumulator tank volume is altered by maximum 50 % are displayed in figures 34, 35 and 36.

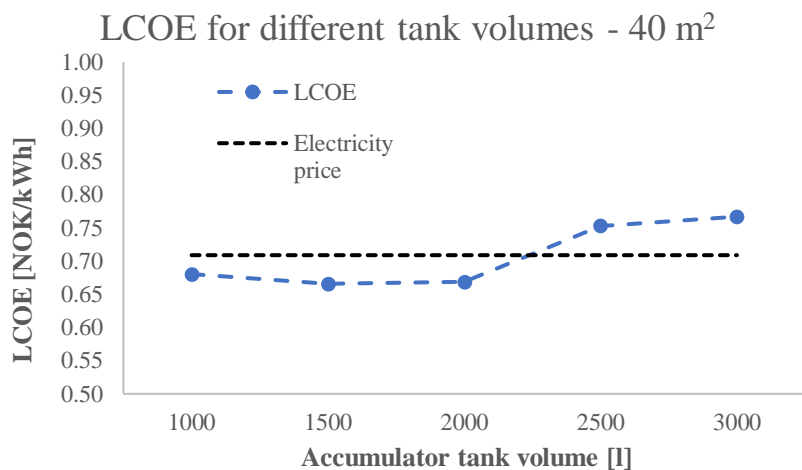


FIGURE 34: The LCOE at accumulator tank volumes of 1000 l, 1500 l, 2000 l, 2500 l and 3000 l.

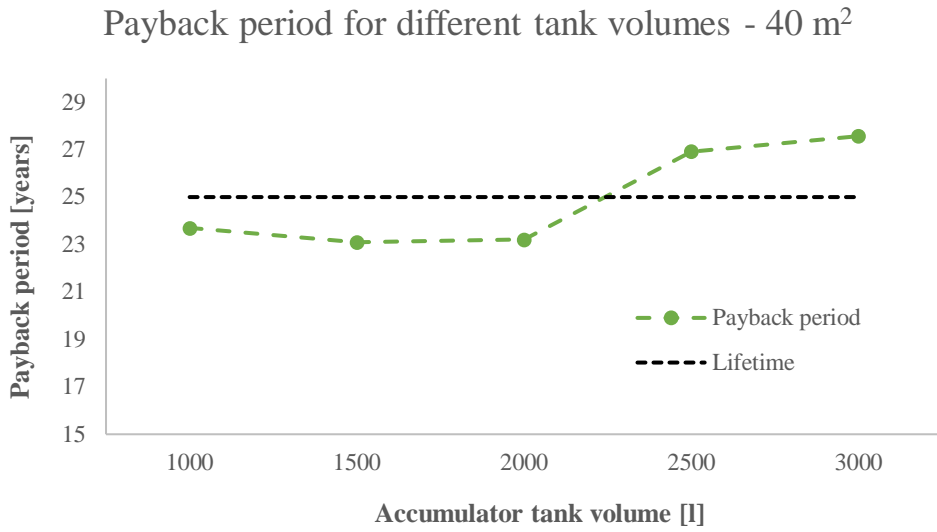


FIGURE 35: The payback period at accumulator tank volumes of 1000 l, 1500 l, 2000 l, 2500 l and 3000 l.

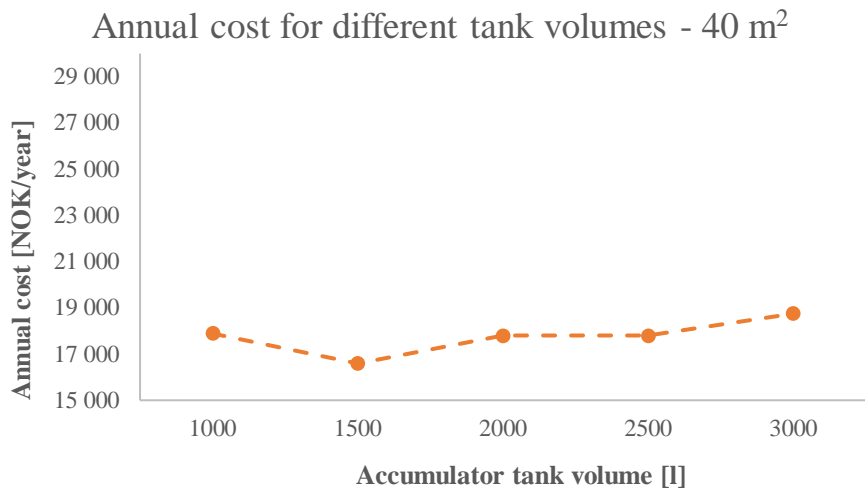


FIGURE 36: The annual cost at accumulator tank volumes of 1000 l, 1500 l, 2000 l, 2500 l and 3000 l.

All the economic parameters have minimum values for a tank volume of 1500 l. The maximum values occur for a 3000-l tank, where the value of LCOE is 76.7 øre/kWh and the payback period is 27.6 years. 3000-l and 2500-l tanks are not profitable for this system size. The annual cost is subject to very small changes.

Figures 37, 38 and 39 show the changes in the technical characteristics with different accumulator tank volumes.

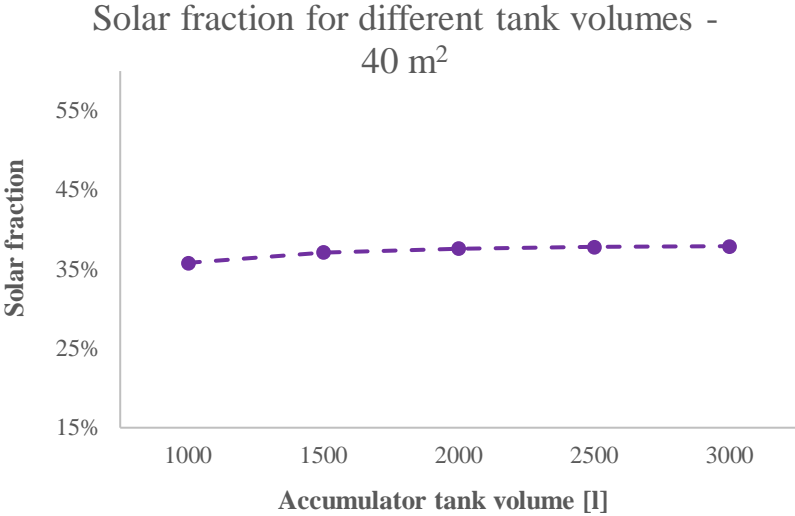


FIGURE 37: The solar fraction at accumulator tank volumes of 1000 l, 1500 l, 2000 l, 2500 l and 3000 l.

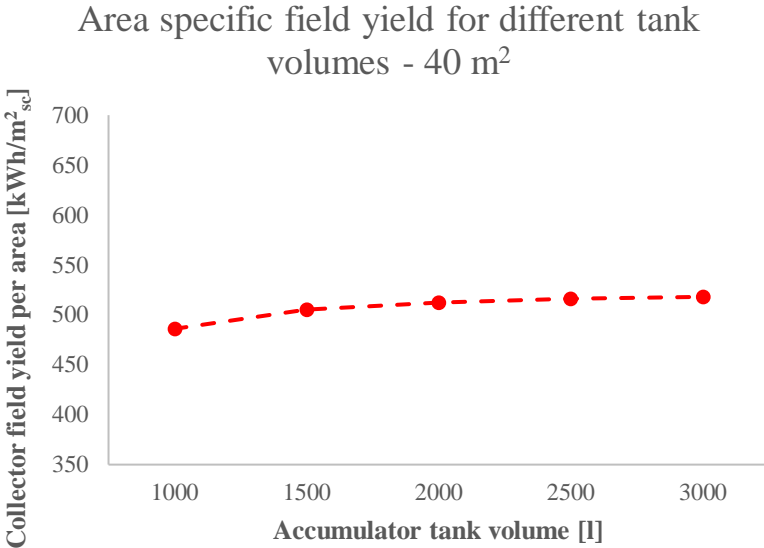


FIGURE 38: The collector field yield relating to gross area at accumulator tank volumes of 1000 l, 1500 l, 2000 l, 2500 l and 3000 l.

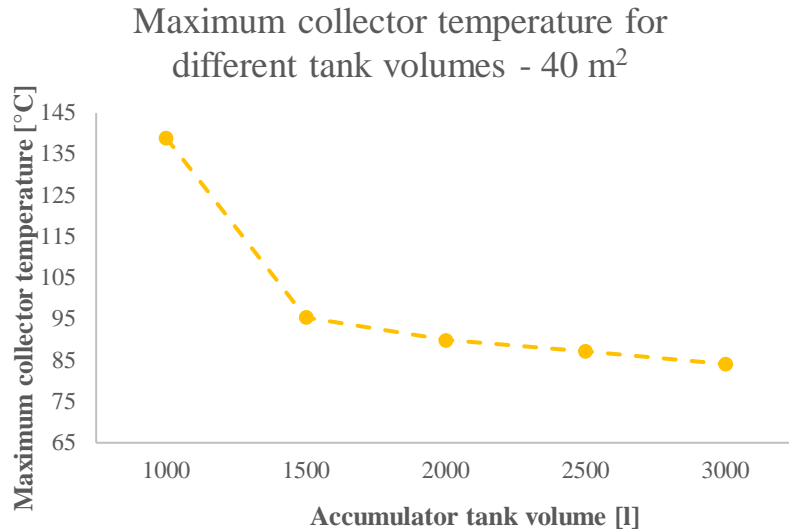


FIGURE 39: The maximum collector temperature at accumulator tank volumes of 1000 l, 1500 l, 2000 l, 2500 l and 3000 l.

Both the solar fraction and area specific field yield increase with larger accumulator tanks, but the changes are very small. The maximum collector temperature decreases with increasing tank volume. A 1000-l tank gives a maximum collector temperature of 139 °C, which is almost at the chosen boiling limit. The biggest drop in this temperature of 31 % happen with a change from 1000 l to 1500 l.

4.1.4 LARGE SYSTEM

Figure 40 displays the LCOE of a system with a collector area of 80 m² for different accumulator tank volumes. The tank volumes are based on the dimensioning options 50 l/m²_{sc}, 62.5 l/m²_{sc} and 75 l/m²_{sc}.

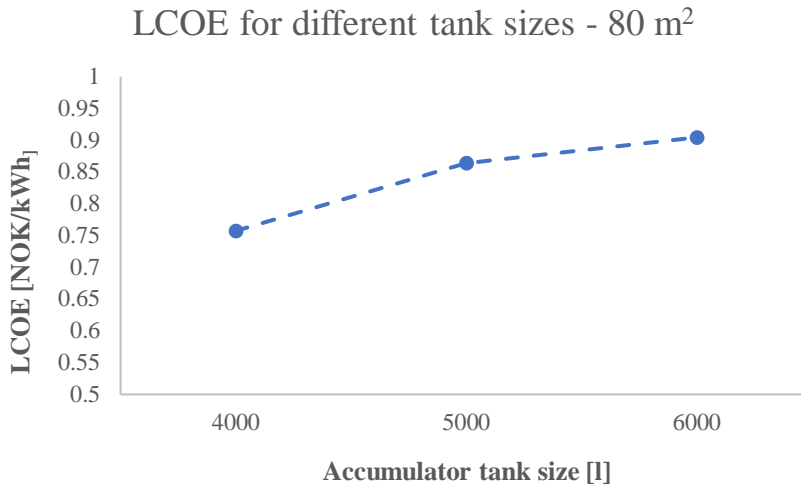


FIGURE 40: The LCOE for a system of 80 m² with tank volumes of 4000 l (50 l/m²_{sc}), 5000 l (62.5 l/m²_{sc}) and 6000 l (75 l/m²_{sc}).

Out of the three tank volumes, the smallest one has the lowest LCOE and hence, the following combination was chosen for simulation of the large system:

- Solar collector area – 80 m²
- Accumulator tank volume – 4000 l
- Tilt angle – 55°

Table 9 comprises the economic parameters together with the values which are part of the calculations. The LCOE, payback period and annual cost are based on equations (18), (19) and (21) respectively. The LCOE is larger than the electricity price and the payback period is longer than the lifetime. Both of these coherences pledge that the system is not profitable.

TABLE 9: The LCOE, payback period and annual cost for the large system. The economic factors needed for the calculations are also included.

Large system - economic	
Discharge rate	6 %
Construction lifetime	25 years
Electricity price	70.9 øre/kWh
Investment cost	469 617 NOK
Operating and maintenance costs	4696 NOK/year
Pump electricity cost	15 NOK/year
Total energy demand	56 530 kWh/year
Produced solar energy	31 023 kWh/year
Electricity use	25 507 kWh/year
LCOE	75.7 øre/kWh
Payback period	27.2 years
Annual cost	18 939 NOK/year

Table 10 comprises the technical parameters. All the numbers refer to a time frame of one year. The solar fraction and area specific field yield are calculated using equations (22) and (23), respectively. Both the solar fraction and the area specific field yield is within the recommended range.

TABLE 10: The solar fraction, collector field yield relating to gross area and maximum collector temperature over a year for the large system.

Large system - technical	
Solar fraction	56.2 %
Collector field yield per area	388 kWh/m ² _{sc}
Maximum collector temperature	130 °C

4.1.5 SMALL SYSTEM

Figure 41 displays the LCOE of a system with a collector area of 20 m² for different accumulator tank volumes. The tank volumes are based on the dimensioning options 50 l/m²_{sc}, 62.5 l/m²_{sc} and 75 l/m²_{sc}.

LCOE for different tank volumes - 20 m²

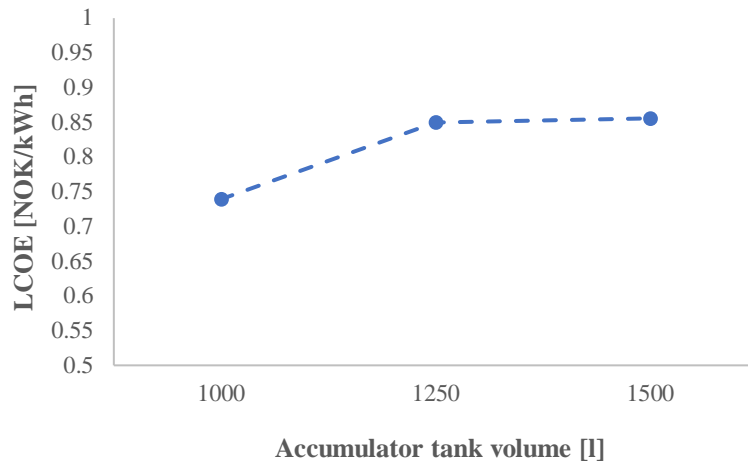


FIGURE 41: The LCOE for a system of 20 m² with tank volumes of 1000 l (50 l/m²_{sc}), 1250 l (62.5 l/m²_{sc}) and 1500 l (75 l/m²_{sc}).

Out of the three tank volumes, the smallest one has the lowest LCOE and hence, the following combination was chosen for simulation of the large system:

- Solar collector area – 20 m²
- Accumulator tank volume – 1000 l
- Tilt angle – 45°

Table 11 comprises the economic parameters together with the values which are part of the calculations. The LCOE, payback period and annual cost is based on equations (18), (19) and (21) respectively. The LCOE is larger than the electricity price and the payback period is longer than the lifetime. Both of these coherences pledge that the system is not profitable.

TABLE 11: The LCOE, payback period and annual cost for the small system. The economic factors needed for the calculations are also included.

Small system - economic	
Discharge rate	6 %
Construction lifetime	25 years
Electricity price	70.9 øre/kWh
Investment costs	175 377 NOK
Operating and maintenance costs	1754 NOK/year
Pump electricity cost	21 NOK/year
Total energy demand	56 323 kWh/year
Produced solar energy	11 890 kWh/year
Electricity use	44 433 kWh/year
LCOE	73.9 øre/kWh
Payback period	26.3 years
Annual cost	18 349 NOK/year

Table 12 comprises the technical parameters. All the numbers refer to a time frame of one year. The solar fraction is calculated using equation (22) and is below the recommended range. The area specific field yield is calculated using equation (23) and is within the suggested interval, near the maximum limit.

TABLE 12: The solar fraction, collector field yield relating to gross area and maximum collector temperature over a year for the small system.

Small system - technical	
Solar fraction	22.0 %
Collector field yield per area	594 kWh/m ² _{sc}
Maximum collector temperature	75.9 °C

4.1.6 COMPARISON BETWEEN SYSTEM SIZES

The differences in the economic parameters for the most profitable, the large and the small system are displayed in figures 42, 43 and 44.

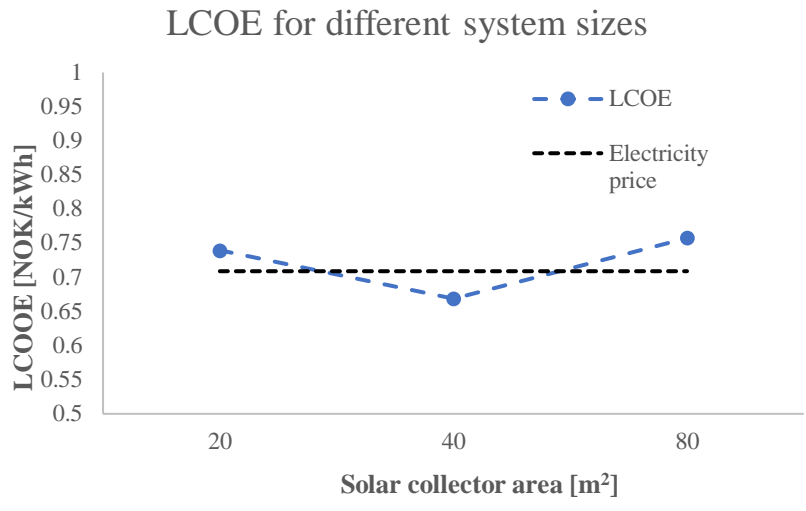


FIGURE 42: The LCOE for system sizes of 20 m², 40 m² and 80 m².

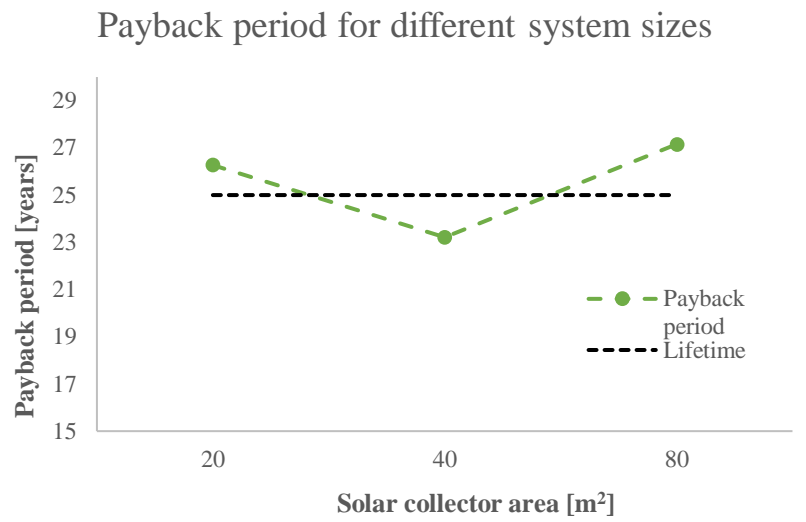


FIGURE 43: The payback period for system sizes of 20 m², 40 m² and 80 m².

Annual cost for different system sizes

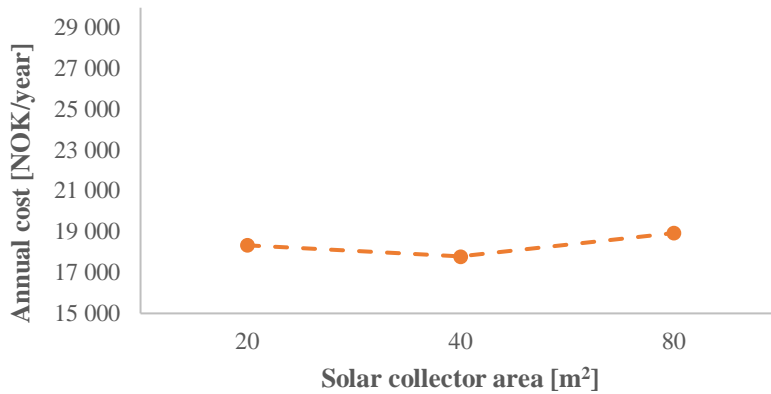


FIGURE 44: The annual cost for system sizes of 20 m², 40 m² and 80 m².

All three parameters have minimum values at the most profitable solution, with a collector area of 40 m². The corresponding maximum values occur for the largest system, but the values for the smallest system are only 2-3 % lower. Merely the 40-m² system is considered profitable. The annual cost is approximately constant.

Figures 45, 46 and 47 show the changes in the technical characteristics for different system sizes.

Solar fraction for different system sizes

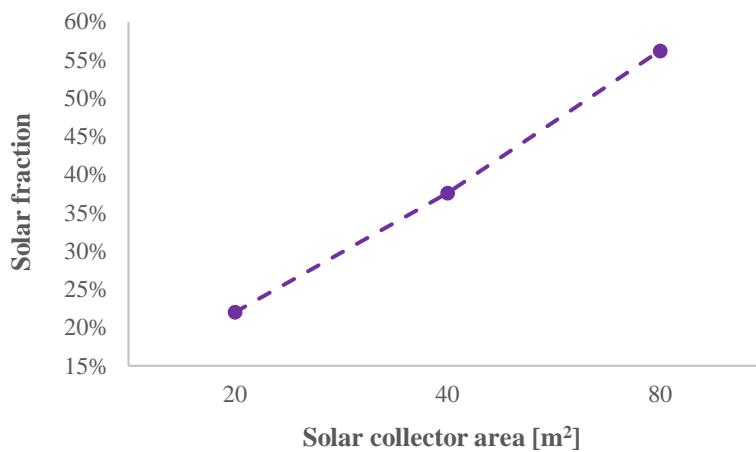


FIGURE 45: The solar fraction for system sizes of 20 m², 40 m² and 80 m².

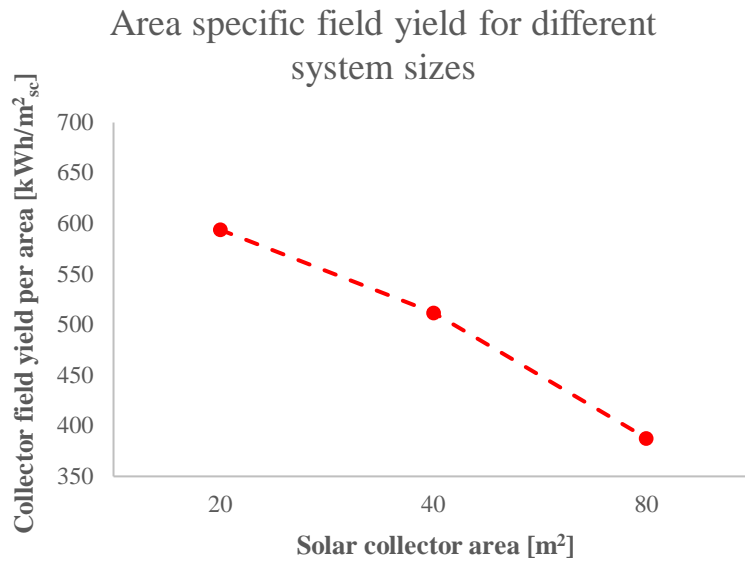


FIGURE 46: The collector field yield relating to gross area for system sizes of 20 m², 40 m² and 80 m².

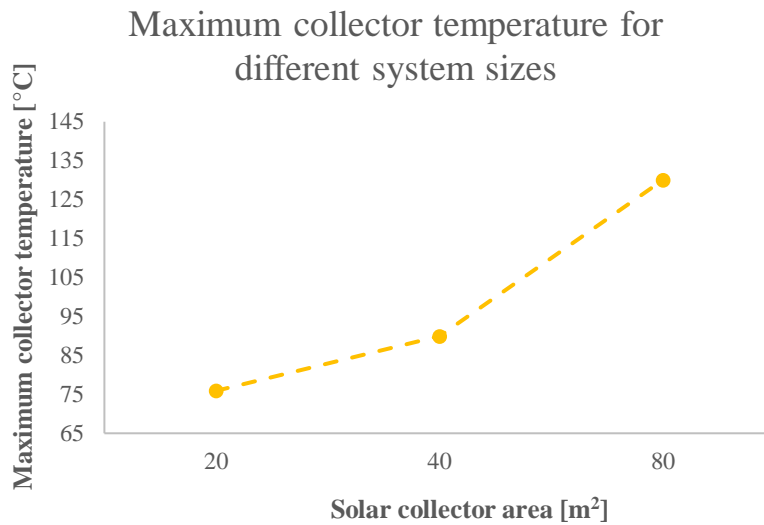


FIGURE 47: The maximum collector temperature for system sizes of 20 m², 40 m² and 80 m².

Both the solar fraction and maximum collector temperature increase with larger system sizes. Regarding the maximum collector temperature, the biggest growth occurs from 40 m² to 80 m². The area specific field yield decreases with increasing system size.

4.1.7 SENSITIVITY ANALYSES

4.1.7.1 INVESTMENT COST

The changes in the economic parameters when the investment cost was altered by $\pm 30\%$ are displayed in figures 48, 49 and 50.

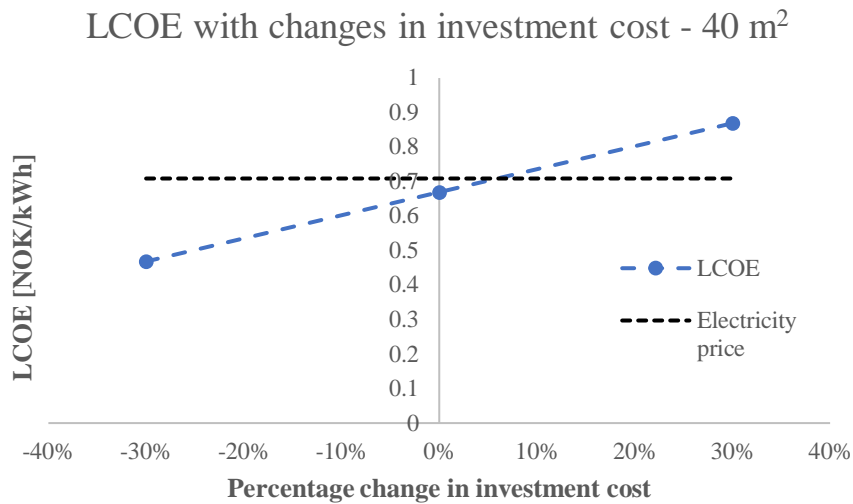


FIGURE 48: The LCOE with changes in the investment cost of $\pm 30\%$. The electricity price remains constant and is included in the graph.

A 30% change in the investment cost results in a 30% change in the LCOE. The LCOE decreases with smaller investment costs and is only above the electricity price for the highest cost.

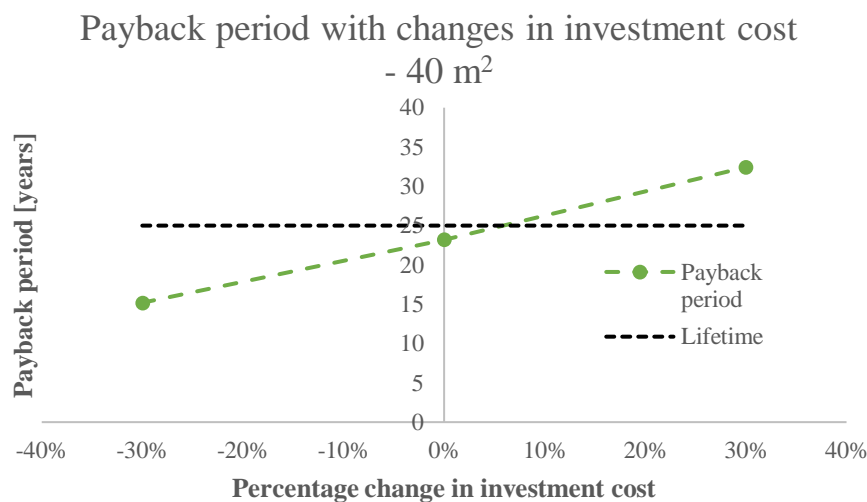


FIGURE 49: The payback period with changes in the investment cost of $\pm 30\%$. The lifetime is included in the graph.

The payback period is altered with around 37 % following changes in the investment cost of ± 30 %. It is longer than the construction lifetime only for the highest cost.

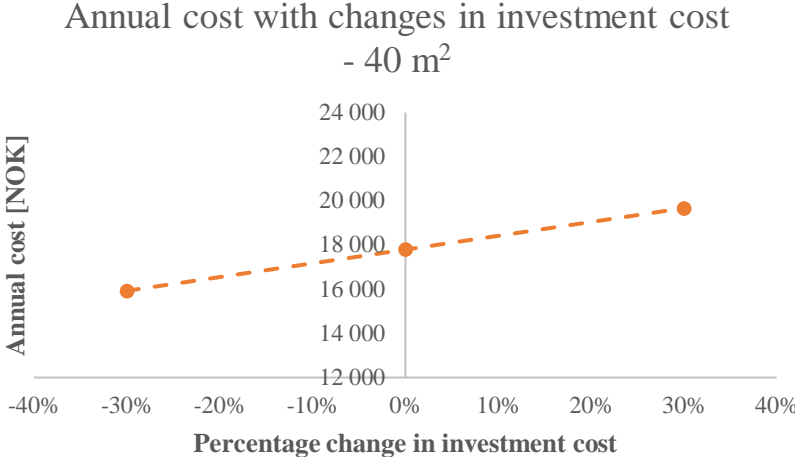


FIGURE 50: The annual cost with changes in the investment cost of ± 30 %.

The annual cost changes with almost ± 11 % for alterations in the investment cost, in a proportional manner.

4.1.7.2 ELECTRICITY PRICE

The changes in the economic parameters when the electricity price is altered by ± 30 % are displayed in figures 51, 52 and 53.

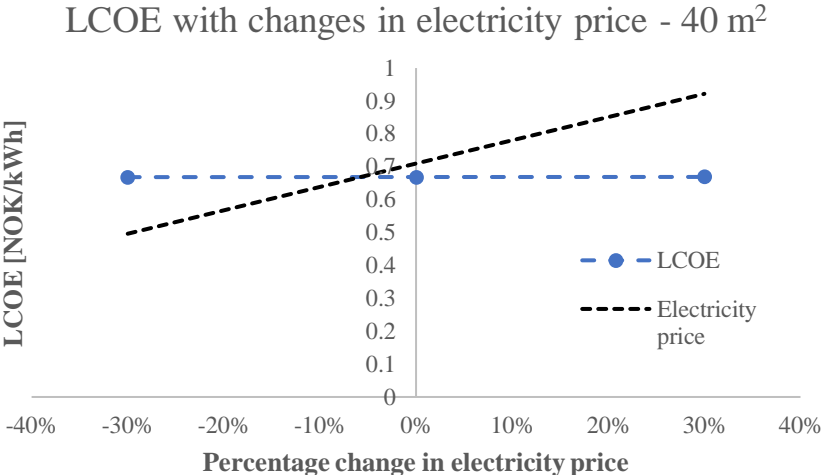


FIGURE 51: The LCOE with changes in the electricity price of ± 30 %. The electricity price is included in the graph.

A 30 % change in the electricity price results in nearly no changes in the LCOE. The LCOE is only above the electricity price for the lowest price.

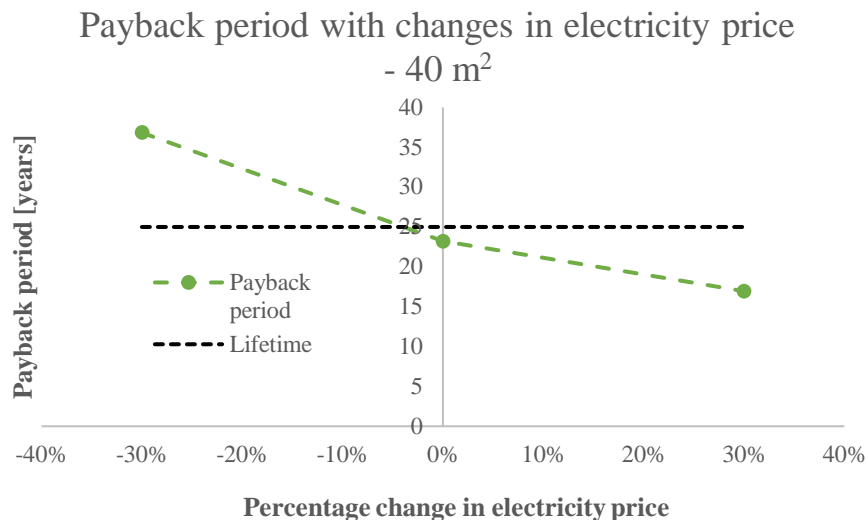


FIGURE 52: The payback period with changes in the electricity price of ± 30 %. The lifetime is included in the graph.

The payback period increases with 59 % and decreases with 27 % following changes in the electricity price of ± 30 %, compared to the original cost. It is longer than the construction lifetime only for the lowest price.

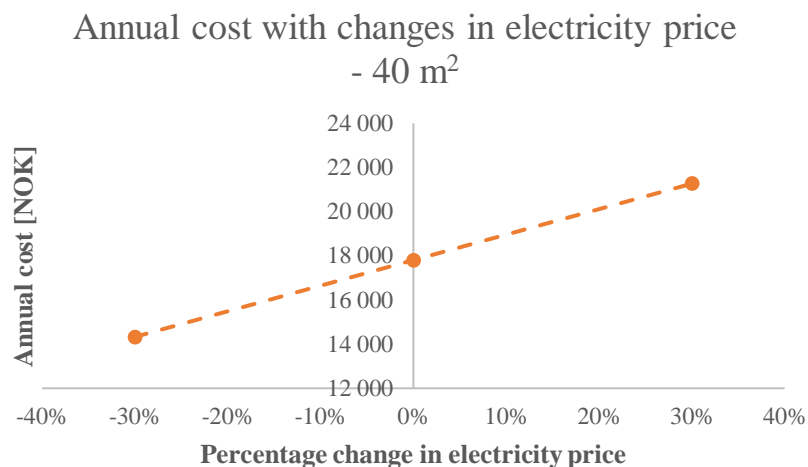


FIGURE 53: The annual cost with changes in the electricity price of ± 30 %.

The annual cost changes with $\pm 19\%$ for alterations in the electricity price, in a proportional manner.

4.2 LARGER CONSUMPTION

Figures 54, 55 and 56 show the changes in the economic parameters for DHW consumptions two and three times as large as the nursing home DHW demand. Simulations with the quadrupled amount gave a warning that the energy demand was not met.

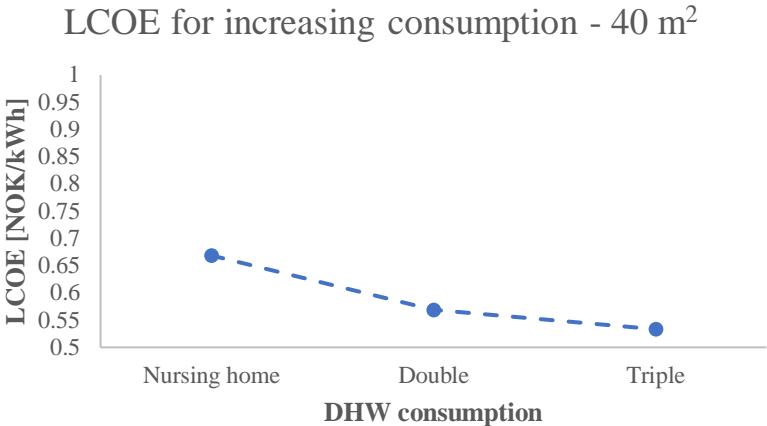


FIGURE 54: The LCOE for increasing DHW consumption equivalent to the double and triple of the nursing home demand.

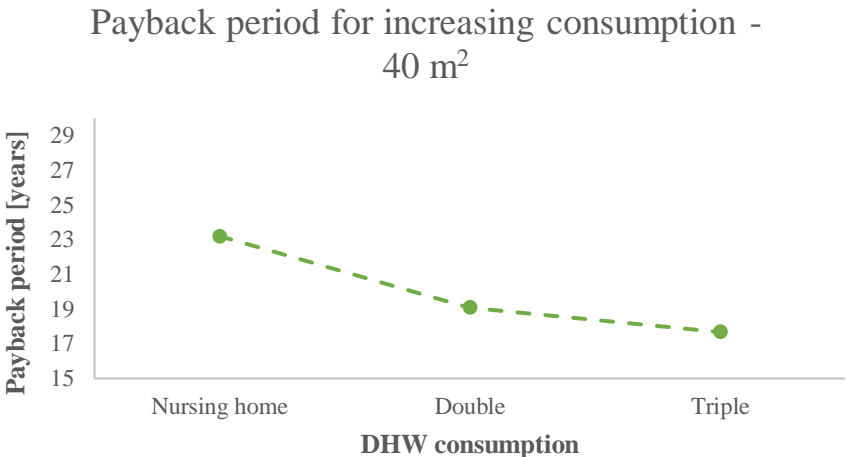


FIGURE 55: The payback period for increasing DHW consumption equivalent to the double and triple of the nursing home demand.

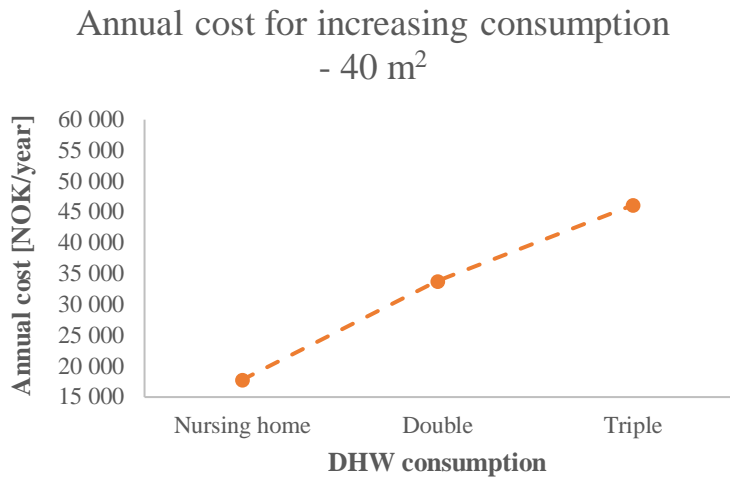


FIGURE 56: The annual cost for increasing DHW consumption equivalent to the double and triple of the nursing home demand.

Both the LCOE and the payback period decrease with larger consumption and all the consumptions give profitable results. The annual cost increases with growing DHW demand, mostly for a doubling with 90 %.

The alterations in the technical parameters with higher consumptions are represented in figures 57, 58 and 59.

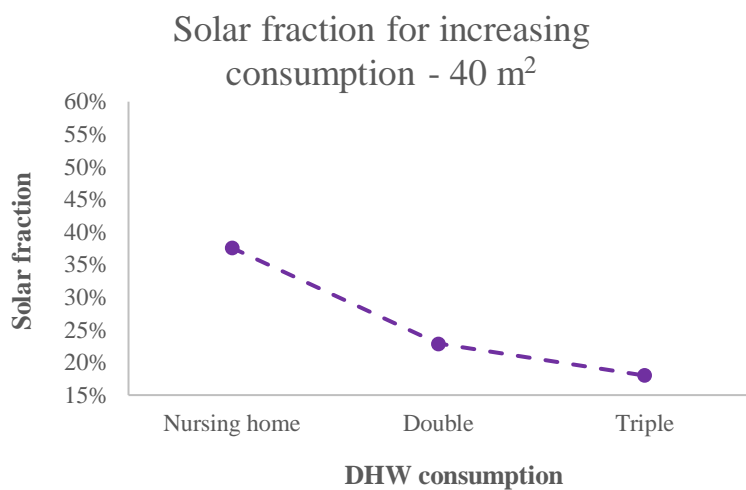


FIGURE 57: The solar fraction for increasing DHW consumption equivalent to the double and triple of the nursing home demand.

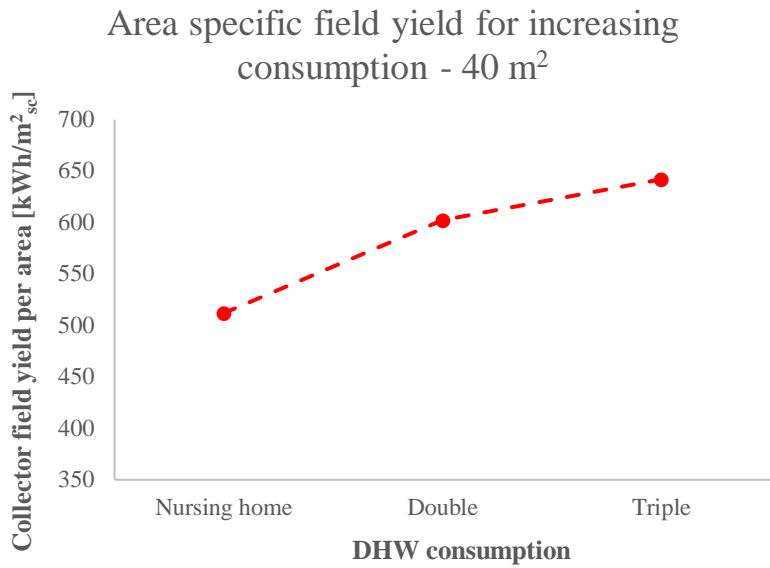


FIGURE 58: The collector field yield relating to gross area for increasing DHW consumption equivalent to the double and triple of the nursing home demand.

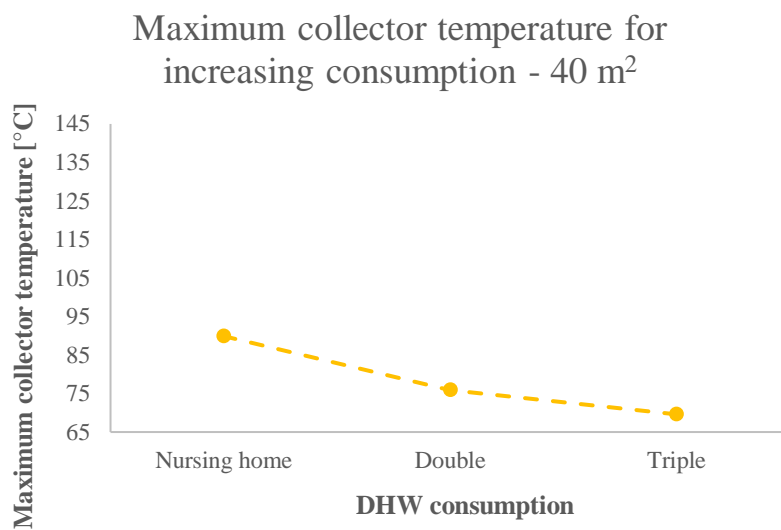


FIGURE 59: The maximum collector area for increasing DHW consumption equivalent to the double and triple of the nursing home demand.

Both the solar fraction and the maximum collector temperature decrease with growing DHW demand, while the area specific field yield increases. The changes are largest for the solar fraction.

4.3 RESULTS BASED ON NORMED INPUTS FROM SN/TS 3031

4.3.1 FINDING THE BEST CONFIGURATION

Figure 60 graphically represents the area specific collector field yield for various tilt angles, resulting from round 1 of the parametrization. The maximum occurs at a 50° angle for both collector areas.

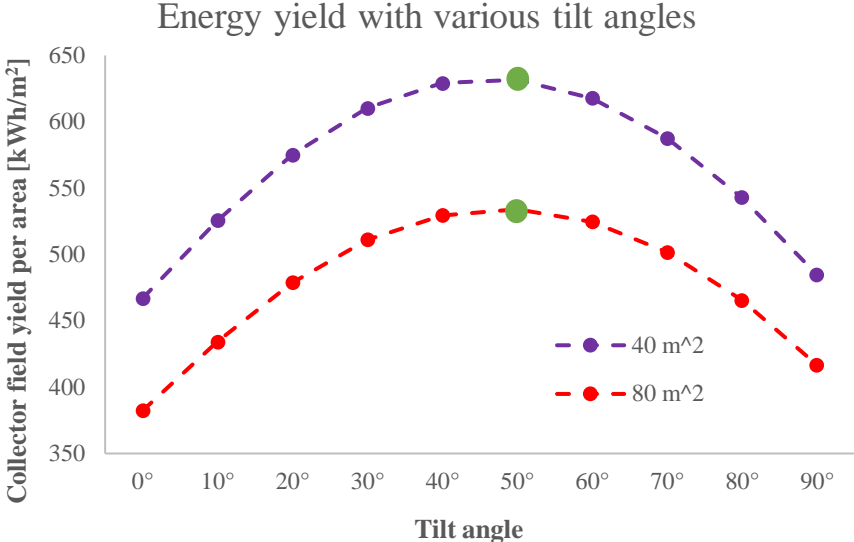


FIGURE 60: The collector field yield relating to gross area for collector areas of 40 m² and 80 m² at different tilt angles, based on SN/TS 3031. The maximum occurs at 50° for both areas.

In round 2 of the parametrization, the collector field yield per area was examined at tilt angles 45°, 50° and 55°. Comparing the energy yield at the three different tilt angles gave an overview of the best solution in the range of collector areas. Table 13 gives a representation of the results.

TABLE 13: Collector field yield relating to gross area for a variation of collector numbers and tilt angles, based on SN/TS 3031. For 10-60 m² collector area 45° have the highest value and for 70-100 m² the maximum is at 50°. 55° is not the best tilt angle for any of the collector areas in the range. The relevant values are marked in green.

Collector area [m ²]	Collector field yield per area [kWh/m ² _{sc}]		
	45°	50°	55°
10	692.4	690.1	683.5
20	683.6	681.8	675.8
30	659.7	658.4	652.8
40	632.5	631.6	626.7
50	605.6	605.1	600.8
60	580.0	579.9	576.1
70	555.9	556.1	552.8
80	533.6	534.1	531.2
90	513.4	514.1	511.3
100	494.2	495.3	493.0

In table 13, all the results for 10-100 m² collector areas are reproduced. The tilt angle being the best regarding energy yield varies with collector area, explained more detailed in the table text.

The graphs in figure 61 shows the LCOE for different solar collector areas, calculated using equation (18). The minimum is 53.9 øre/kWh and occurs at a solar collector area of 50 m² with a tank volume of 2500 l.

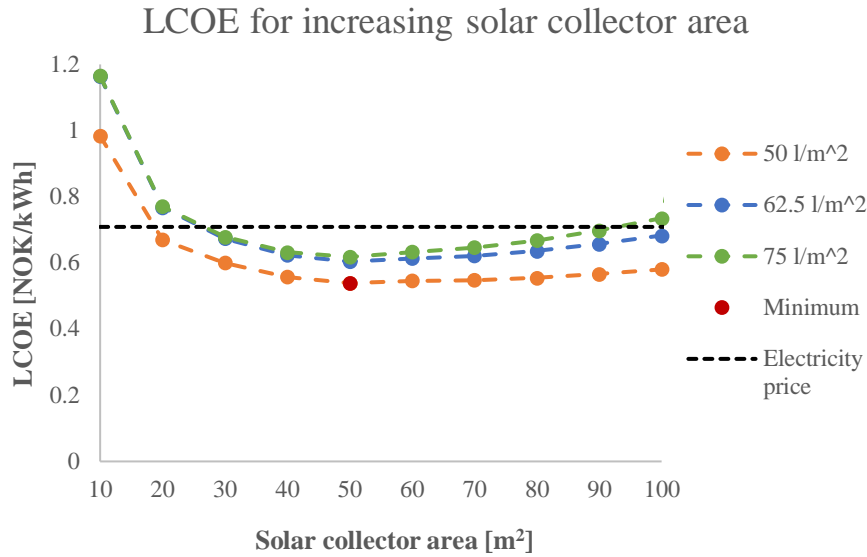


FIGURE 61: The LCOE at different solar collector areas from 10 m² to 100 m² based on SN/TS 3031. The minimum point occurring at 50 m² with a tank of 2500 l is marked with a red dot. The electricity price is also included.

The maximum collector temperature for the most profitable system was 78 °C, which is below the limit value.

4.3.2 THE MOST PROFITABLE SOLUTION

Based on these simulations, the following parameters ended up in the best combination for SN/TS 3031:

- Solar collector area – 50 m²
- Accumulator tank volume – 2500 l
- Tilt angle – 45°

Results from simulations of this configuration with normed inputs from SN/TS 3031 and collected data from the nursing home are compared in the following paragraphs. The differences in the economic parameters are displayed in figures 62, 63 and 64.

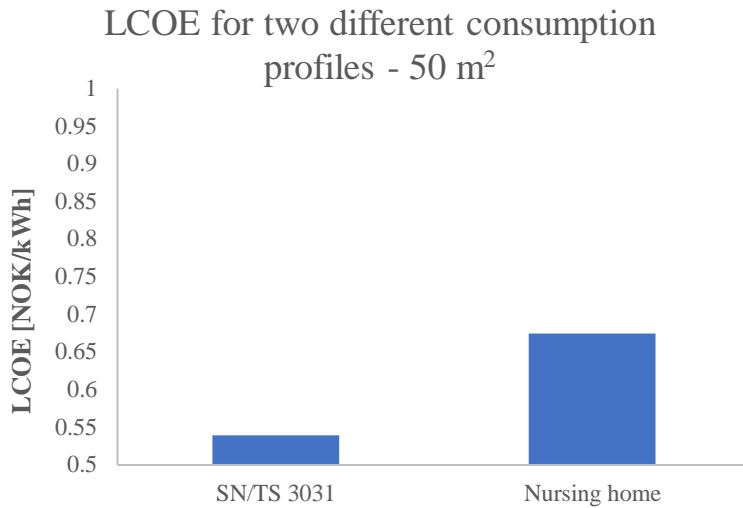


FIGURE 62: The LCOE of a construction with 50 m² solar collector area. Two different consumption profiles are considered – normed inputs from SN/TS 3031 and the collected data from the nursing home.

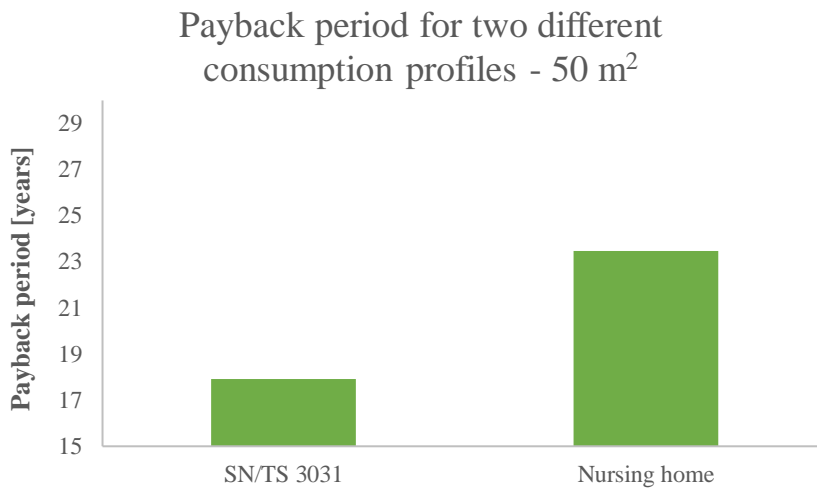


FIGURE 63: The payback period of a construction with 50 m² solar collector area. Two different consumption profiles are considered – normed inputs from SN/TS 3031 and the collected data from the nursing home.

Annual cost for two different consumption profiles - 50 m²

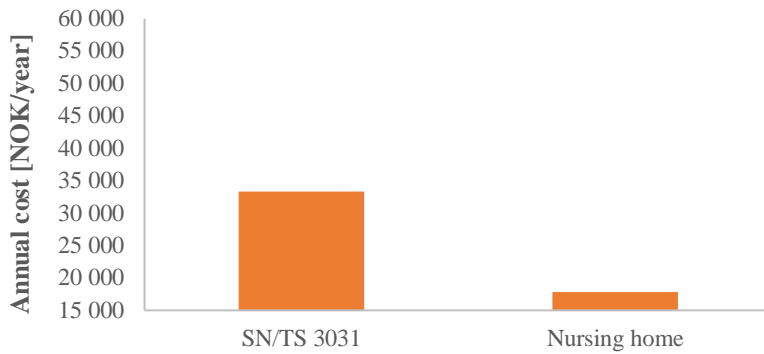


FIGURE 64: The annual cost of a construction with 50 m² solar collector area. Two different consumption profiles are considered – normed inputs from SN/TS 3031 and the collected data from the nursing home.

The LCOE based on the collected data from the nursing home is 25 % higher than the LCOE using the normed standard. The payback period for the nursing home consumption profile is 31 % higher than the payback period based on SN/TS 3031. The annual cost is 47 % lower when the consumption is based on the nursing home.

Figures 65, 66 and 67 show the changes in the technical characteristics.

Solar fraction for two different consumption profiles - 50 m²

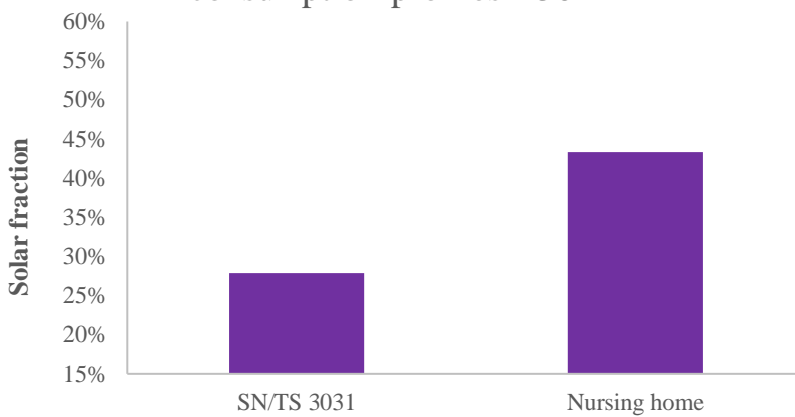


FIGURE 65: The solar fraction of a construction with 50 m² solar collector area. Two different consumption profiles are considered – normed inputs from SN/TS 3031 and the collected data from the nursing home.

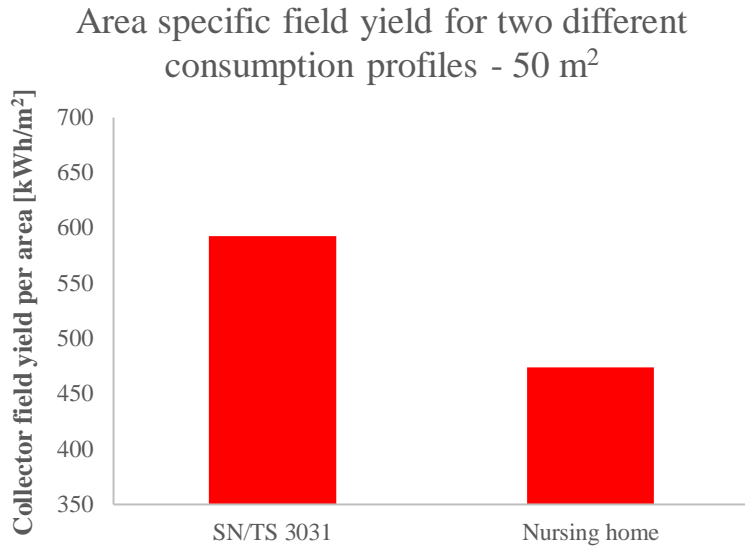


FIGURE 66: The collector field yield relating to gross area of a construction with 50 m² solar collector area. Two different consumption profiles are considered – normed inputs from SN/TS 3031 and the collected data from the nursing home.

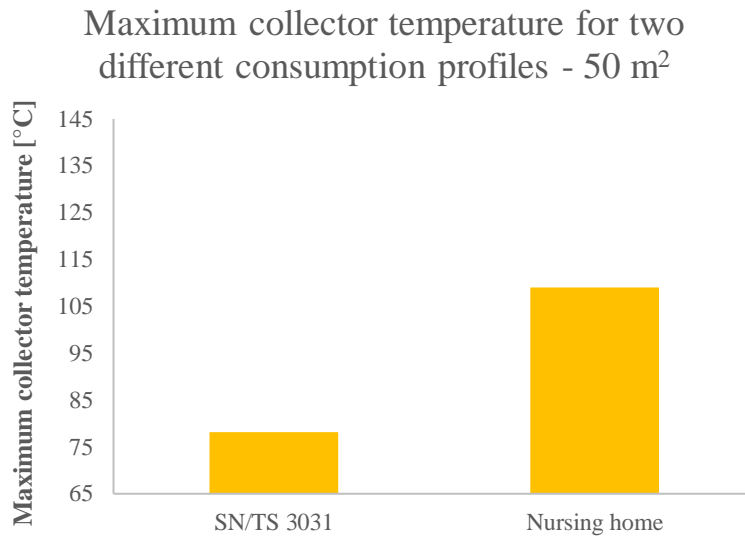


FIGURE 67: The maximum collector temperature of a construction with 50 m² solar collector area. Two different consumption profiles are considered – normed inputs from SN/TS 3031 and the collected data from the nursing home.

The solar fraction is around 55 % higher based on the collected data from the nursing home, compared to the normed inputs from SN/TS 3031. The corresponding value for the maximum

collector temperature is around + 39 %. The area specific field yield is 36 % lower based on the measured data from the nursing home, compared to the normed inputs from SN/TS 3031.

5 DISCUSSION

This chapter will discuss the assumptions and choices made in the research of this thesis. The applied data will also be considered. Lastly, an assessment of the results is included.

5.1 ASSUMPTIONS

5.1.1 MAXIMUM SOLAR COLLECTOR AREA AND ACCUMULATOR TANK VOLUME

The area limitation for the solar collectors was set to 100 m^2 with a corresponding accumulator tank volume limit of 7500 l, following a tank dimension principle of $75 \text{ l/m}^2_{\text{sc}}$. This was assumed to be large enough for the given DHW consumption. The results for both the nursing home consumption and SN/TS 3031 show that the best system has a size which is well within these upper limits.

Regarding the accumulator tank, its height is set to 2 m, independent of the volume. This leads to a 2000 l tank having a diameter of around 1 m, while a tank of 7000 l would have a diameter about twice as large. In case of space limitations, there is a possibility of changing the tank dimensions and/or connect several smaller tanks together. However, the latter would increase both costs and heat losses. Projects for buildings will have given limits based on the size of the roof and tank room.

5.1.2 IRRADIATION AND SHADING

The roof was assumed to be flat for simplification. This is an idealistic situation and most roofs tend to be sloped and oriented in different directions. A possible consequence of this assumption is an overestimation of the solar irradiation on the collectors.

Another simplification which may cause exaggerated irradiation values is the choice of placing all the collectors on one array. There will be no shading from collectors lying in front, which lead to a constant irradiation intensity when the sky is clear. This configuration may also be practically impossible with many collectors.

Lastly, no horizon profile was defined in this research. This was mainly to generalise, but also functioned as a simplification. The collectors will experience no shadow unless there are clouds in the sky, similarly to the previous point. Using a more practical solution would probably result in lower irradiation values, leading to a smaller solar fraction and area specific field yield,

among others. However, the changes would happen to all the parameters and the relationship between them would most likely not be any different.

5.2 WEATHER DATA AND DHW CONSUMPTION

The chosen weather data source was an inbuilt function in Polysun. Using this, there was no need for an assembly of data. Additionally, this method minimised the probability of potential difficulties arising during data import.

Meteonorm collects weather information from a large number of years. The disadvantage of using a tool based on a time series of several years is that the consumption in this case corresponds to the weather of a specific year, January 11th, 2018 to January 10th, 2019. No years have the same weather profile, and some years have anomalies. The most sensational about 2018 was the long and dry summer (Skaland et al., 2019). In the period of May until July, the average temperature was 3.1 °C above normal throughout the whole of Norway. This period was also the fourth driest in the country since 1900. Additionally, Blindern weather station in Oslo had a record amount of sunshine hours during a year (Elster, 2018). The same principles apply for the standard, SN/TS 3031, which is based on another weather profile than Polysun.

Having DHW data only from the specified year, and not the corresponding weather, makes it impossible to know how the weather may have influenced the consumption in the nursing home. Given that the consumption is subject to relatively small variations throughout the year, the effects can be assumed negligible. However, an increased quantity of sun naturally causes more irradiation on the solar collectors and, in turn, a higher contribution to the water heating. More research is necessary to draw any clear conclusions.

The consumption profile which was put into Polysun was converted from energy use of the heating elements into heated volume. The electrical heating happened inside the tank while the volume flow was located in the tap. It takes some time for the heated water to move from the tank to the tap. For this reason, the conversion might have led to an offset in time between the real consumption and the one in Polysun. The consumption could appear to take place at an earlier time in Polysun, which would affect its interaction with solar irradiation. However, the effects on the results are assumed to be negligible.

5.3 SYSTEM CHOICES

5.3.1 PIPES

In the simulations, it is assumed that all the pipes are made of the same material, have equal dimensions and identical insulation. They are also set to be straight and the pressure losses are non-existing. If the friction between the pipes and the liquid was to be considered, the pipe characteristics would be more important. As equation (6) shows, the pressure losses are dependent on both material and dimensions. In a cost perspective, such losses might increase the electricity costs for the operation of the pumps. Further research taking this into account could give more accurate results. However, due to the neglecting of the friction losses, the choice of pipe features is justified.

The insulation thickness of 100 mm is significantly larger than what is used by for instance De Dietrich (2017). This choice was made to make the heat losses a less important part of the energy equation and is reflected by the negligible contribution in figure 33. There would be a cost increase due to the larger thickness, but the amount is not considered.

5.3.2 SOLAR COLLECTOR

Regarding the type of solar collector, a generic flat plate version was chosen. The fact that it has widespread similarities with a solar collector on the market makes the choice sensible. The resemblance also supports the cost calculations. Evacuated tube collectors were deselected. Using this type would most likely increase the collector efficiency but may have a higher price.

5.3.3 ACCUMULATOR TANK

The tanks which were chosen were also generic versions from the Polysun catalog. PU foam is an insulation material used on the Akvaterm accumulator tanks which is supplied by SGP Armatec (SGP Armatec AS, n.d.-a). Based on the recommendations from Vela Solaris, an insulation thickness of 150 mm was selected (Vela Solaris, 2018). According to the product sheets of the Akvaterm tanks, a common choice is a thickness of 100 mm (SGP Armatec AS, n.d.-a). The larger thickness might increase the cost of the tank and decrease the heat losses, but the amount is difficult to decide. Considering its dimensions, a height of 2 m seems normal, although some are higher (SGP Armatec AS, n.d.-a). There are also other aspects which are not identical to a real accumulator tank. In any case, the tank's features and cost are merely estimations.

5.3.4 SOLAR LIQUID

The choice of antifreeze fraction in the solar liquid was based on SGP Armatec's use. On February 26th 2018, the temperature in Drammen was -22.2 °C, but such cold is very rare (Jansen, 2018). Referring to this extreme temperature, a mix giving a freezing point of -21.5 °C is barely within limits. However, the liquid in the solar collector probably holds a higher temperature than the outside environment. Additionally, a propylene glycol solution of at least 33 % does not freeze to solid ice, rather it becomes a gelatinous mass, according to Vela Solaris (2018). This means that the freezing of 40 % concentration antifreeze will not completely stop the flow, but it might slow down. The negative effects of mixing water and antifreeze, namely decreased heat capacity and increased viscosity, will assert themselves more with a growing glycol concentration. All in all, the chosen concentration is considered to be within acceptable limits for the specified location.

Since the boiling temperature of the heat carrier is dependent on the antifreeze concentration and pressure, it is assumed that other solar liquids with similar features have the same boiling point. A buffer of 6 °C was selected for precautionary reasons.

5.3.5 TEMPERATURES

There are several temperatures set in the system. The defined profile of the cold water was based on assumptions in collaboration with SINTEF Byggforsk (2019). The monthly values are detailed enough for this purpose. In the hot water end, the temperature is set to 5 °C higher than the recommended limit at 60 °C for precautionary reasons. For the same reason, the contents in the electrically heated water tank is attempted to keep 70 °C by configuring the heating element to turn on if the temperature is below 67.5 °C and off again at 72.5 °C, in one of the low tank levels. The cut-in temperature difference of the pump in the solar loop of 6 °C is within the area recommended by SINTEF Byggforsk (Andresen, 2008).

5.3.6 HEAT AND PRESSURE LOSSES

As can be derived from figure 33, the heat losses make up around 7 % of the total energy output from the system. This low share is probably caused by the thick insulation on both pipes and tanks. The dimensions of the pipes and tanks are also contributing factors. In this case, some of the pipes have a shorter length than they would have in a building.

The pressure losses are removed in total by choosing a friction factor equal to zero. A consequence of this choice is an additional underestimation of the system losses in the results. According to equation (6), the thinner, longer and rougher the pipes, the higher the losses would be. In this regard, a larger building would have more losses given that the material and diameter of the pipes are equal, because their length increases. However, the pressure losses are even more dependent on the flow velocity, which again is decided by the pumps. In the case of including the pressure losses, the flow rate would play a more important role, and more consideration on this choice should be taken.

Another consequence of eliminating the pressure losses is a negligible amount of pump operation, illustrated in figure 33. The percentage of the total electricity use which goes to the pumps is negligible, only 0.07 %. This is also reflected in the low costs for this purpose in tables 7, 9 and 11. The electricity which is used is most likely linked to starting and stopping the flow when temperatures are outside of the limits.

5.3.7 WATER HEATER AND PUMPS

The volume of the water heater tank of 1000 l and the power of the heating element at 30 kW was chosen independently of the rest of the system. Alterations of these values might result in changes in the different parameters. As long as the energy demand has been covered by the simulated systems, the change of capacity of the water storage heater has not been considered. This was probably the limiting factor when the Drammen nursing home consumption was quadrupled.

The pumps in the solar system can be controlled in various ways. In this thesis, a specific flow rate function was selected. Based on the area of operation of the pumps in SGP Armatec's solar stations, the middle value of 27.5 l/h per m² solar collectors was chosen (SGP Armatec AS, n.d.-b). Another possibility of pump control is called matched flow. This function enables the selection of a target outflow temperature from the collectors.

Figure 68 shows the variation of the LCOE using different pump control modes for the most profitable 40 m² system. The minimum value occurs at a specific flow rate of 33.75 l/h per m² solar collectors. This a larger value than the one used in this research. However, the change from the highest to the lowest LCOE in this graph is only 1.5 %. Based on this analysis, the choice of pump control has negligible effect on the results.

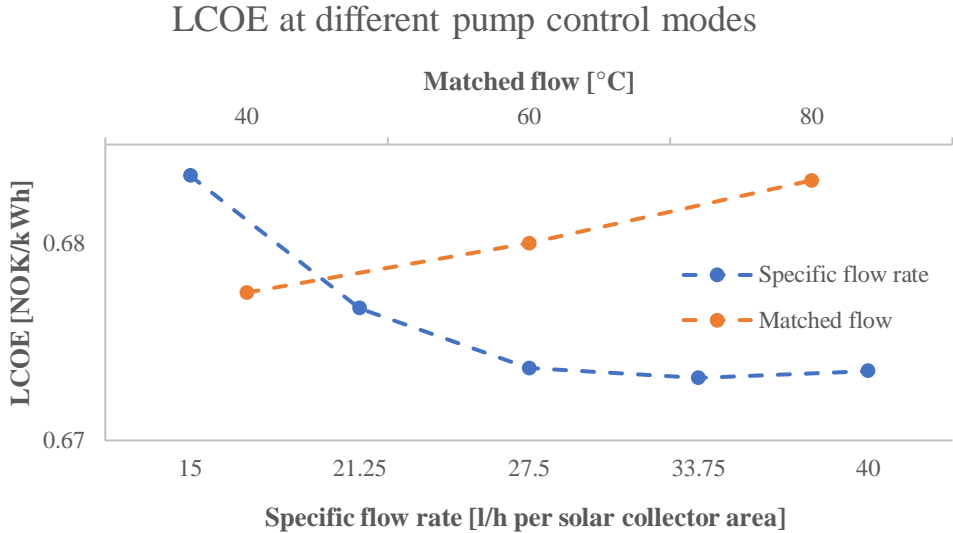


FIGURE 68: The LCOE as a function of two different pump control modes – matched flow and specific flow rate. A selection of variables within these modes is tested.

5.4 METHODS LIMITATIONS

5.4.1 RESULT PARAMETERS

A selection of result parameters had to be chosen. Among the economic parameters, the LCOE was a natural choice because this value determined the most profitable solution. The payback period was included because it explains the electricity savings in an understandable way, especially when compared to the construction lifetime. To present a more direct picture of the expenses, annual cost was added.

On the technical side, the solar fraction was considered important to describe the solar energy contribution throughout the year. Collector field yield per area give a notion of the system’s performance in relation to its size. The maximum collector temperature was included to observe whether the solar liquid was prone to boil.

5.4.2 SOFTWARE

The results of this paper are solely based on simulations performed by Polysun. Using other types of software might give different results as each program has its own algorithms and structure. Other software programs might prioritise differently and offer their own set of inputs. These variations could be examined by comparing programs, but that is not done in this research.

5.4.3 DIMENSIONING

In comparison to the tank dimensioning principle of 50-75 l/m²_{sc}, NVE used tank dimensions of 50-83 l/m²_{sc} in their report (Sidelnikova et al., 2015). A collection of prices from different suppliers in another report resulted in 35-100 l/m²_{sc} accumulator tank volumes, where the majority was around 60 l/m²_{sc} (Norsk Solenergiforening & Asplan Viak, 2015).

When testing a variety of tank volumes in this thesis, the findings favoured an accumulator tank of 37.5 l/m²_{sc}. This makes an expansion of the dimension interval towards lower values interesting. At even lower tank volumes, there is reason to believe that the maximum collector temperature would have risen above the boiling point. In any case, the chosen dimensioning principle seems to be in a sensible range.

In the part where the best tilt angle was determined, an accumulator tank volume of 10 000 l was selected. This large tank volume was chosen to avoid possible storage limitations in the simulations. 10 000 l correspond to a construction of 200 m², given a principle of 50 l/m²_{sc}. Using 75 l/m²_{sc}, this tank volume refers to a solar collector area of 133 m². This is larger than the most profitable solution considering the DHW consumption of both the nursing home and based on SN/TS 3031. The use of an accumulator tank of a different volume might have given lower values of the area specific field yield but, as in figure 38, the changes would most likely have been negligible. Applying the same changes to all the solar collector areas would most likely not alter the relationship between the tilt angles.

5.4.4 CONSTRUCTION LIFETIME

It is assumed that the whole construction has a lifetime of 25 years. The pumps may have a shorter lifetime, but that is not taken into account in this thesis. Additionally, the efficiency of the solar collectors might deteriorate after some time, before the end of the lifetime. This would

lead to a decrease in the amount of produced solar energy, and hence a higher LCOE and longer payback period. These possibilities are not considered in the results.

5.5 CHOICE OF COSTS

5.5.1 INSTALLATION COST

The installation costs are based on percentage values of two different system sizes from a 2015 NVE report (Sidelnikova et al., 2015). The linear trend line in figure 12 is not a coherence which is real, it is merely a simplification to calculate the installation cost as a function of solar collector area. Even though it is an assumption, the fact that installation costs per collector area for small constructions are higher than for large facilities is preserved.

5.5.2 ACCUMULATOR TANK COST

Similar to the installation costs, the accumulator tank costs are based on trend lines. However, these trend lines are exponential and does not match all the data points. From figure 22 it is clear that some points are underestimated while others are overestimated. The coefficient of determination has a value of $R^2 = 0.9855$. This might lead to incorrect investment cost estimations and affect the final results.

An additional consequence of this method is that a price is found for each 100-150 l accumulator tank volume, depending on the dimension principle used. Based on SGP Armatec's products, the accumulator tank volumes normally have an increase step of 1000 l. Yet, there might be tanks on the commercial market with a lower minimum volume difference. Nevertheless, this simplification is important to have in mind when studying the results.

5.5.3 INVESTMENT COST

The economic results in this thesis are based on material price information from only one supplier, in addition to other cost assumptions, resulting in an estimation of investment costs. Without any further research it is difficult to state where these costs lie in relation to other offers and how much they might differ. However, similar surveys have been done by NVE, NSF and Asplan Viak, and SINTEF (Norsk Solenergiforening & Asplan Viak, 2015; Sidelnikova et al., 2015; Skeie et al., 2016).

NVE found in 2015 that the average investment cost of a solar thermal construction varies between around 7400 NOK/m²_{sc} and 3300 NOK/m²_{sc}, decreasing with an increase in facility size of 6-300 m². In comparison, the calculated investment costs of the most profitable solutions in this thesis are 6300 NOK/m²_{sc} (SN/TS 3031) and 6900 NOK/m²_{sc} (Drammen nursing home). Based on these results, the applied investment cost in this thesis seem to be within sensible limits, trending towards the higher value. The variation in the costs collected by NVE was ± 20-30 %. (Sidelnikova et al., 2015)

Another study from the same year, by NSF and Asplan Viak, concluded with an average investment cost for small installations of 7200 NOK/m²_{sc}. The costs were collected from ten different suppliers. This report's findings also showed larger variations in the investment costs than the NVE report. For constructions of 100-160 m² solar collector area, the investment cost ranged from 3000 NOK/m²_{sc} to 5700 NOK/m²_{sc}. These estimates agree well with the values used in this research, given that the most profitable constructions are smaller than 100 m². (Norsk Solenergiforening & Asplan Viak, 2015)

Based on costs from four suppliers, a SINTEF report from 2016 registered differences in investment costs of almost 100 % for solar collector constructions for heating DHW. A comparison of a variety of heating sources found that waterborne systems had an investment cost which was more than twice as high as for systems producing electricity. (Skeie et al., 2016)

The NVE report also did a sensitivity analysis of the LCOE to observe its dependency of different parameters. The results showed, among others, that the LCOE depend largely on the investment cost. Additionally, NVE extrapolates a reduction in investment costs of solar thermal constructions of around 40 % from 2014 to 2035 and a reduction in the LCOE of around 30 % towards the same year. These numbers are based on a learning curve of 20 %. (Sidelnikova et al., 2015)

The sensitivity analysis in this thesis looks at investment costs ranging from around 4800-8900 NOK/m²_{sc}. This interval covers the highest costs derived from the mentioned reports. To include the lowest costs, the decrease would have had to be larger than 30 %. However, the lowest investment costs refer to the largest constructions and are not equally relevant for this research.

5.5.4 ELECTRICITY PRICE

The power price in this thesis is calculated from the forward price for 2022 in addition to marks and taxes in the prevailing market. The grid rent is based on statistics from 2017. Figure 69 displays graphs of end-consumer electricity prices from the last eight years, including the first twelve weeks of 2019 (Tekniske Nyheter DA, 2019).

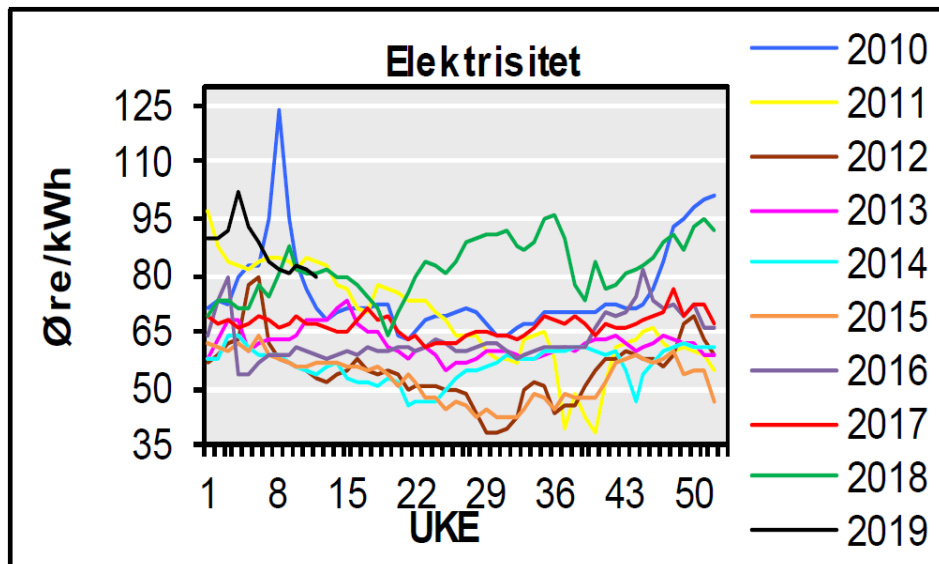


FIGURE 69: Historical electricity prices for industry consumers. Used with kind permission from Tekniske Nyheter DA. (Tekniske Nyheter DA, 2019)

The values range from around 36 øre/kWh in week 29 of 2012 to just below 1.25 NOK/kWh in week 8 of 2010. The maximum electricity price in this graphic is almost 350 % larger than the minimum. These numbers are the extremes in electricity price differences.

Taking 2018 as an example, the electricity prices in summer were the highest during the last eight years, with a peak of just above 95 øre/kWh. There is reason to believe that the dry weather conditions this year was a significant contributor of the large increase (Skaland et al., 2019).

Considering other reports where economic calculations have been done, various electricity prices are used. This thesis has used the same power price approach as the 2015 NVE report, but the prices has changed during the four years to this date (Sidelnikova et al., 2015). The SINTEF report from 2016 made estimations based on an energy price of 1 NOK/kWh (Skeie et al., 2016), while research for Campus Evenstad had 59.2 øre/kWh as the corresponding value (Selvig et al., 2017).

There has been no variation in the electricity price in this research. In the sensitivity analysis in the thesis, electricity prices from 50-92 øre/kWh was considered (figures 51-53). This range includes the majority of the prices illustrated in figure 69. Further examination on both higher and lower electricity prices would probably extrapolate the tendencies observed.

5.6 RESULTS DISCUSSION

5.6.1 SN/TS 3031

Simulations using normed inputs from the standard SN/TS 3031 resulted in a larger collector area being most profitable, compared to the system based on the collected data from the nursing home. This is not a surprising outcome as the annual consumption according to the standard is a doubling of the nursing home data collection over a year. The result indicates that the standard might overestimate the size of a solar thermal construction as DHW energy source at nursing homes if information about actual use is not available. Comparing the nursing home results in figures 62-67 to the corresponding values in tables 7 and 8, the 50 m² construction is less suitable than the one of 40 m². However, the changes are small in this case, the largest alteration being + 21 % for the maximum collector temperature.

Due to the fact that SN/TS 3031 assumes a DHW consumption which is almost twice as large as the demand at the Drammen nursing home, the results for the most profitable system might be estimations for the best solution in case of a doubling in consumption at the nursing home. Further increasing the DHW demand would most likely lead to a growth in the system size considered to be economically best.

5.6.2 LCOE

The changes in the pump electricity costs are neglected in the discussion of the LCOE because they comprise a share of less than 1 % of the total costs.

Figures 26 and 61 show that the LCOE increases with growing accumulator tank volume, within the dimensioning principle 50-75 l/m²_{sc}. Larger tanks give a rise in the costs, contributing to a higher LCOE. On the other hand, the produced solar energy increases, which contributes to lower the LCOE. However, the cost growth seems to affect the LCOE more than the rise in

solar contribution in this case. This effect can also be observed in figure 34 for an increase in tank volume from 2000 l to 3000 l, and in figures 40 and 41 for a large and small system.

The LCOE had its minimum value with a 1500-l tank, which implies a growth for a decreasing tank volume as well. Smaller tanks have lower costs, but a smaller amount of solar energy is transferred to the system. Apparently, the decrease in costs are not sufficient to outweigh the drop in produced solar energy. The biggest difference in LCOE is for a tank volume change from 2000 l to 2500 l, which can be explained by the exponential growth of the accumulator tank cost. This applies for all the economic parameters.

Similar results as for varying accumulator tank volumes appear for simulations of different system sizes, displayed in figure 42. Figure 24 shows that the investment cost per collector area is considerably larger for an area of 20 m² compared to a 40 m² system size. Larger systems have lower investment costs per collector area. However, they have a tendency to produce more energy than what is needed, resulting in heat waste.

Alterations in the investment cost by $\pm 30\%$ show that the LCOE act proportionally to the varying parameter, illustrated in figure 48. This can be explained by the investment cost representing a large share of the total costs, and the operation and maintenance costs changing equally much. In consequence, more than 99 % of the costs are altered. Figure 51 shows, on the other hand, that the electricity price has little influence on the LCOE. The reason for this is the negligible amount composed by the pump electricity cost of the total costs, as mentioned above.

For a solar thermal construction of 40 m², an increasing consumption gives a decrease in the LCOE, displayed in figure 54. The construction is identical, which means that the costs are the same. This leaves the produced solar energy as the only factor remaining to affect the LCOE. There is a growing need for energy and when the sun is generous, the heating potential is used to the fullest. The profit gets better with larger demands, as long as the energy need is covered.

The opposite effect can be observed when using SN/TS 3031. From figure 62, it is clear that the LCOE has a higher value with the nursing home consumption, compared to the expected value based on the standard. A small DHW demand require less heat energy, which results in a decreased need for the production based on the sun's irradiation. In consequence, the LCOE is higher for demands which are lower than the construction size is based on.

5.6.3 PAYBACK PERIOD

The growth in the payback period with larger accumulator tanks, displayed in figure 35, shows that the increase in investment, operation and maintenance costs exceeds the savings in electricity costs. As with the LCOE, the payback period is longer for the smallest accumulator tank and the reasons are the same. A similar development can be observed in figure 43 when various system sizes are tested.

The payback period is proportionally related to the investment cost changes, but inversely proportional to the altering of the electricity price, shown in figures 49 and 52. Both the reactions are self-explanatory, considering equation (19). A combination of even lower investment costs and higher electricity prices would give a further decrease in the payback period.

Doubling and tripling of the DHW demand on the same system lead to a more frequent use of energy, but the savings in electricity costs also increase. This is because a larger portion of the produced solar heat is used. The construction is identical; the investment, operating and maintenance costs stay constant. Hence, the payback period shortens as consumption grows, illustrated in figure 55.

Similar to the LCOE, the payback period has a higher value with nursing home consumption than expected from SN/TS 3031. This is displayed in figure 63. The electricity cost savings is the contributing factor for changes in the payback period. These savings are lower for a small consumption because a lower share of the solar energy produced is exploited.

Even though the payback period of 23.2 years for the most profitable system is below the assumed construction lifetime of 25 years, it is still a long-term investment. The decrease of the investment cost and increase of the electricity cost giving 15.2 years and 16.9 years payback periods, respectively, is still a long time. People might find it difficult to choose this solution for economic reasons exclusively. It can be necessary to focus on other advantages a solar thermal construction could bring, such as a degree of independence and a contribution for a “greener” energy production.

5.6.4 ANNUAL COST

It can be seen from figure 36 that the annual cost also has a minimum value for a 1500-l accumulator tank. This tank volume ensures the economically best balance between the costs and the produced solar energy for the most profitable system size. Smaller tanks are not able to deliver enough heat from the solar collectors and larger tanks are too expensive. Changes in system size give similar results (figure 44).

Changes in the investment cost cause variations in the annual cost of almost 11 % and electricity price deviations result in an increase/decrease of 19 %. Hence, the changes in the cost of heating element electricity affects the annual cost more than alterations in the investment costs. The interactions are illustrated in figures 50 and 53.

A larger DHW demand leads to a more frequent use of the heating element, which again gives increased electricity costs. In consequence, the annual cost is higher, shown in figure 56. The annual cost using the measured nursing home demand is lower than expected from the standard because the electricity costs are smaller (figure 64).

5.6.5 AREA SPECIFIC COLLECTOR FIELD YIELD

The results in tables 6 and 13 show that the area specific field yield decreases with growing system size. The most probable reason for this is that the solar thermal construction gets too large in relation to the DHW demand. Heat is produced and transferred to the liquid, but if there is no need for the energy the warm water will stay in the system. Then the pumps will stop because the temperature difference between the tank and the collectors fall below 2 °C. If irradiation continues, the temperature in the collectors increases and this leads to more heat losses and possibly boiling. The potential of the solar collectors is not fully used. This can also be observed in figure 46, which shows a fall in collector field yield per area with increasing system size. Furthermore, applying the larger standard based solar construction on the measured consumption from the nursing home shows the same effect, in figure 66.

The opposite outcome occurs when the system stays the same, but the DHW consumption grows. This leads to an improvement in the area specific field yield, as figure 58 shows, because the need for heat prevents the decrease in the temperature difference and the pumps keep operating. The full potential of the solar thermal construction is taken advantage of.

The results from finding the best tilt angle made clear that the collector field yield per area is dependent on both system size and tilt angle. There is a tendency of an increase in the best tilt angle with growing solar collector area, displayed in figure 25 and tables 6 and 13. This is most likely linked to the decrease in area specific field yield with increasing collector area. Figure 7 illustrates that the higher the tilt angle, the more irradiation is incident on the collectors during winter. In summer, the irradiation is lower on large slopes because the sun is high in the sky. The DHW consumption has a tendency to be lower in summer, confirmed by figures 17 and 31. To avoid possible overheating in large systems, a high tilt angle can be useful. This weakens the irradiation hitting the collectors in summer and strengthens it during the colder seasons, when the DHW demand is larger. A consequence is an improved collector field yield per area throughout the year.

The increase in the area specific field yield with larger tank volumes, observable in figure 38, can be explained by the growth in the capacity to store energy. This capacity rise provides heat storage over a longer period, for instance without sun.

5.6.6 SOLAR FRACTION

In figure 27, the solar fraction was displayed. It is dependent on both the DHW consumption and the solar irradiation onto the collectors. When irradiation increases, more heat is produced in the collectors and there is less need for the heating element. Since the DHW demand is approximately constant throughout the year, the amount of sun dominates the development. The solar fraction is highest in July, which can also be observed in figure 28.

As with the area specific field yield, the solar fraction increases with growing accumulator tank volume, due to larger storage capacity (figure 37). The solar fraction also grows proportionally to the construction size, showed in figure 45. A larger collector area has the possibility to gather more heat energy and the need for auxiliary electrical energy is less. Hence, the solar thermal installation covers a larger proportion of the DHW demand. Figure 65 displays the same principles for the collected nursing home consumption on the standard based system.

On the contrary, an increase of DHW consumption makes the use of the heating element more necessary. A consequence of this is a decrease in the solar fraction, illustrated in figure 57.

5.6.7 MAXIMUM COLLECTOR TEMPERATURE

The high maximum collector temperature with a small accumulator tank is consequence of a deficit in capacity. In periods of intensive solar irradiation and low consumption, the pumps are turned off sooner for a smaller tank, leaving the liquid in risk of boiling. The development is illustrated in figure 39.

The maximum collector temperature increases with a growth in system size, as figure 47 shows. Similarly, when the nursing home consumption is simulated on the most profitable system for the SN/TS 3031 demand, the maximum collector temperature is higher than expected (figure 67). As explained in the chapter on area specific collector field yield, the system most likely becomes too large for the given consumption. The pumps might stop, making the liquid in the collectors subject to intensive solar irradiation.

For the same reasons as the increase in collector field yield per area with larger DHW consumption, the maximum temperature experiences a fall. The high consumption keeps the pumps operating and the solar liquid is not stationary in the collectors.

All the simulations resulted in a maximum collector temperature which was below the given boiling limit of 140 °C, ranging from 70 °C to 139 °C. The maximum temperature for the most profitable system based on the Drammen nursing home consumption was 90 °C, which is even below the boiling point of water at standard pressure. It is safe to assume that no boiling occurs at that temperature. The temperature closer to 140 °C, however, might result in boiling.

5.6.8 TEMPERATURE OUT OF THE ACCUMULATOR TANK

The temperature out of the accumulator tank changes from the different weeks of the year. Figures 30 and 32 show examples of week 1 in 2019 and week 26 in 2018. Comparing these temperatures to the corresponding week in figures 29 or 31, it seems like the highest values occur after the difference between the produced solar energy and the DHW demand has been small, and opposite. The maximum temperatures are results of a surplus of solar energy yield. These outcomes are most likely due to a large accumulation of heat in the tank when the solar irradiation is strong and DHW consumption is low. When there is a deficit in solar energy

production in relation to the DHW demand, the temperature does not have much time to rise before the heat is utilised.

5.6.9 USEFULNESS

The results derived from the simulations in this thesis are specific for the exact chosen structure of each system and the given DHW consumption. Any alterations in the inputs would change the outputs more or less.

However, this does not mean that the results are useless. The outcomes give an idea on the approximate size of a solar thermal construction which will give the lowest LCOE. Additionally, changes in various parameters for different configurations can be observed.

A comparison between the collected DHW consumption and the normed inputs from the standard SN/TS 3031 shows considerable differences. In relation to dimensioning a solar thermal facility, the standard might be in need for some adjustments.

6 CONCLUSION

This thesis has examined the most profitable solar collector facility for measured and standard based DHW consumptions in nursing homes, and changes in various economic and technical parameters with specified alterations. The focus has been on a pressurised system in combination with an electric water heater. The most profitable solution was the one with the lowest LCOE out of solar collector areas of 10-100 m² with accumulator tank dimensions of 50 l/m²_{sc}, 62.5 l/m²_{sc} and 75 l/m²_{sc}. The best tilt angle was found doing specified simulations. In addition to the LCOE, the payback period and annual cost were considered. Technical parameters included in the results were the solar fraction, area specific collector field yield and maximum collector temperature.

Measurements of the energy use for DHW at a nursing home in Drammen gave an annual consumption of 53.9 MWh. The most profitable system based on the collected consumption data from this nursing home consisted of a solar collector area of 40 m² with a tilt angle of 50° and an accumulator tank of 2000 l. For this solution, the LCOE was 66.9 øre/kWh, the payback period was 23.2 years and the annual cost was 17 798 NOK/year. The solar fraction was 38 %, the area specific field yield was 512 kWh/m²_{sc} and the maximum collector temperature was 90 °C.

Alterations in the accumulator tank volume of maximum ± 50 % lead to various changes. The lowest economic values occurred for a tank of 1500 l, but the increasing costs of a growing tank volume from 2000 to 2500 l dominated the results of the LCOE and payback period. All the technical parameters were most optimal for the largest tank. These improvements were small, except from a steep decrease in the maximum collector temperature with a change in tank volume from 1000 l to 1500 l, as a result of larger storage capacity.

The tests of different system sizes showed that the tank dimension principle of 50 l/m²_{sc} was most profitable for all three solutions. For the large system (80 m²), the LCOE was 75.7 øre/kWh, the payback period was 27.2 years, the solar fraction was 56 %, the area specific field yield was 388 kWh/m²_{sc} and the maximum collector temperature was 130 °C. For the small system (20 m²), the LCOE was 73.9 øre/kWh, the payback period was 26.3 years, the solar fraction was 22 %, the area specific field yield was 594 kWh/m²_{sc} and the maximum collector

temperature was 76 °C. The annual cost was subject to negligible changes. The middle-sized facility had the lowest LCOE, payback period and annual cost, which confirmed it was the best choice. Only the solar fraction had its best value for the system of 80 m². The other technical parameters favoured a solar collector area of 20 m². A small solar thermal construction achieves better technical results because the large system is overdimensioned in relation to the DHW consumption.

Both the investment cost and the electricity price are factors which influence the economic results. All three economic parameters had the best outcomes for the smallest investment cost. In that case, the LCOE was 46.8 øre/kWh, the payback period was 15.2 years and the annual cost was 15 928 NOK/year. This is not surprising as higher costs on the same system only makes it less profitable. Alterations of the electricity price gave the shortest payback period at the highest value, of 16.9 years. This is because the payback period focuses on the savings in the electricity cost, which are larger with increasing electricity price. The LCOE and annual cost had their maximum values at the highest electricity price due to a growth in the electricity costs, though the changes in the LCOE was negligible. The annual cost for the lowest electricity price was 14 329 NOK/year.

The solar thermal construction of 40 m² becomes more profitable with increasing consumption, a tripling giving an LCOE of 53.3 øre/kWh. A larger DHW demand keeps the solar system running more frequently, avoiding too much accumulation of heat in the collectors. Hence, heat loss is decreased. This also reflects well upon the area specific field yield and the maximum collector temperature. A tripling gives corresponding values of 642 kWh/m²_{sc} and 70 °C, respectively. The solar fraction is worsened to 18 % for a tripling, but this is a necessary sacrifice to improve the other parameters. However, because of the given capacity of the heating element, the system is only able to deliver enough energy up to a certain limit. It seems that the DHW demand in the nursing home is too small to achieve very lucrative outcomes from the use of solar collectors as energy source.

When the normed inputs from the standard SN/TS 3031 was used as consumption profile, the most profitable solution ended up having a solar collector area of 50 m² with a tilt angle of 45° and a 2500-l accumulator tank. This system is larger than the resulting solution for the collected nursing home data. The most probable reason for this is that the standard based DHW demand is twice as big as the measured one. Testing this system with the consumption of the Drammen

nursing home showed signs of it being overdimensioned. All the parameters, with an exception of the annual cost and solar fraction, had worse results than expected from the standard, when implementing the measured DHW consumption. This kind of estimation of the demand can give very different outcomes than predicted.

The results in this thesis show the importance of enhanced research on the use of domestic hot water. Both costs and use of energy can be minimised if the actual consumption of the building in each individual case is examined in advance of the installation of a solar thermal construction. A decrease in the costs of solar thermal facilities and/or an increase in the electricity price would make it a more desirable alternative.

Implementation of solar collectors in buildings contributes to increase the share of renewable energy sources and decrease the load on the power system. The need for hot water will not diminish in the future. More research on this subject gives expanded knowledge which improves the methods used in the future and our understanding of the way we live.

6.1 FURTHER RESEARCH

The analyses in this thesis are subject to limitations. There are a number of possibilities for further research on this topic.

Firstly, to achieve more realistic results concerning the heat losses in the system, the pressure losses in the pipes could be included. The inclusion of these losses gives rise to a more thorough examination of the dimensions of the pipes. Additionally, thinner insulation on both pipes and tanks may be applied.

Secondly, the most profitable dimensioning of a solar thermal construction can be analysed for DHW consumption values of various magnitudes. This may make it easier to estimate the best facility size, exclusively based on a given DHW demand.

Thirdly, a different kind of system may be examined. Alterations to the solar thermal system could be done, e.g. choosing a drain-back type or using evacuated tube collectors. An alternative option is to focus on another energy source, e.g. heat pumps.

Fourthly, the simulations might be done with a different software than Polysun or several softwares for comparison. Examples of other software are T*SOL and TRNSYS. A different weather data service could also be tested.

Lastly, similar analyses could be done on other building types than nursing homes. For instance, the project VarmtVann2030 also include measurements from hotels and residential buildings.

7 REFERENCES

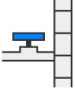
- Aashammer, H. (2016). *Analyse av termisk energiforsyning ved Hotell Scandic Lerkendal*: NTNU.
- Alternative Energy Tutorials. (2019a). *Evacuated Tube Collector*. Available at: <http://www.alternative-energy-tutorials.com/solar-hot-water/evacuated-tube-collector.html> (accessed: 29.01.19).
- Alternative Energy Tutorials. (2019b). *Flat Plate Collector*. Available at: <http://www.alternative-energy-tutorials.com/solar-hot-water/flat-plate-collector.html> (accessed: 01.02.19).
- Amin, S., Hanania, J., Stenhouse, K., Yyelland, B. & Donev, J. (2018). *Solar energy to the Earth: Energy Education*. Available at: [https://energyeducation.ca/encyclopedia/Solar energy to the Earth](https://energyeducation.ca/encyclopedia/Solar_energy_to_the_Earth) (accessed: 24.01.19).
- Andresen, I. (2008). *Planlegging av solvarmeanlegg for lavenergiboliger og passivhus. En introduksjon*, 22: SINTEF Byggforsk.
- Borgnakke, C. & Sonntag, R. E. (2013). *Fundamentals of Thermodynamics*. 8 ed.: Wiley.
- Cooper, C. (n.d.). *What is Thermal Conduction? Introduction to Heat Transfer: Part One*: Bright Hub Engineering. Available at: <https://www.brighthubengineering.com/hvac/47238-what-is-thermal-conduction/> (accessed: 24.01.19).
- De Dietrich. (2017). *Solar installations - Solar collectors, tanks and systems for individual and collective installations*.
- Elster, K. (2018). Oslo har satt norgesrekord i soltimer. Available at: <https://www.nrk.no/norge/oslo-har-satt-norgesrekord-i-soltimer-1.14329425> (accessed: 20.03.19).
- Engineering ToolBox. (2003a). *Energy Equation - Pressure Head Loss in Ducts, Tubes and Pipes*. Available at: https://www.engineeringtoolbox.com/major-loss-ducts-tubes-d_459.html (accessed: 25.01.19).
- Engineering ToolBox. (2003b). *Hydraulic Diameter*. Available at: https://www.engineeringtoolbox.com/hydraulic-equivalent-diameter-d_458.html (accessed: 25.01.19).
- Engineering ToolBox. (2003c). *Reynolds Number*. Available at: https://www.engineeringtoolbox.com/reynolds-number-d_237.html (accessed: 25.01.19).
- Engineering ToolBox. (2003d). *Water - Density, Specific Weight and Thermal Expansion Coefficient*. Available at: https://www.engineeringtoolbox.com/water-density-specific-weight-d_595.html (accessed: 15.02.19).
- Engineering ToolBox. (2008a). *Colebrook Equation*. Available at: https://www.engineeringtoolbox.com/colebrook-equation-d_1031.html (accessed: 25.01.19).
- Engineering ToolBox. (2008b). *Pipes and Fluid Flow Velocities*. Available at: https://www.engineeringtoolbox.com/pipe-velocity-d_1096.html (accessed: 25.01.19).
- Engvold, O. (2018). *Sola*: Store norske leksikon. Available at: <https://snl.no/Sola> (accessed: 23.01.19).
- Enova. (2016). *Solfanger*. Available at: <https://www.enova.no/privat/alle-energitiltak/solenergi/solfanger/> (accessed: 05.02.19).
- Enova. (2019). *Enovas byggstatistikk 2017*.
- Enova. (n.d.). *Varmesentraler*. Available at: <https://www.enova.no/bedrift/bygg-og-eiendom/varmesentraler/> (accessed: 15.03.19).
- European Commission. (2017). *The PVGIS project, a bit of background*. Available at: http://re.jrc.ec.europa.eu/pvg_static/about_pvgis.html (accessed: 21.02.19).
- European Commission. (2019). *Typical Meteorological Year (TMY)*. Available at: <https://e3p.jrc.ec.europa.eu/articles/typical-meteorological-year-tmy> (accessed: 03.04.19).
- Fidorów-Kaprawyl, N. & Dudkiewicz, E. (2017). The impact of the hot tap water load pattern in the industrial hall on the energy yield from solar collectors. *E3S Web of Conferences*, 22.
- Folkehelseinstituttet. (2018). *Legionellose*. Available at: <https://www.fhi.no/nettpub/smittevernveilederen/sykdommer-a-a/legionellose/> (accessed: 20.02.19).
- Fredly, K. (2014). *Vurderinger av ulike fornybare energiløsninger for Fredrikshald Brygge*: NMBU.

- Fuchs, J. (2013). *Mind Teaser - Water Heater Wars*. Available at: <https://techblog.ctgclean.com/2013/09/mind-teaser-water-heater-wars/> (accessed: 13.05.19).
- G., L. & Donev, J. (2017). *Payback*. Available at: <https://energyeducation.ca/encyclopedia/Payback> (accessed: 14.03.19).
- Hanania, J., Stenhouse, K. & Donev, J. (2017). *Radiant heat*: Energy Education. Available at: https://energyeducation.ca/encyclopedia/Radiant_heat (accessed: 23.01.19).
- Hanania, J., Sheardown, A., Stenhouse, K. & Donev, J. (2019). *Infrared radiation*: Energy Education. Available at: https://energyeducation.ca/encyclopedia/Infrared_radiation (accessed: 23.01.19).
- Hauge, Å. L., Sørnes, K., Godbolt, Å. L., Kristjansdottir, T., Sørensen, Å. L., et al. (2014). *Suksessfaktorer for økt bruk av solvarme*.
- IPCC. (2014). *Climate Change 2014 - Synthesis Report - Summary for Policymakers*.
- Isachsen, O. K. (2017). *Revidert kostnadsrapport*: NVE.
- Jansen, A. (2018). Kaldeste dag på flere år i Drammen: 22,2 minusgrader! (21.03.19). Available at: <https://drm24.no/nyheter/vaeret/vinterens-hittil-kaldeste-dag-i-drammen-22-2-minusgrader-1822700>.
- Jones, A. Z. (2017). *What Is Fluid Dynamics?*: ThoughtCo. Available at: <https://www.thoughtco.com/what-is-fluid-dynamics-4019111> (accessed: 24.01.19).
- Kartverket. (n.d.). *Norgeskart*. Available at: <https://www.norgeskart.no/#!?project=norgeskart&layers=1002&zoom=4&lat=7197864.00&lon=396722.00> (accessed: 26.02.19).
- Keul, A. L. (2010). *Solvarmeanlegg for vann-og romoppvarming*: NTNU.
- Klima- og miljødepartementet. (2017). *Klimaloven*.
- Kommunal- og moderniseringsdepartementet. (2017). *Byggteknisk forskrift*.
- Larsen, E. K. (2014). *Varmtvannssirkulasjon*. Prenøk - Prosjektering av energianlegg.
- Larsen, G. S., Aalrust, T. S. & Karayazgan, K. D. (2011). *Prosjektering og Modellering av Varme-og VAV-anlegg for A-bygg*: Høgskolen i Oslo.
- Meteotest. (n.d.). *Meteonorm Features*. Available at: <https://meteonorm.com/en/meteonorm-features> (accessed: 26.02.19).
- Moratal, A. M. & Bermejol, A. L. (2013). *Energy audit at Vallbacksskolan for future possible refurbishment*: University of Gävle.
- Norges vassdrags- og energidirektorat. (2018). *Solenergi*. Available at: <https://www.nve.no/energiforsyning/solenergi/?ref=mainmenu> (accessed: 23.01.19).
- Norsk Solenergiforening & Asplan Viak. (2015). *Solvarmeanlegg i Norge*.
- Norsk solenergiforening, Sørensen, Å. L., Torp, C. B. & Nylund, H. K. (2017). *Solvarme i kombinasjon med andre varmekilder*.
- Quaschnig, V. (2004). *Solar thermal water heating*. Available at: <https://www.volker-quaschnig.de/articles/fundamentals4/index.php> (accessed: 26.04.19).
- Selvig, E., Wiik, M. K. & Sørensen, Å. L. (2017). *Campus Evenstad - Statsbyggpilot. Jakten på nullutslippsbygget ZEB-COM.*: Statsbygg.
- SGP Armatec AS. (2019). *Conversation with Malin Helander*.
- SGP Armatec AS. (n.d.-a). *Akkumulatortanker*. Available at: <https://sgp.no/produktkategori/akkumulatortanker/akkumulatortanker-akkumulatortanker/> (accessed: 18.04.19).
- SGP Armatec AS. (n.d.-b). *Solstasjoner*. Available at: <https://sgp.no/produktkategori/solvarmere/solstasjoner/> (accessed: 18.04.19).
- Sidelnikova, M., Weir, D. E., Groth, L. H., Nybakke, K., Stensby, K. E., et al. (2015). *Kostnader i energisektoren - Kraft, varme og effektivisering, 2-2015*: Norges vassdrags- og energidirektorat.
- SINTEF Byggforsk. (2011). *Væskebaserte solfangere. Funksjon og energiutbytte*. Byggforskserien, 552.455.
- SINTEF Byggforsk. (2019). *Discussions with Harald Taxt Walnum*.
- SINTEF Byggforsk. (n.d.). *VarmtVann2030*. Available at: <https://www.sintef.no/projectweb/varmtvann/english/#/> (accessed: 16.01.19).
- Skaland, G. R., Colleuille, H., Andersen, A. S. H., Mamen, J., Grinde, L., et al. (2019). *Tørkesommeren 2018*.

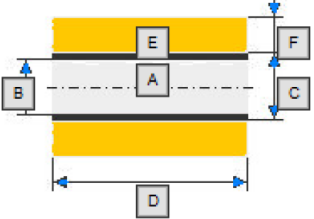
- Skatteetaten. (2019). *Avgift på elektrisk kraft*. Available at: <https://www.skatteetaten.no/bedrift-og-organisasjon/avgifter/saravgifter/om/elektrisk-kraft/> (accessed: 09.04.19).
- Skeie, K. S., Lien, A. G., Svensson, A. & Andresen, I. (2016). *Kostnader for nye småhus til høyere energistandard*: SINTEF.
- Spilde, D., Lien, S. K., Ericson, T. B. & Magnussen, I. H. (2018). *Strømforbruk i Norge mot 2035*, 43-2018: Norges vassdrags- og energidirektorat.
- Standard Norge. (2016). *Inndata for normert energiberegning*. Available at: <https://www.standard.no/ns3031> (accessed: 12.03.19).
- Standard Norge. (2017). *SN/TS 3031:2016 for beregning av energibehov og energiforsyning*. Available at: <https://www.standard.no/nyheter/nyhetsarkiv/bygg-anlegg-og-eiendom/2016/snts-30312016-for-beregning-av-energiebehov-og-energiforsyning/> (accessed: 12.03.19).
- Starakiewicz, A. (2018). Coverage of energy for the preparation of hot tap water by installing solar collectors in a singlefamily building. *E3S Web of Conferences*, 49.
- Statistisk sentralbyrå. (2018). *Elektrisitet*. Available at: <https://www.ssb.no/energi-og-industri/statistikker/elektrisitet/aar> (accessed: 14.03.19).
- Stickney, B. (2017). *Propylene Glycol: Solar Heat Transfer Fluid*. Available at: <https://www.phcpropros.com/articles/5189-propylene-glycol-solar-heat-transfer-fluid> (accessed: 13.05.19).
- Tekniske Nyheter DA. (2019). EnergiRapporten. 11:2019: p. 6, 10 (accessed: 08.04.19).
- Time and Date AS. (2019). *Klima og gjennomsnittsvær i Oslo, Norge*. Available at: <https://www.timeanddate.no/vaer/norge/oslo/klima> (accessed: 10.04.19).
- Twidell, J. & Weir, T. (2006). *Renewable Energy Resources*. 2 ed.: Taylor & Francis.
- TYFOROP Chemie GmbH. (2015). *Technical Information - TYFOCOR L Concentrate*. Available at: https://tyfo.de/downloads/TYFOCOR-L_en_TI.pdf.
- United Nations Framework Convention on Climate Change. (n.d.). *What is the Paris Agreement?* Available at: <https://unfccc.int/process-and-meetings/the-paris-agreement/what-is-the-paris-agreement> (accessed: 18.01.19).
- Vela Solaris. (2018). *Polysun Simulation Software User Manual*.
- Vela Solaris. (2019). *Polysun Designer Student*. Available at: <https://www.velasolaris.com/products/polysun-designer-student/?lang=en> (accessed: 26.02.19).
- Weiss, W. & Spörk-Dür, M. (2018). *Solar Heat Worldwide*.
- Young, H. D. & Freedman, R. A. (2012). *Sears and Zemansky's University Physics*. 13 ed.: Addison-Wesley.
- Zijdemans, D. (2014). *Varmtvannsforsyningsanlegg - type, systemer og komponenter*. Prenøk - Prosjektering av energianlegg: Skarland Press AS.

APPENDIX A: COMPONENTS IN POLYSUN

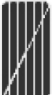
Appendix A includes screenshots of the settings of the different components of the chosen system in Polysun.

@	Name	Value	Unit	Schematic diagram
	Description			
	Show in report	▼ visible		
	Cold water calculation	▼ Catalog		
	Cold water supply	📍 Norway		
	- Mean temperature	8	°C	
	- Temperature range	4	K	
	- Warmest month	September		
	Temperature shift	0	K	

APPENDIX FIGURE 1: Screenshot of the settings for the cold-water inlet of the chosen system in Polysun.

@	Name	Value	Unit	Schematic diagram
	Description	5		
	Show in report	▼ visible		
A	Pipe	📍 Copper pipe 22x1		
B	- Internal diameter	20	mm	
C	- External diameter	22	mm	
D	Length	1	m	
	Linear form factor	1		
	Friction factor	0		
E	Insulation	📍 Loose glass fibres and mineral wool		
F	Thickness of insulation	100	mm	

APPENDIX FIGURE 2: Screenshot of the settings for the pipes of the chosen system in Polysun.

@	Name	Value	Unit	Schematic diagram
	Description			
	Show in report	▼ visible		
	External heat exchanger	📍 medium		
	- Transfer capacity	10,000	W/K	
	- Number of heat exchanger plates	30		

APPENDIX FIGURE 3: Screenshot of the settings for the heat exchanger of the chosen system in Polysun.

@	Name	Value	Unit
	Description	Transfer circuit	
	Show in report	▼ visible	
	Loop description		
	Pump	Eco, small	
	Pumping level	▼ 1	
	Flow rate-controlled	▼ Flow rate setting	
	Energy source	Electricity	

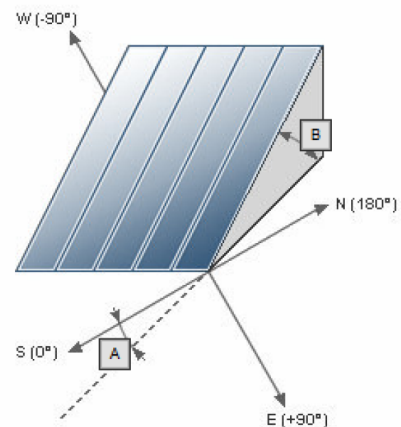
Schematic diagram



APPENDIX FIGURE 4: Screenshot of the settings for the pumps of the chosen system in Polysun.

@	Name	Value	Unit
	Description		
	Show in report	▼ visible	
	Test Standard	▼ Europe	
	Collector	Flat-plate, good quality	
	- Collector type	Flat-plate collector	
	- Testing standard Solar Keymark	EN 12975	
	Reference value for the area	▼ Number of collectors	
	Total gross area	40	m ²
	Total aperture area	36	m ²
	Total absorber area	36	m ²
	Number of collectors	20	
	Number of arrays	1	
	Wind speed at the collector array	50	%
A	Orientation (E=+90°, S=0°, W=-90°)	0	°
B	Tilt angle (hor.=0°, vert.=90°)	50	°
	Rotation	0	°
	Tracking	▼ No tracking	
	Maximum collector temperature	▼ No	

Schematic diagram



APPENDIX FIGURE 5: Screenshot of the settings for the solar collector of the chosen system in Polysun. This example is of a collector area of 40 m².

@	Name	Value	Unit
	Description		
	Show in report	▼ visible	
	Loop description		
	Use consumption profile	▼ Yes	
	Profile	[REDACTED]	
	Nominal flow rate automatic	▼ Yes	
	Temperature	65	°C
	Average volume withdrawal	1,997.3	l/day
	Annual demand ca	48,493	kWh
	Annual demand	729	m ³
	Enable hot water circulation	▼ No	
	Load profile automatic	▼ No	
	Load profile	▼ M (5.845 kWh/d)	

Schematic diagram



APPENDIX FIGURE 6: Screenshot of the settings for the tap of the chosen system in Polysun. This example is of the Drammen nursing home consumption (its name is censored).

APPENDIX B: CONTROLLERS IN POLYSUN

Appendix B includes screenshots of the settings of the different controllers of the chosen system in Polysun.

@	Name	Value	Unit
	Description		
	Show in report	▼ visible	
	Show input lines	▼ no	
	Show output lines	▼ no	
	Sign of output	▼ normal	
	Computation priority	2	
	Maximum collector temperature	130	°C
	Maximum tank temperature	90	°C
	Cut-in temperature difference	6	dT(°C)
	Cut-off temperature difference	2	dT(°C)
	Definition flow rate setting	▼ Specific flow rate	
	Specific flow rate	27.5	l/h/m ²
	Tank discharge mode	▼ no	

Control inputs		
Name	Value	Unit
Collector temperature	Collector: Outflow temperature	°C
Tank temperature	Storage tank 5: Bottom layer	°C
Collector aperture area (optional)	Collector: Collector aperture area	m ²
Upper tank temperature (optional)		°C

Control outputs		
Name	Value	Unit
On/Off pump 1	Pump Solar loop: On/Off	%
On/Off pump 2 (optional)	Pump Transfer circuit: On/Off	%
Pumping capacity pump 1 (optional)	Pump Solar loop: Flow rate	l/h
Pumping capacity pump 2 (optional)	Pump Transfer circuit: Flow rate	l/h

Availability times		<input checked="" type="radio"/> Timer	<input type="radio"/> Switching profile																				
1	2	3	4	5	6	7	8	9	10	11	12	13	14	15	16	17	18	19	20	21	22	23	24
<input checked="" type="checkbox"/>	<input checked="" type="checkbox"/>	<input checked="" type="checkbox"/>	<input checked="" type="checkbox"/>	<input checked="" type="checkbox"/>	<input checked="" type="checkbox"/>	<input checked="" type="checkbox"/>	<input checked="" type="checkbox"/>	<input checked="" type="checkbox"/>	<input checked="" type="checkbox"/>	<input checked="" type="checkbox"/>	<input checked="" type="checkbox"/>	<input checked="" type="checkbox"/>	<input checked="" type="checkbox"/>	<input checked="" type="checkbox"/>	<input checked="" type="checkbox"/>	<input checked="" type="checkbox"/>	<input checked="" type="checkbox"/>	<input checked="" type="checkbox"/>	<input checked="" type="checkbox"/>	<input checked="" type="checkbox"/>	<input checked="" type="checkbox"/>	<input checked="" type="checkbox"/>	<input checked="" type="checkbox"/>
Mon	Tue	Wed	Thu	Fri	Sat	Sun																	
<input checked="" type="checkbox"/>	<input checked="" type="checkbox"/>	<input checked="" type="checkbox"/>	<input checked="" type="checkbox"/>	<input checked="" type="checkbox"/>	<input checked="" type="checkbox"/>	<input checked="" type="checkbox"/>																	
Jan	Feb	Mar	Apr	May	Jun	Jul	Aug	Sep	Oct	Nov	Dec												
<input checked="" type="checkbox"/>	<input checked="" type="checkbox"/>	<input checked="" type="checkbox"/>	<input checked="" type="checkbox"/>	<input checked="" type="checkbox"/>	<input checked="" type="checkbox"/>	<input checked="" type="checkbox"/>	<input checked="" type="checkbox"/>	<input checked="" type="checkbox"/>	<input checked="" type="checkbox"/>	<input checked="" type="checkbox"/>	<input checked="" type="checkbox"/>	<input checked="" type="checkbox"/>	<input checked="" type="checkbox"/>	<input checked="" type="checkbox"/>	<input checked="" type="checkbox"/>	<input checked="" type="checkbox"/>	<input checked="" type="checkbox"/>	<input checked="" type="checkbox"/>	<input checked="" type="checkbox"/>	<input checked="" type="checkbox"/>	<input checked="" type="checkbox"/>	<input checked="" type="checkbox"/>	<input checked="" type="checkbox"/>

APPENDIX FIGURE 7: Screenshot of the settings for the pump controllers of the chosen system in Polysun.

@	Name	Value	Unit
	Description		
	Show in report	▼ visible	
	Show input lines	▼ no	
	Show output lines	▼ no	
	Sign of output	▼ normal	
	Computation priority	3	
	Logic relation temperature sensor 1 a...	▼ None	
	Reference for temperature sensors 1	▼ Fixed value	
	Cut-in tank temperature 1	67.5	°C
	Cut-off tank temperature 1	72.5	°C
	Minimum operation time	0	min
	Minimum downtime	0	min
	Maximum tank temperature	140	°C

Control inputs		
Name	Value	Unit
Layer temperature sensor on 1	Storage tank Stand-by storage tan...	°C
Layer temperature sensor off 1	Storage tank Stand-by storage tan...	°C
Flow rate heat generator (optional)		l/h
Inlet temperature heat generator (optional)		°C
Flow rate setting 2nd switch on/off (optional)		l/h

Control outputs		
Name	Value	Unit
On/Off heating device	Internal heater [1]: On/Off	%
On/Off switch (optional)		
Controlled power heat generator (optional)		W
On/Off feedwater pump (optional)		
On/Off heating loop pump (optional)		
Controlled flow rate 2nd switch on/off (optio...		l/h

Availability times		<input checked="" type="radio"/> Timer	<input type="radio"/> Switching profile																				
1	2	3	4	5	6	7	8	9	10	11	12	13	14	15	16	17	18	19	20	21	22	23	24
<input checked="" type="checkbox"/>	<input checked="" type="checkbox"/>	<input checked="" type="checkbox"/>	<input checked="" type="checkbox"/>	<input checked="" type="checkbox"/>	<input checked="" type="checkbox"/>	<input checked="" type="checkbox"/>	<input checked="" type="checkbox"/>	<input checked="" type="checkbox"/>	<input checked="" type="checkbox"/>	<input checked="" type="checkbox"/>	<input checked="" type="checkbox"/>	<input checked="" type="checkbox"/>	<input checked="" type="checkbox"/>	<input checked="" type="checkbox"/>	<input checked="" type="checkbox"/>	<input checked="" type="checkbox"/>	<input checked="" type="checkbox"/>	<input checked="" type="checkbox"/>	<input checked="" type="checkbox"/>	<input checked="" type="checkbox"/>	<input checked="" type="checkbox"/>	<input checked="" type="checkbox"/>	<input checked="" type="checkbox"/>
Mon	Tue	Wed	Thu	Fri	Sat	Sun																	
<input checked="" type="checkbox"/>	<input checked="" type="checkbox"/>	<input checked="" type="checkbox"/>	<input checked="" type="checkbox"/>	<input checked="" type="checkbox"/>	<input checked="" type="checkbox"/>	<input checked="" type="checkbox"/>																	
Jan	Feb	Mar	Apr	May	Jun	Jul	Aug	Sep	Oct	Nov	Dec												
<input checked="" type="checkbox"/>	<input checked="" type="checkbox"/>	<input checked="" type="checkbox"/>	<input checked="" type="checkbox"/>	<input checked="" type="checkbox"/>	<input checked="" type="checkbox"/>	<input checked="" type="checkbox"/>	<input checked="" type="checkbox"/>	<input checked="" type="checkbox"/>	<input checked="" type="checkbox"/>	<input checked="" type="checkbox"/>	<input checked="" type="checkbox"/>												

APPENDIX FIGURE 8: Screenshot of the settings for the heating element controller of the chosen system in Polysun.

@	Name	Value	Unit
	Description		
	Show in report	▼ visible	
	Show input lines	▼ no	
	Show output lines	▼ no	
	Sign of output	▼ normal	
	Computation priority	1	
	Definition temperature setting	▼ Variable value	
	Temperature shift	5	dT(°C)

Control inputs		
Name	Value	Unit
Upper temperature level (optional)	Pipe 2: Temperature	°C
Lower temperature level (optional)	Pipe 6: Temperature	°C
Variable temperature setting (optional)	Hot water demand: Temperature s...	°C

Control outputs		
Name	Value	Unit
Mixing valve (optional)	Three-way valve Domestic hot wat...	%

Availability times		<input checked="" type="radio"/> Timer	<input type="radio"/> Switching profile																				
1	2	3	4	5	6	7	8	9	10	11	12	13	14	15	16	17	18	19	20	21	22	23	24
<input checked="" type="checkbox"/>	<input checked="" type="checkbox"/>	<input checked="" type="checkbox"/>	<input checked="" type="checkbox"/>	<input checked="" type="checkbox"/>	<input checked="" type="checkbox"/>	<input checked="" type="checkbox"/>	<input checked="" type="checkbox"/>	<input checked="" type="checkbox"/>	<input checked="" type="checkbox"/>	<input checked="" type="checkbox"/>	<input checked="" type="checkbox"/>	<input checked="" type="checkbox"/>	<input checked="" type="checkbox"/>	<input checked="" type="checkbox"/>	<input checked="" type="checkbox"/>	<input checked="" type="checkbox"/>	<input checked="" type="checkbox"/>	<input checked="" type="checkbox"/>	<input checked="" type="checkbox"/>	<input checked="" type="checkbox"/>	<input checked="" type="checkbox"/>	<input checked="" type="checkbox"/>	<input checked="" type="checkbox"/>
Mon	Tue	Wed	Thu	Fri	Sat	Sun																	
<input checked="" type="checkbox"/>	<input checked="" type="checkbox"/>	<input checked="" type="checkbox"/>	<input checked="" type="checkbox"/>	<input checked="" type="checkbox"/>	<input checked="" type="checkbox"/>	<input checked="" type="checkbox"/>																	
Jan	Feb	Mar	Apr	May	Jun	Jul	Aug	Sep	Oct	Nov	Dec												
<input checked="" type="checkbox"/>	<input checked="" type="checkbox"/>	<input checked="" type="checkbox"/>	<input checked="" type="checkbox"/>	<input checked="" type="checkbox"/>	<input checked="" type="checkbox"/>	<input checked="" type="checkbox"/>	<input checked="" type="checkbox"/>	<input checked="" type="checkbox"/>	<input checked="" type="checkbox"/>	<input checked="" type="checkbox"/>	<input checked="" type="checkbox"/>												

APPENDIX FIGURE 9: Screenshot of the settings for the mixing valve controller of the chosen system in Polysun.

APPENDIX C: SPECIFICATIONS OF SOLAR COLLECTOR AND ACCUMULATOR TANK

Appendix C includes specifications of the chosen types of solar collector and accumulator tank of the chosen system in Polysun.

APPENDIX TABLE 1: Specifications of the solar collector used in the chosen system. Some of the specifications are explained below the table.

Solar collector specifications	
Name	Flat-plate, good quality
Manufacturer	Anonymous
Data source	SPF
Collector type	Flat-plate collector
Test date	2005
Quality test	No
Absorber area	1.8 m ²
Aperture area	1.8 m ²
Gross area	2 m ²
Eta0 (laminar)	0.75
Eta0 (turbulent)	0.8
A1 (without wind)	3.5 W/m ² /K
A1 (with wind)	4 W/m ² /K
A2	0.02 W/m ² /K ²
Dynamic heat capacity	5000 J/K
Volume	1.5 l
Internal pipe diameter	9 mm
Single pipe length	18 m
Parallel piping	1
Pipe roughness	0.1 mm
Linear form factor	1
Friction factor	0
Fluid for test	Water
Test flow rate	100 l/h
Maximum flow rate	2000 l/h
Maximum pressure	10 bar
Maximum temperature	220 °C

The following explanations on some of the specifications in appendix table 1 are a direct rendering from Polysun:

- SPF is the testing institute, the Institute for Solar Technology.

- The areas are according to ISO EN 9488. The aperture area is the surface area of the collector, through which light can enter and reach the absorber. The gross area is the largest projected area of a collector module without mounting fixtures or hydraulic connections.
- η_0 is the optical efficiency value of laminar/turbulent flow of the heat transfer medium in the collector piping when the collector temperature equals the ambient temperature. A_1 (without wind) is the linear heat loss coefficient with a measurement without artificial ventilation (no standard value). A_1 (with wind) is the linear heat loss coefficient according to EN standard 12975, i.e. for a wind speed of 3 ± 1 m/s. A_2 is the quadratic heat loss coefficient according to EN 12975.
- The dynamic heat capacity is related to dynamic equilibrium, i.e. for a stationary heat flow (absorbed energy is equal to output energy).
- The single pipe length is the length between the manifold pipes. Parallel piping means piping sections connected in parallel. The pipe roughness is the average value of the surface roughness of the internal pipe wall. The linear form factor is a pressure drop multiplier to account for pipe bends. The friction factor is a pressure drop multiplier for dynamic pressure due to hydraulic elements.
- The maximum flow rate and pressure are specified by the manufacturer.

APPENDIX TABLE 2: Specifications of the accumulator tank used in the chosen system. Some of the specifications are explained below the table.

Accumulator tank	
Manufacturer	Anonymous
Height	2 m
Bulge height	100 mm
Material	Stainless steel
Wall thickness	3 mm
Insulation	Rigid PU foam
Thickness of insulation	150 mm
Ports	No S-bending
Position P[1]	0 %
Position P[2]	35 %
Position P[5]	0 %
Position P[8]	100 %

Following are explanations on some of the specifications in appendix table 2:

- S-bending in the ports means that a downward curving piece is installed right at the output of the tank, to minimise connection heat losses (Vela Solaris, 2018). Such an implementation is not applied in this research.
- P[1] refers to the port connected to the pipe which contains the water giving the inlet temperature to the solar collector. P[2] refers to the port connected to the pipe which contains the water heated by the outlet water from the solar collector. P[5] refers to the port connected to the pipe which contain the water from the cold inlet. P[8] refers to the port connected to the pipe which contain the water flowing from the accumulator tank to the water heater. The positions in percent correspond to figure 19.



Norges miljø- og biovitenskapelige universitet
Noregs miljø- og biovitenskapelige universitet
Norwegian University of Life Sciences

Postboks 5003
NO-1432 Ås
Norway